Palacký University Olomouc

Master thesis

Olomouc 2023 **Jakub Lemberk**

Palacký University Olomouc

Faculty of Science

Department of Cell Biology and Genetics

Study of root angle determination in barley (*Hordeum vulgare* L.)

Master thesis

Jakub Lemberk

Study programme: Biology

Field of study: Molecular and cell biology

Form of study: Full time

Olomouc 2023

Supervisor: Véronique Hélène Bergougnoux-Fojtik, Ph.D.

UNIVERZITA PALACKÉHO V OLOMOUCI

Přírodovědecká fakulta

Akademický rok: 2021/2022

ZADÁNÍ DIPLOMOVÉ PRÁCE

(projektu, uměleckého díla, uměleckého výkonu)

Jméno a příjmení:	**Bc. Jakub LEMBERK**
Osobní číslo:	**R21927**
Studijní program:	**N0511A030046 Molekulární a buněčná biologie**
Téma práce:	**Studium kontrolované změny úhlu kořene ječmene (Hordeum vulgare L.)**
Zadávající katedra:	**Katedra buněčné biologie a genetiky**

Zásady pro vypracování

1. Study of scientific literature related to root system development in cereals, genetic control of root angle determination and methods to study root phenotype. This will lead to the identification of genes with a potential role in the developmental process.
2. Firstly, using in vitro cultivation, different barley accessions will be screened for their contrasted root angle.
3. Based on the literature, genes will be selected for their potential role in root angle development in barley. The expression of these candidates will be determined by qPCR in different organs but also among different barley accessions identified in 2)
4. Using CRISPR-Cas9 methodology, knock-out plants will be prepared. In the frame of the master thesis, the student will be able to prepare the constructs, obtain the T0 generation and genotype for K0 plants.
5. Based on the results, the student will be forming hypothesis concerning the role of the chosen candidate gene during root system angle determination

Rozsah pracovní zprávy:	
Rozsah grafických prací:	
Forma zpracování diplomové práce:	**tištěná**
Jazyk zpracování:	**Angličtina**

Seznam doporučené literatury:

Guyomarc'h S., *et al.* (2012): Early development and gravitropic response of lateral roots in Arabidopsis thaliana. Philosophical Transactions of the Royal Society B: Biological Sciences 367: 1509-1516.

Guseman J. M., *et al.* (2017): DRO 1 influences root system architecture in Arabidopsis and Prunus species. The Plant Journal 89(6): 1093-1105.

Tomita A., *et al.* (2017): Genetic variation of root angle distribution in rice (Oryza sativa L.) seedlings. Breeding Science, Japanese Society of Breeding. 67: 181-190.

Toal T. W., *et al.* (2018): Regulation of Root Angle and Gravitropism. G3 Genes|Genomes|Genetics 8(12): 3841-3855.

Kitomi Y., *et al.* (2020): Root angle modifications by the DRO1 homolog improve rice yields in saline paddy fields. Proceedings of the National Academy of Sciences 117(35): 21242-21250.

Vedoucí diplomové práce:	**Véronique Hélene Bergougnoux-fojtik, Ph.D.** Centrum regionu Haná
Datum zadání diplomové práce:	**4. listopadu 2021**
Termín odevzdání diplomové práce:	**31. července 2023**

L.S.

doc. RNDr. Martin Kubala, Ph.D.
děkan

prof. RNDr. Zdeněk Dvořák, DrSc.
vedoucí katedry

V Olomouci dne 5. listopadu 2021

Bibliographical identification

Author's first name and surname: Jakub Lemberk

Title: Study of root angle determination in barley (*Hordeum vulgare* L.)

Type of thesis: master

Department: Department of Cell Biology and Genetics, Faculty of Science Palacký University Olomouc

Supervisor: Véronique Hélène Bergougnoux-Fojtik, Ph.D.

The year of presentation: 2023

Keywords: Barley, root growth angle, *DEEPER ROOTING 1* (*DRO1*), *DRO1*-like (*DRL1*), CRISPR/Cas9

Number of pages: 89

Number of appendices: 0

Language: English

SUMMARY

Root system architecture, specifically root growth angle and spatial distribution of roots, is an important factor for plant in acquiring resources from the soil. Plants with narrow root growth angle could exploit resources from greater depth and avoid drought. Recently, the role in the root system architecture of the two rice genes Os*DRO1* and *qSOR/DRL1* was recognized. In this work, we identified gene *HORVU.MOREX.r3.5HG0480470* in barley as putative homolog of rice gene Os*DRO1* (81,6% identity), and gene *HORVU.MOREX.r3.2HG0125600* in barley as putative homolog of rice gene *qSOR/DRL1* (94,7% identity). Based on screened root growth angles of the landrace HOR1122 (53,8 °), and two modern cultivars cv. Golden Promise (45,5 °) and cv. Maythorpe (37,9 °) after *in vitro* cultivation, expression of Hv*DRO1* and Hv*DRL1* was measured in crown of cv. Golden Promise and Maythorpe during crown-root initiation and development using an auxin-based inducible system. Concerning Hv*DRL1* gene, no expression could be detected in the crown of the seedling of none of the cultivar at the start of the initiation. For both genotypes, Hv*DRL1*

transcripts accumulated in the crown 3 days after the start of initiation by auxin. At this moment, “buds” at the surface of the crown were visibly emerging, suggesting the presence of new CR primodium. The expression remains constant during the rest of the kinetic analysed. A low, basal expression of Hv*DRO1* was detected in the crown of seedlings at any time of the kinetic. No significant difference between the two cultivars could be observed. *Agrobacterium tumefaciens*-mediated barley immature embryo transformation was employed to knock-out either Hv*DRO1* or Hv*DRL1* by the CRISPR/Cas^{9} methodology. Despite a huge number of embryo were transformed, only 5 plants were found to contain the T-DNA. Among those plants, one (DRO2-S4/3) was predicted using DECODER to have a 3-base deletion in the Hv*DRO1* gene, 3 bp upstream of PAM sequence. This T_0 plant did not show morphology difference between mutated and nonmutated plant’s above-ground part. The effect of the mutation in the Hv*DRO1* on the plant fitness and root system architecture will be studied in the next generation.

Bibliografické údaje

Jméno a příjmení autora: Jakub Lemberk

Název práce: Studium kontrolované změny úhlu kořene ječmene (*Hordeum vulgare* L.)

Typ práce: diplomová

Pracoviště: Katedra buněčné biologie a genetiky, PřF UP v Olomouci

Vedoucí práce: Véronique Hélène Bergougnoux-Fojtik, Ph.D.

Rok obhajoby práce: 2023

Klíčová slova: Ječmen, úhel růstu kořene, *DEEPER ROOTING 1* (*DRO1*), *DRO1*-like (*DRL1*), CRISPR/Cas9

Počet stran: 89

Počet příloh: 0

Jazyk: anglický

ABSTRAKT

Architektura kořenového systému, konkrétně úhel růstu kořenů a prostorové rozložení kořenů, je důležitým faktorem pro rostliny při získávání zdrojů ze země. Rostliny, u kterých rostou kořeny pod úzkým úhlem mohou využívat zdroje z větší hloubky a vyhnout se tak suchu. Nedávno byla rozpoznána role dvou rýžových genů Os*DRO1* a *qSOR/DRL1* v architektuře kořenového systému. V této práci jsme u ječmene identifikovali gen *HORVU.MOREX.r3.5HG0480470* jako možný homolog rýžového genu Os*DRO1* (81,6% shoda) a gen *HORVU.MOREX.r3.2HG0125600* jako možný homolog rýžového genu *qSOR/DRL1* (94,7% shoda). Na základě zkoumaného úhlu růstu kořenů z krajové odrůdy HOR1122 (53,8°) a dvou moderních kultivarů cv. Golden Promise (45,5°) a cv. Maythorpe (37,9°) pěstovaných *in vitro*, byla měřena exprese genů Hv*DRO1* a Hv*DRL1* v koruně cv. Golden Promise a Maythorpe během iniciace a vývoje kořenů pomocí auxinového indukčního systému. Pokud jde o gen Hv*DRL1*, nebylo možné detekovat žádnou expresy v koruně u žádného z kultivarů na začátku iniciace. Pro oba genotypy se při použití auxinu hromadily transkripty Hv*DRL1* v koruně 3 dny po zahájení iniciace. V této době se na povrchu koruny viditelně

objevovaly "poupata", což naznačovalo přítomnost nových CR primordií. Exprese zůstávala konstantní po zbytek analyzovaného kinetického období. V koruně sazenic byla detekována nízká bazální exprese Hv*DRO1* kdykoliv během zkoumaného období. Mezi oběma kultivary nebyl pozorován žádný významný rozdíl. Knock-out genů Hv*DRO1* nebo Hv*DRL1* byl iniciován za použití metodologie CRISPR/Cas9 a transformace nezralých ječmenných embryí *Agrobacterium tumefaciens*. Přestože bylo transformováno obrovské množství embryí, pouze 5 rostlin obsahovalo T-DNA. U jedné z těchto rostlin (DRO2-S4/3) byla pomocí DECODERu předpovězena 3-bázová deleci v genu Hv*DRO1*, 3 bp před PAM sekvencí. Tato rostlina v generaci T_0 nevykazovala žádné morfologické změny v nadzemní části rostliny oproti rostlině bez mutace. Vliv mutace v genu Hv*DRO1* na kondici rostliny a architekturu kořenového systému bude studován v další rostlinné generaci.

I declare that this master thesis was written independently with the help of my supervisor, Véronique Hélène Bergougnoux-Fojtik, Ph.D., using sources listed in the reference.

In Olomouc …… ……

Jakub Lemberk

Acknowledgment:

I would like to thank my supervisor, Véronique Hélène Bergougnoux-Fojtik, Ph.D., for her expert and patient guidance throughout the work on this thesis. Next, I would like to thank Nguyễn Diệu Thu M.Sc and Alexie Techer M.Sc for their willingness to assist me in laboratory. And at last, but not least, I would like to thank Bc. Vendula Svobodová for her help with transformation of barley embryos, and for taking care of the plants.

CONTENT

ABBREVIATIONS

1-NAA	1-Naphthaleneacetic acid
cDNA	complementary DNA
dNTP	deoxynukleosidtriphosphate
CR	crown roots
DRO1	Deeper Rooting 1
DRL1	DRO1-like
EtBr	ethidium bromide
GP	Golden Promise
gRNA	guide RNA
p6i	271p6i-2x35S-TE9 vector
PCR	polymerase chain reaction
NPA	naptalam
scRNA	scaffold RNA
SNP	single nucleotide polymorphisms
qSRO	quantitative trait locus for Soil Surface Rooting 1

FIGURES

TABLES

1 INTRODUCTION

Growing population combined with changing climate with more frequent drought episodes, as well as need to reduce use of fertilizers, poses challenges of nowadays agriculture plant production. For long, due to their hidden nature, roots – the underground part of the plants – have been neglected even though they constitute an important interface with the environment. Indeed, they don't solely permit plant's anchorage in the soil, ensuring water and nutrient uptake. The current study focuses on traits defining the root system architecture, such as density of roots or root growth angle, as they define the 3-dimensional orientation of root system in the soil and predict the root foraging ability towards resources from the soil. Plants with steep root growth angle have longer roots, can acquire water from deep levels of soil and that makes them less drought prone. Understanding molecular mechanisms governing root system development in harsh environment (drought or nutrient deficiency, for example) has a potential for new breeding programs, using either marker-assisted selection or new methods of genetic engineering. A major locus responsible for narrow root growth angle *'DEEP ROOTING 1'* (Os*DRO1*) was identified in rice in 2011 and studies since then specified its role in drought tolerance and improved grain yield in environment with lack of water. The identification of genes that are associated with root architecture thus represents an important task.

2 AIM OF THE THESIS

1 Study of scientific literature related to root system development in cereals, genetic control of root angle determination and methods to study root phenotype. This will lead to the identification of genes with a potential role in the developmental process.

2 Firstly, using in vitro cultivation, different barley accessions will be screened for their contrasted root angle.

3 Based on the literature, genes will be selected for their potential role in root angle development in barley. The expression of these candidates will be determined by qPCR in different organs but also among different barley accessions identified in 2)

4 Using CRISPR-Cas9 methodology, knock-out plants will be prepared. In the frame of the master thesis, the student will be able to prepare the constructs, obtain the T_0 generation and genotype for KO plants.

5 Based on the results, the student will be forming hypothesis concerning the role of the chosen candidate gene during root system angle determination

3 LITERATURE REVIEW

3.1 Root system and architecture of cereals

Cereals have typical fibrous root system consisting of two types of roots: seminal and nodal roots. Seminal roots are formed embryonically and are short-lived. Post-embryonic nodal roots emerge at the lower tiller nodes (Bellini *et. al.*, 2014). In cereals such as rice (*Oryza sativa* L.), barley (*Hordeum vulgare* L.) or maize (*Zea mays* L.), lateral roots originate from pericycle of primary roots, that is surrounded by up to 20 layers of cells, including the endodermis, the mesodermis, the exodermis, the epidermis, and the sclerenchyma layer (Rebouillat *et al.*, 2008). Other post-embryonic roots, that develop from shoots, are typically called crown roots (CR) (Wahbi *et* Gregory, 1995; Coudert *et al.*, 2010).

Root system is an important part of each plant, between two of its main functions belongs absorption of nutrients and water from soil and supporting above-ground part of the plant. The term 'root architecture' is commonly used in association with spatial configuration of the root system. It does not focus on surface attributes of the single root (such as root diameter, hairs, cap etc.) that are subjects of the root morphology, but takes in consideration the shape of the whole root system. More specifically, root architecture refers to the geometric distribution of root axis (Ennos *et* Fitter, 1992; Lynch, 1995).

The architecture differs between species, between genotypes and even between other parts of the same root system. The final look is a result of a widespread elongation of single roots and occurrence of daughter roots along axes, direction in which they grow, their senescence and mortality, and compliance of these procedures to variable soil conditions such as availability of nutrients, water, and oxygen. The last one mentioned is important, because the resources, that plants need for growth, are not distributed in soil evenly. High gradients of water, oxygen, and nutrient availability, as well as gradients of pH and temperature, exist in soil on the order of centimetres. It is also related to topsoil usually being drier, more exposed to temperature fluctuation, but richer in nutrients than subsoil (Fogel, 1985; Ennos *et* Fitter, 1992; Lynch, 1995). Resources in soil could be described as mobile (move with water to deeper layers) and immobile. Between main mobile nutrients belongs nitrogen (N) usually in form

of nitrate and sulfur (S) usually in form of sulfate. Immobile nutrients, such as phosphorus (P), potassium (K) or ammonium are often characterized as nutrients with limited diffusion. Calcium (Ca^{2+}) and magnesium (Mg^{2+}) have medium mobility. In one hand, lack of most of the nutrients can result in limited plant growth, with the most restrictive in agricultural soils being N, P and K, along with water. On the other hand, high concentrations of nutrients can promote elongation and root branching (Drew *et al.*, 1973; Barber, 1995; Havlin *et al.*, 2013).

As mentioned before, the ability of roots to explore the variable soil and exploit the resources depends on root spatial distribution, hence architecture. Main architecture traits responsible for plant uptake of soil resources are root growth angle, number and length of seminal roots, root branching, and root hair length. For example, number of seminal roots is associated with need of water. In dry environments plants develop higher number of seminal roots, as their increased number may result in vivid root branching, denser and longer roots and therefore plant might obtain more water from deeper soil (Manschadi *et al.*, 2006, 2008; Richard *et al*., 2015). Root angle of seminal roots is another important factor in water (and mobile nutrients) acquisition. Plants in droughty environment tend to have narrow angle and consequently a root system that goes deeper. Moreover, genotypes in wet areas where water is not a limiting factor have wide, almost horizontal seminal roots angle and shallow root system. (Rundel *et* Nobel, 1991; Oyanagi, 1994). The shallow root system is also typical for plants in environment with low amounts of immobile nutrients, such as phosphorus, as they are mostly in upper layers of soil. Additionally, study on barley showed, that genotypes with short root hairs have lower grain yield in soil with low P concentration, while genotypes with long root hairs have stable grain yield across the low to high concentrations of P and therefore are better adapted to lack of phosphorus in soil, suggesting association of length of root hairs with the ability to obtain P from surrounding soil (Lynch *et* van Beem, 1993; Gahoonia *et* Nielsen, 2004).

Lynch (2013, 2019) summarized roots phenotypes of maize based on their potential to exploit resources from soil and proposed two main ideotypes: ‘steep, cheap, and deep’ (SCD) and ‘topsoil foraging’. The SCD ideotype has steep root growth angle, smaller number of crown and nodal roots and reduced lateral branching. It should have improved capture of water and nitrate, that tend to leak to deeper layers of soil.

The second ideotype topsoil foraging, is adapted for capture of immobile nutrients (P, K, Ca, Mg) in upper soil layer and its root traits are exactly the opposite to the SCD (Figure 1).

These ideotypes, that focus mainly on root architecture, could promote plant growth in environments, where growth is limited by resources either in deep or shallow layers of soil. But even though having long and deep roots help to acquire water and nitrate, it is not advantageous for exploiting nutrients in upper parts of soil and vice versa. Hence improving uptake of potassium might simultaneously reduce uptake of water. Genotypes with these root ideotypes could be used in highly specific environments, such as terminal drought, but not in conditions with other limitations. The solution could be the plasticity of roots to explore both upper and deeper levels of soil. However, factors like salinity, acidity, and temperature of soil as well influence root architecture and affect acquisition of nutrients (Hodge, 2004; Lynch, 2019; van der Bom *et. al.*, 2020).

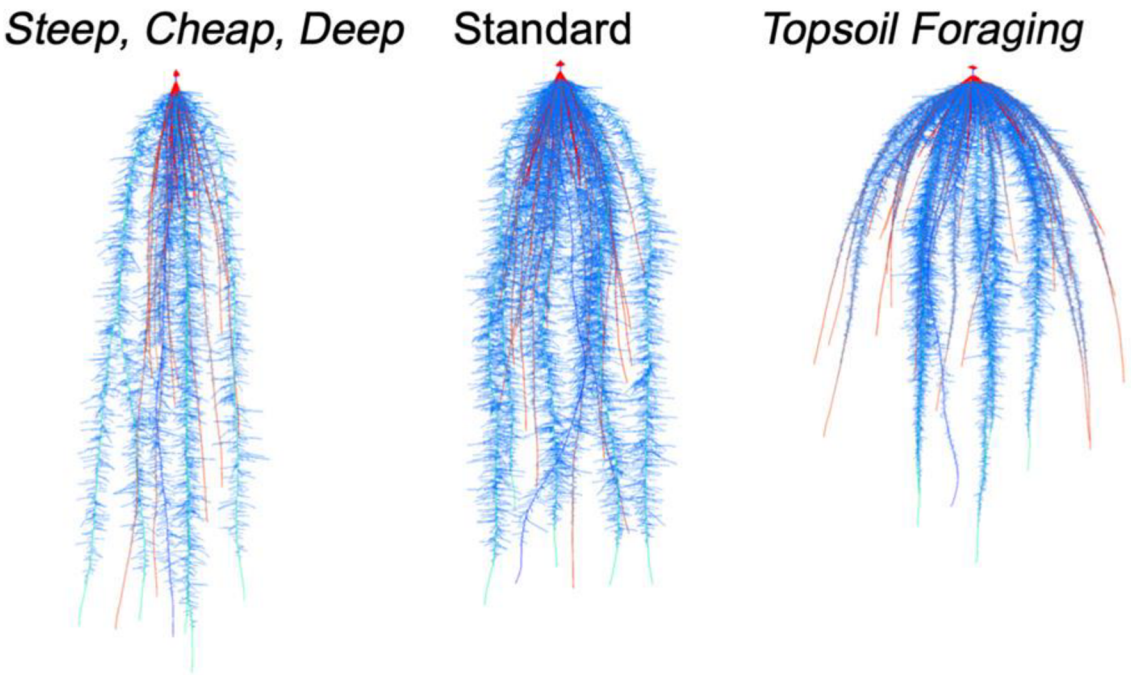

Figure 1: Different root ideotypes of maize (from: Lynch, 2019).

3.2 How to study roots

Visualisation of plant root system is essential for its study. There are many different methods of root phenotyping, and each has its advantages and disadvantages. They can be divided into laboratory-based methods and methods conducted in field, further to destructive and non-destructive, to soil and non-soil techniques, *ex vivo*, *in situ* or *in vitro*, and many more.

3.2.1 Field phenotyping

For quantitative measurement of length and mass of roots the simplest technique is to collect intact plants in field, wash the soil from the roots and quantify the properties (Oliviera *et al.*, 2000; Pierret *et al.*, 2005). This destructive field phenotyping technique is often referred to as "shovelomics". Dug up plants with carefully washed away soil to expose the roots (using 0,5% detergent) are then subjected to various tools and techniques to measure different root traits By studying traits such as root length, thickness, angle, or branching pattern, researchers can gain insights into how plants respond to different environmental conditions, such as soil texture, nutrient availability, and water stress. This method is optimal for basic characterisation of root system architecture, but doesn't allow researcher to study spatial distribution of roots (Trachsel *et al.*, 2011).

Observing 3-D features in field is quite difficult. The use of rhizotrons, that were first introduced in 1937 (Bates, 1937), with the progress of image analysis in recent years, helped to almost surpass this problem. Minirhizotrons are hollow round glass or plastic tubes, typically 1.5 to 2 meters long and 0.5 m in diameter. Tubes are buried in the ground either vertically, horizontally, or slightly tilted (Figure 2). The last orientation is preferred because, unlike vertical distribution, it avoids soil artefacts and is not as difficult to position in the ground as horizontal orientation. Inside the tube, there is a moveable camera, nowadays with 600 DPI high-resolution, and digital sensors. As the minirhizotron is buried in the ground, its surface is exposed to growing roots that can be repeatedly recorded by camera without any significant effects on rooting of a plant. Minirhizotrons provide information about plant root growth in time, from its birth to death, and an insight to its spatial distribution (McMichael & Taylor, 1987; Majdi, 1996; Johnson *et al.*, 2001; Vamerali *et al.*, 2011). Moreover, it can be used to study

interactions of roots with soil fauna such as N-fixing bacteria (Pritchard *et* Rogers, 2000), mycorrhizae (Pritchard *et al.,* 2008) or nematodes (Smit *et* Vamerali, 1998).

The main disadvantage of this technique is that as the roots grow along the minirhizotron, a part of roots remain undetected as the minirhizotron can monitor only those that grow on its surface. The number of observable roots decreases as the average root diameter of the plant increases (Nagel *et al.*, 2012). The result is a picture of 2-dimensional area that does not represent the total expansion of the root system in the soil. Furthermore, introducing minirhizotrons into the ground disturbs the soil dynamics and hence it is suggested to wait 6 to 17 months after the tube installation to the ground before the start of the experiment (Johnson *et al.*, 2001; Joslin *et al.*, 2006; Pritchard *et al.*, 2008).

Overall, minirhizotrons are useful non-destructive technique for studying plant roots in natural habitat. It is not surprising, that few commercial companies, such as Vienna Scientific Instruments (VSI, 2023), or Bartz Technology Corporation (BTC, 2023) develop and sell their own minirhizotrons including software and hardware. However, the use of "home-made" minirhizotrons is not uncommon (Johnson *et* Meyer, 1998; Vamerali *et al.*, 2003).

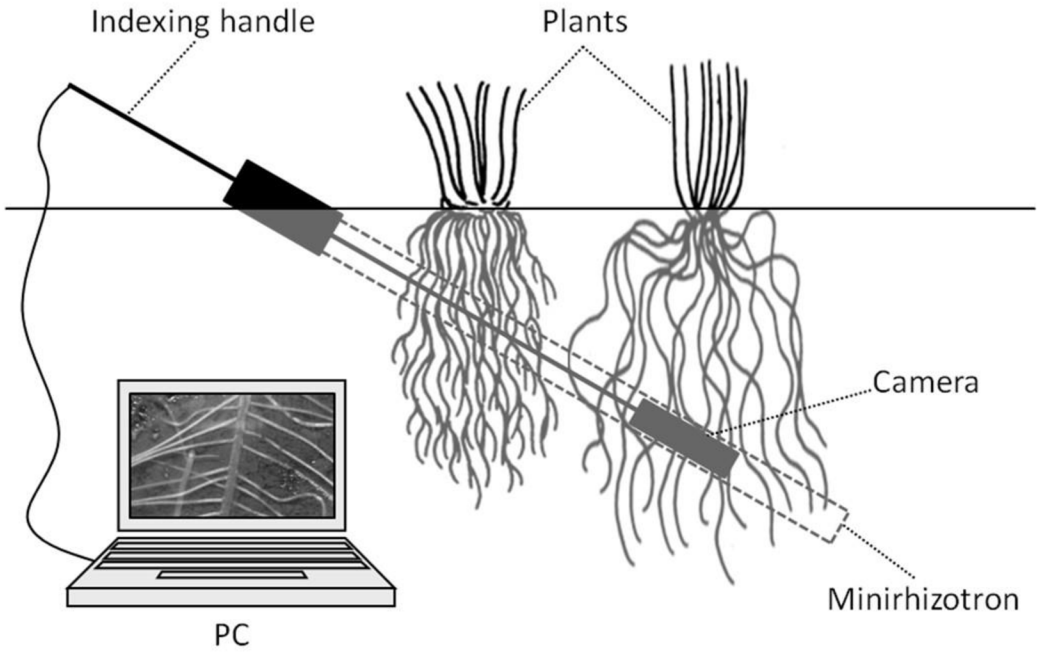

Figure 2: Minirhizotron root observation system. (from Vamerali *et. al.*, 2011).

3.2.2 Laboratory-based techniques

A common tool used to study traits of large population of plants are germination pouches, also known as seed germination bags. The pouches are made of a sterile, transparent, and breathable material that allows monitoring of the seedling's development, while providing a controlled environment. This non-destructive approach is typically used to measure root angle, root depth and diameter, and to observe the germination process. Moreover, it helps to identify the effects of different conditions on seed germination, such as temperature, light, and moisture levels. It is also used to quantify herbicide dose-response and resistance. In plant breeding, germination pouches allow researchers to monitor the germination success of seeds and select the most promising plants for further cultivation (Zhang *et al.*, 2015; Huang *et al.*, 2020).

Technique, that is popular not only in biology, is X-ray computed tomography (CT). CT is a non-invasive imaging technique that uses X-ray beams to produce detailed, 3-D images of the internal structure of objects. It is a useful tool to study structure and function of plant roots. Imaging is performed by CT scanner, which rotates around the sample and takes multiple 2-D projections (radiographs) from different angles. These images are then reconstructed using computer algorithms to produce a 3D model of the root system. The resulting images provide valuable insights into the architecture and function of plant roots, including their length, diameter, branching patterns, spatial orientation, and density. One of the main advantages of CT is its ability to non-destructively image the internal structure of the roots without damaging or altering them. This makes possible to study the same root system over time to monitor changes in response to different treatments or environmental conditions. Such series of radiographs is sometimes referred to as 4-D image, i.e., 3-D including time (Withers *et al.*, 2021). CT imaging can also reveal the presence of air pockets and water-filled spaces or help to study the effects of environmental factors such as soil moisture and other features on root growth and nutrient uptake. It can also be used to evaluate the effectiveness of different management practices for optimizing root growth and nutrient uptake in agricultural systems. In conclusion, X-ray CT is a valuable tool for plant root research, providing detailed and accurate information about the root system without damaging the roots. This allows researchers to gain insights into the root morphology and architecture that are crucial for plant growth and development (Gregory *et al.*, 2003;

Lontoc-Roy *et al.*, 2006; Perret *et al.,* 2007; Taina *et al.*, 2008; Hargreaves *et al.*, 2009; Mooney *et al.*, 2012; Mairhofer *et al.*, 2013; Withers *et al.*, 2021).

In controlled laboratory conditions the use of plates with medium represents fast and non-invasive method to study early plant development. Medium contains substances needed for plant growth such as amino acids, micro and macronutrients, growth regulators, solidifying agents (agar), vitamins, etc. (Murashige & Skoog, 1962; Saad & Elshahed, 2012). Seedlings grown in gel chamber, that was introduced by Bengough *et al*. (2004), on optically clear agar under optimal temperature and lightning settings are visible and therefore easily screened by scanner. Observed features are in 2-D and could serve for simple measurement of root traits, such as length, root growth angle, density, or number of seminal roots. However, the growth of plants is limited by the size of the chamber and hence this method could be used to study only early stages of development. Moreover, it is important to maintain sterile conditions throughout the process to prevent contamination from microorganisms that could affect the growth of the plants and interfere with the observations. Even though 2-dimensional results might not sufficiently represent a real 3-D root system in natural environment, Hargreaves *et al.* (2009) after converting 3-D data from X-ray CT to 2-D projection observed: "completely analogous results to the 2-D gel plates", proving that this method is eligible for studying 3-D oriented traits. Additionally, it is important to simulate as natural conditions as possible. Roots grow in natural environment underground in darkness and exposing them to light even for small period of time induces release of reactive oxygen species (ROS) (Yokawa *et al.*, 2011). Furthermore, plants growing with uncovered roots develop longer roots in total with higher density of hair, increased presence of PIN2 (efflux carrier protein of auxin) in root apexes, associated with stronger gravitropism, than in plants with roots grown in darkness. These findings indicate the importance of maintaining natural conditions in laboratories during experiments (Xu *et al.*, 2013). Nevertheless, growing plants in laboratory on agar-plate, or nowadays within embedded fluidic channels in agar (Aziz *et al.*, 2020), provides a controlled environment that can be adjusted to the specific needs of the plants and allows for the precise control of factors such as temperature, light intensity, and nutrient availability, which can be difficult to achieve in the field, making it possible to study the effects of specific deficiencies. Moreover, the observation is easy, and it is feasible to

replicate experiments and obtain consistent results (Bengough *et al.*, 2004; Hargreaves *et al.*, 2009; Xu *et al.*, 2013; Aziz *et al.*, 2020).

The last-mentioned method in this review is hydroponics. It is a method of growing plants without soil, but instead with the use of a nutrient-rich solution to provide the necessary nutrients for the plants to grow. The word "hydroponics" comes from the Greek words "hydro" (meaning water) and "ponos" (meaning labor). In hydroponics, plants are typically grown in containers filled with a growing medium, which provides support for the plant's roots, and the freely circulating nutrient solution, that is usually composed of water and a mixture of essential minerals and nutrients, such as nitrogen, phosphorus, and potassium. Hydroponics has several advantages over traditional soil-based growing methods, including greater control over nutrient uptake, more efficient use of water and space, and the ability to grow plants in environments where soil-based agriculture is not possible (Khan *et al.*, 2021). Additionally, American agency National Aeronautics and Space Administration (NASA) studies hydroponics as a method, that could in future long-duration missions in space provide astronauts with freshly grown plants, that would not only provide a healthy diet, but would also create oxygen and reduce carbon dioxide level (Heiney, 2004; Pierce, 2021).

3.3 Identification of genes

3.3.1 Methods

Identifying new genes can lead to better understanding the genetic basis of numerous traits and potentially recognize new targets for genetic manipulation. A common approach is the use of recombinant inbred lines (RILs) (Bailey, 1971) to identify a specific region of DNA − Quantitative Trait Loci (QTL), that is associated with a particular trait, such as height, root growth angle or root length. Recombinant inbred lines are created by crossing two parents that differ in the trait of interest and then inbreeding F1 hybrids for multiple generations until the resulting lines become homozygous at almost all loci. This means that each RIL will be genetically identical to all other lines at most loci, except for those regions where recombination has occurred. Recombination leads to the formation of new combinations of numerous genetic markers, such as SNP, along the chromosomes. By analysing the phenotypic variation among the RILs, with the help of statistical methods, and genotyping them with the use

of genetic markers, it is possible to identify regions of the genome that are associated with the trait of interest. Identification of QTL can help to better understand the genetic basis of complex traits and may ultimately lead to the development of more targeted and effective breeding strategies in agriculture and other fields (Goffinet *et* Gerber, 2000; Pollard, 2012).

Another option is Genome-wide association study (GWAS). The study is used to identify genetic variations, such as copy-number variants or more common single-nucleotide polymorphism (SNP), that are statistically associated with a specific trait of interest. The approach typically involves genotyping many thousands of SNPs across the genome of a large number of subjects (e. g. plants, humans) with the trait of interest and a control group without the trait, and then analysing data for an association between each SNP and the trait. The results can help to link specific phenotype to genotype and identify potential targets for further investigation (Pearson *et* Manolio, 2008; Manolio, 2010; Yang *et al.*, 2013; Uffelmann *et al.*, 2021).

Once the gene is identified, it is possible to use approaches of reverse genetics. Reverse genetic studies the function of genes in organisms by manipulating the genes *in vitro* or *in vivo* and observing the changes in phenotype (Thorneycroft *et al.*, 2001). One common approach is to "knock-out" specific gene by introducing direct mutation and then determine its role in a biological process. Nowadays, with the development of the CRISPR/Cas9 methodology, this can be done very precisely with a very low frequency of mutating unwanted genes (Doudna *et* Charpentier, 2014; Kumar *et al.*, 2019). Reverse genetics can also be used to silence the expression of specific genes throughout an entire organism or cell line through post-transcriptional gene silencing by RNA interference (Han, 2018).

3.3.2 Studies focused on root development

The goal of many researchers and breeders is to improve cereals (and other plants) tolerance to stress and increase yield and nutrients income. Roots monitor changing environment of the soil, level of toxins, nutrients and water attainability and are therefore essential for plant´s adaptation to biotic and abiotic stress. Development of roots is a complex process that is affected by the environment and impacted by various

endogenous factors (such as phytohormones), their transcription factors and controlled by numerous sets of genes (Coudert *et al.*, 2010; Gowda *et al.*, 2011).

Phytohormones as growth regulators play a crucial role in development by regulating cell division, differentiation, and growth. Auxins and cytokinins (CK) are two groups of plant hormones with highest impact on root development, but other phytohormones, such as abscisic acid, salicylic acid, gibberellins, brassinosteroids, jasmonic acid, ethylene or strigolactones, are also important, constituting a complex interplay (Malamy, 2005; Dun *et al.*, 2009; Orman-Ligeza *et al.*, 2013). Naturally occurring auxins, such as indol-3-acetic acid (IAA) or indol-3-butyric acid (IBA) are produced in the developing root meristem and promote cell division and elongation. CK are produced in the shoot and promote cell differentiation. They work as antagonists of auxin and inhibit formation of roots (Thimann and Skoog; 1933; Laplaze *et al.*, 2007; Ongaro *et al.*, 2008; Ramirez-Carvajal *et al.*, 2009; Shimizu-Sato *et al.*, 2009; Lavenus *et al.*, 2013).

The molecular regulatory mechanisms of root development in cereals have been intensively studied in rice, identifying role of many genes, transcription factors and phytohormones (reviewed by Meng *et al.*, 2019). The main genes and other factors involved in root development are shown in Figure 3.

Maintaining the balance between promotion and inhibition of root development is vital for plant growth and it is regulated by several genes associated with phytohormones. Genes affecting auxin signalling pathway *AUXIN RESPONSE FACTOR 12* (Os*ARF12*), *TRANSPORT INHIBITOR RESPONSE 1* (Os*TIR1*) and *AUXIN SIGNALLING F-BOX 2* (Os*AFB2*) play a role in elongation of primary and adventitious roots. Genes Os*TIR1* and Os*AFB2* encode auxin receptors, that bind AUXIN/INDOLE ACETIC ACID (A/IAA) regulatory protein (Bian *et al.*, 2012; Qi *et al.*, 2012). Os*IAA23*, gene of IAA family expressed in the centre cells of the root tip, is indispensable for development of primary, lateral, and crown roots. Knocking-out this gene resulted in plants without any crown roots, lateral roots and without root cap (Ni *et al.*, 2011). Two genes duplicates, *NARROW LEAF 2*, and *NARROW LEAF 3*, encode WUSCHEL-RELATED HOMEOBOX 3A (OsWOX3A), that through auxin signalling pathway mediates development of lateral roots (Cho *et al.*, 2013).

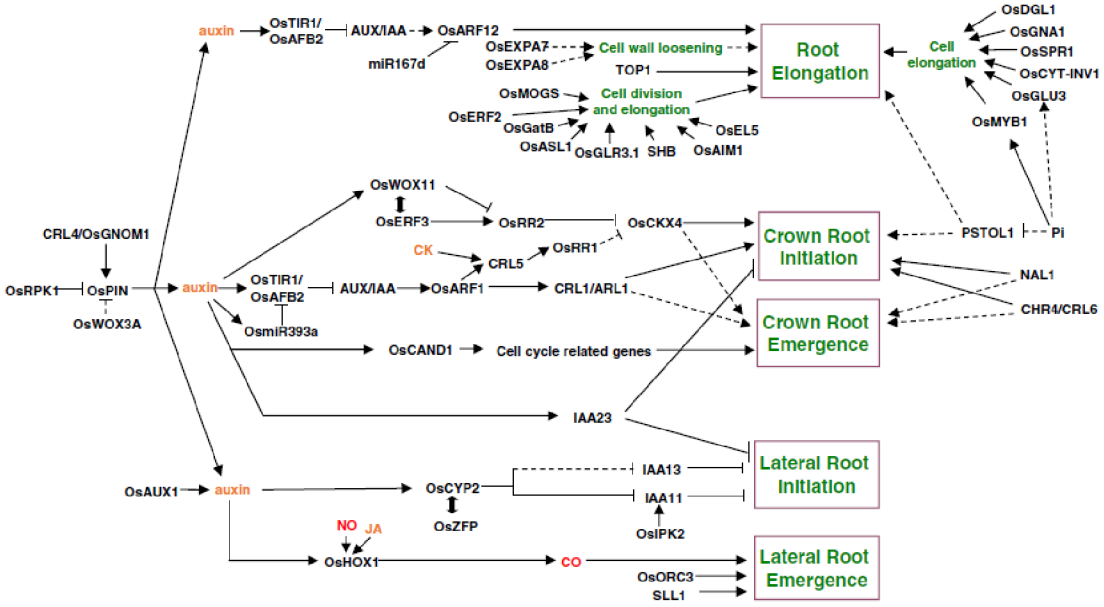

Figure 3: The molecular mechanisms involved in regulation of root development in rice. From: Meng *et al.*, 2019. Legend: colours code: black – genes or protein, yellow – phytohormones, red – signals, green – biological processes; positive regulatory actions are labelled with an arrow; flat head ending of lines represents a negative regulatory action; dashed lines indicates interaction yet not experimentally confirmed

Auxin is also related to crown root development. Plants with overexpressed gene Os*YUCCA1*, that plays a role in auxin biosynthesis, had higher levels of auxin and increased number of crown roots (Yamamoto *et al.*, 2007). Genes *NARROW LEAF 1* (*NL1*), *PIN-formed 1* (Os*PIN1*) and *CULLIN-ASSOCIATED AND NEDDYLATION-DISSOCIATED 1* (*CAND1*) promote crown root development. *NL1* encodes TRYPSIN-LIKE SERINE/CYSTEINE PROTEASE, Os*PIN1* encodes efflux carrier protein. Both products play a role in auxin transport. Os*CAND1* is associated with activity of UBIQUITIN LIGASE SCF^{TIR1}, that targets A/IAA protein (Feng *et al.*, 2004; Xu *et al.*, 2005; Wang *et al.*, 2011; Cho *et al.*, 2014). Gene *CRL4/OsGNOM1*, named either after crown rootless phenotype of mutans (*CRL4*) or after its product GUANINE NUCLEOTIDE EXCHANGE FACTOR OF THE ADP-RIBOSYLATION FACTOR G PROTEIN (Os*GNOM1*), mediates transport of polar auxin via efflux carrier proteins of the PIN1 family and is suggested to play a role in initiation of crown roots (Kitomi *et al.*, 2008; Liu *et al.*, 2009). Additionally, there is evidence, that *CROWN ROOTLESS 6*,

also called *CHROMATIN REMODELLING 4*, which encodes a helicase/ATPase and DNA-binding domain protein, have an effect on crown root development via signalling pathway of auxin (Zhao *et al.*, 2012; Wang *et al.*, 2016). Furthermore, gene *ADVENTITIOUS ROOTLESS 1/CROWN ROOTLESS 1* (Os*ARL1*/Os*CRL1*) encoding a LOB-domain transcription factor is a specific target of auxin response factor 1. Knocked-out allelic mutant *arl1* containing 20-bp deletion grew no adventitious root nor adventitious root primordia, mutant *crl1* with single amino acid mutation produced crown roots once in a while later on development. Promoter of Os*CRL1* is consisted of 2 auxin responsive elements, one is necessary for the gene expression in the base of the stem, associated with crown root emergence (Inukai *et al.*, 2005; Liu *et al.*, 2005).

Probably the most studied gene associated with cytokinin regulating development of crown root is WUSCHEL-related homeobox gene *OsWOX11*. The gene is mostly active in emerging crown roots and in dividing cells of the root meristem. Plants overexpressing Os*WOX11* have longer and bulkier crown roots, while loss-of-function of this gene results in lower number and significantly shorter roots. Os*WOX11* binds to the promoter of *Response Regulator 2* (*RR2*), responsive gene of cytokinin signalling that is expressed in the primordia of crown roots, and represses it. Even though during initiation of crown root development, OsERF3, an interacting protein of Os*WOX11*, regulates the expression of *RR2* positively, during crown root elongation, Os*WOX11* creates a complex with OsERF2 and represses *RR2* expression. OsWOX11 can also make a complex with ADA2-GCN5 histone acetyltransferase and regulate genes associated with crown root proliferation, including phytohormone response in root meristem, energy metabolism, and biosynthesis of cell wall (Zhao *et al.*, 2009, 2015; Zhou *et al.*, 2017).

Another two genes, *CROWN ROOTLESS 5* (*CRL5*) and *CYTOKININ OXIDASE/DEHYDROGENASE 4* (*OsCKX4*) play a role in crown root formation and development, via affecting cytokinin signalling pathway. *CRL5* encodes a transcription factor AP2/ERF. It has positive effect on *RESPONSE REGULATOR 1*, that represses cytokinin signalling, and also promotes auxin signalling to mediate crown root initiation. Os*CKX4* is a target of CK response regulators RR2 and RR3, but also target of auxin response factor OsARF25. Plants overexpressing Os*CKX4* have higher number of crown roots, but lower height (Kitomi *et al.*, 2011; Gao *et al.*, 2014).

Strigolactones and brassinosteroids are also important for initiation and development of crown roots, as mutated plants with dysfunctional biosynthesis of mentioned phytohormones develop less adventitious roots than wild type (Mori *et al.*, 2002; Arite *et al.*, 2012; Sun *et al.*, 2015). Root growth is promoted by transcription factor OsEIL1, that plays a part in ethylene signalling pathway (Mao *et al.*, 2006). Moreover, gene associated with biosynthesis of salicylic acid, Os*AIM1*, is responsible for accumulation of ROS and is another key player in root elongation (Xu *et al.*, 2017). Initiation of lateral roots is controlled by jasmonic acid through regulating HEME OXYGENASE 1, an enzyme needed for producing carbon monoxide (Hsu *et al.*, 2012). Additionally, abscisic acid with polyethylene glycol and salt enhances expression of basic helix-loop-helix transcription factor OsbHLH120. This transcription factor is a product of quantitative trait loci *qRT9*, that affects root length and thickness (Li *et al.*, 2015).

Root development is a complex process. Except for genes involved in signalling pathways of phytohormones, factors associated with biosynthesis of cell wall (Os*EXPANSION*, Os*GLU3*), biosynthesis of UDP-N-acetylglucosamine (Os*GNA1*), ubiquitin E3 ligase (OsEL5), cell division (Os*GLR3.1*), DNA replication (Os*OEC3*), biosynthesis of arginine (OsASL1), and fatty acid desaturation (*SLL1*) are required for normal, flawless root development (Jiang *et al.*, 2005; Li *et al.*, 2006; Koiwai *et al.*, 2007; Zhang *et al.*, 2012; Chen *et al.*, 2013; Shelley *et al.*, 2013; Wang *et al.*, 2014b; Xia *et al.*, 2014).

Important roles in root development and elongation also play genes that are involved in sugar metabolism and sugar-based modification of proteins. A 48 kDa subunit precursor of DOLICHYL DIPHOSPHOOLIGOSACCHARIDE-PROTEIN GLYCOSYL-TRANSFERASE, encoded by Os*DGL1*, function with association of Oligosacharyltransferase complex. A mutation in Os*DGL1* affected root cells, which were either shorter or dead, and also degreased the size of root meristems. These alternations were cause by defective N-glycosylation in the root (Qin *et al.*, 2013). Gene Os*CYT-INV1*, that encodes alkaline/neutral invertase, is another key player in regulation of root growth. Mutation in this gene caused plants to have shorter roots, lower level of hexose, and increased amount of sucrose. Wild-type phenotype could be re-gained after supply of glucose (Jia *et al.*, 2008). Additionally, Mannosyl-oligosaccharide glucosidase regulates root elongation through N-glycan maturation (Wang *et al.*, 2014a).

3.4 Root growth angle

Growth angle of roots is largely affected by gravitropism response through hoarding of statoliths, specific type of plastids containing starch, in gravity sensitive cells called statocytes. Gravity signal transduction complex transpositions auxin efflux carrier proteins PIN2 and PIN3 to lower membrane of the statocytes, which results in asymmetric accumulation of auxin at downward side of a root tip and sedimentation of statoliths at the bottom of a root. Gradient of auxin regulates genes responsible for elongation of cells at the root tip and as a result of unequal distribution of auxin, cells at the lower side elongate faster and root tip bends downward towards the gravitational force (Boonsirichai *et al.*, 2003; Morita *et* Tasaka, 2004; Abas *et al*., 2006; Lucas *et al.*, 2008; Morita, 2010).

Recently, Uga *et al.* (2011) identified a major QTL on chromosome 9 in rice (*Oryza sativa* L.) named *DEEPER ROOTING 1* (Os*DRO1*), that was involved in control of root growth angle. Os*DRO1* encodes 2 putative N-myristoylation sites associated with lipid modification in plasma membrane and is mostly expressed in root meristem. It is associated with elongation of cells in root tips, downward growth of roots, and, as name hints, deeper rooting. Os*DRO1* is "early-auxin-response" gene, controlled by ARF. Auxin also works as negative regulator of Os*DRO1*. Introducing Os*DRO1* into near isogenic line IR64 with shallow root system resulted in deeper roots, higher grain yield and better photosynthesis under drought condition. Nor shoots or roots biomass was decreased, suggesting, that Os*DRO1* plays a role only in control of growth angle of root, and not in development of upper parts of plant. Os*DRO1* is promising QTL to focus on for breeders, as it promotes drought avoidance and does not affect other aspects of growth (Uga *et al.*, 2013). Moreover, homolog of Os*DRO1*, *SOIL SURFACE ROOTING 1 (qSOR1*), was found to improve yield of rice under saline conditions. Plants with loss-of-function allele qsor1 grew shallower roots on the surface of soil and therefore were able to avoid stress from saline paddy soils (Kitomi *et al.*, 2020).

3.5 Breeding methods used in agriculture

Researchers worldwide study traits associated with the yield of crops, as growing population worldwide puts higher demands on production of food. In classical breeding programs, marker-assisted selection (MAS) is a technique used to assist in the selection of desirable traits in plants based on molecular markers, such as SNPs, simple sequence repeats (SSRs), and amplified fragment length polymorphisms (AFLPs). MAS involves the use of these markers to considerably accelerate the breeding process by improving selection accuracy, and enabling the selection of traits that are difficult to evaluate directly (Hasan *et al.*, 2021).

Two most commonly used methods in molecular plant biology to produce adjusted plants are RNA interference (RNAi) and very recently discovered CRISPR/Cas9. RNAi is a natural process that involves the silencing of specific genes by small RNA molecules, known as small interfering RNAs (siRNAs) or microRNAs (miRNAs). These small RNA molecules can specifically bind to messenger RNAs, which are the templates for protein synthesis, and trigger their degradation or inhibit their translation, resulting in reduced expression of the targeted genes. The gene silencing mechanism has significant implications in agriculture research as it can be used to study role of genes by selectively silencing them, which is helpful in studies where the gene of interest plays a vital role and complete knock-out would be lethal. It can also reduce disease severity and incidence by improving resistance of plants to viruses, bacteria, fungi, and other pathogens. RNAi inhibits the replication and spread of pathogens in organism by expressing siRNAs that specifically target and degrade viral or pathogen-derived mRNAs. This approach can help reduce the reliance on chemical pesticides and contribute to the development of disease-resistant crops (Fire *et al.*, 1998; Wilson & Doudna, 2013; Sherman *et al.*, 2015; Rosa *et al.*, 2018).

The newest method used in agriculture and breeding is CRISPR/Cas9. It is a revolutionary gene editing tool used in genetic engineering to selectively modify DNA sequences within an organism's genome. It is a system that is adapted from the natural defence mechanism found in bacteria against viral infections. The CRISPR/Cas9 system consists of two main components: the Clustered Regularly Interspaced Short Palindromic Repeats (CRISPR), which are specific DNA sequences found in the bacterial genome, and the CRISPR-associated (Cas) proteins, which are enzymes that

can cut DNA. Cas9 protein is consisted of two nuclease domains, PAM interacting site and nuclear localisation signal enabling transport of the protein into a nucleus. By combining Cas9 protein with designed guide RNA (gRNA), a small RNA molecule that carries a specific sequence that matches the target DNA site to be edited and consists of a scaffold sequence (scaffold RNA) that creates secondary structure that can bind to Cas9 protein, is created functional CRISPR/Cas9 construct that could be introduced into the target cells. Complex searches in the genome of the cell for the target DNA sequence and binds to it through base pairing mechanism between gRNA and the target DNA. It is important to mention protospacer-adjacent motif (PAM) that is recognised by PAM interacting site of Cas9 and is essential for successful editing as Cas9 usually makes double-stranded break (DSB) 3 nucleotide upstream of PAM sequence. The cell's natural DNA repair mechanisms then activates, trying to repair the DSB. There are two main repair pathways: non-homologous end joining (NHEJ) and homology-directed repair (HDR). NHEJ is an error-prone repair pathway that often results in small insertions or deletions (indels) at the site of the DSB, leading to gene disruptions or knockouts. HDR is a more precise repair pathway that needs a template in order to work. By providing specific sequence as the template within the gRNA, CRISPR/Cas9 can also be used for knock-in (Fischer *et al.*, 2012; Doudna & Charpentier, 2014; Nishimasu *et al.*, 2014; Bortesi & Fischer, 2015; Kumar *et al.*, 2019).

In agriculture and breeding, CRISPR/Cas9 has the potential to revolutionize the way we produce food by allowing us to create crops and livestock that are more resistant to diseases, pests, and environmental stressors, as well as produce more nutritious and healthier foods. By targeting specific genes in the plant's DNA, plants that are naturally resistant to diseases and pests can be created, reducing the need for harmful pesticides and herbicides. This could help to reduce the environmental impact of agriculture and make food production more sustainable. Another way CRISPR/Cas9 can be used in agriculture is to create crops that are more tolerant to environmental stressors, such as drought, heat, and cold. By editing the genes that control a plant's response to these stressors, such as DRO1, crops that are better able to survive in harsh conditions can be produced, hence improving food security in regions with challenging climates. In breeding, CRISPR/Cas9 can be used to introduce desirable traits into livestock and crops more quickly and with greater precision than traditional breeding methods. This

could lead to the development of healthier, more productive livestock and crops that require fewer resources to grow (Nadolska-Orczyk *et al*., 2017; Kumar *et al*., 2019).

However, due to regulation approved by the Court of Justice of the European Union from 25th of July 2018, that "classified genome-edited plants as genetically modified organisms (GMO) and thus subjected them to prohibitive premarket risk evaluations" (Urnov *et al.*, 2018), mutagenesis and new breeding techniques, including CRISPR/Cas9, can be used in laboratory for the purpose of scientific research only (Vives-Vallés & Collonnier C, 2020; Van Der Meer *et al.*, 2023).

4 MATERIALS AND METHODS

4.1 Biological material

- Grains of barley (*Hordeum vulgare*, L.)
  - cultivar Golden promise, generation 1 DH 1−6, harvested on 17. 7. 2020
  - cultivar Maythorpe
  - *Hordeum vulgare* L. convar. *distichon* (L.), a Greek landrace registered under the accession number HOR1122 (internal number: 181) in the barley collection stored at the Leibniz Institute of Plant Genetics and Crop Plant Research, Gatersleben, Germany
- Chemical competent *Escherichia coli* TOP10 (New England BioLabs, cat. n. C3019)
- Electrocompetent *Agrobacterium tumefaciens* strain AGL1 (John Innes centre)

4.2 Chemicals, kits, and solutions

Chemicals

- 1-Naphthaleneacetic acid (NAA) (Sigma-Aldrich, cat. n. N0640)
- 5X Green GoTaq® Reaction Buffer (Promega, cat. n. M791A)
- 96−100% ethanol (Lach-Ner, cat. n. 20025-A96)
- Agar powder (Himedia, cat. n. GRM026)
- Agarose (Sigma-Aldrich, A9539)
- *Bsa*I_HF® Restriction Enzyme (New England BioLabs, cat. n. R3733S)
- Carbenicillin Disodium (Duchefa Biochemie, cat. n. C0109)
- Chloroform:Isoamyl alcohol 24:1 (Sigma-Aldrich, cat. n. C0549)
- DNase Reaction Buffer 10X (Invitrogen, cat. n. AM2239)
- dNTP Mix (10 mmol·dm^{-3} each) (Promega, cat. n. U1511)
- GeneRuler 1kb Plus DNA ladder (ThermoFisher Scientific, cat. n. SM1331)
- GoTaq® DNA Polymerase (Promega, cat. n. M300A)
- *Hind*III_HF® Restriction Enzyme (New England BioLabs, cat. n. R3104S)
- Kanamycin Sulphate Monohydrate (Duchefa Biochemie, cat. n. K0126)
- *Kpn*I_HF® Restriction Enzyme (New England BioLabs, cat. n. R3142S)
- Kristalon™ Start (AGRO CS a.s.)
- Luna® Universal qPCR Master Mix (New England BioLabs, cat. n. M3003L)

- MES Monohydrate (Duchefa Biochemie, cat. n. M1503)
- Murashige & Skoog basal salt mixture medium (Duchefa Biochemie, cat. n. M0221)
- Naptalam (NPA) (Sigma-Aldrich, cat. n. 33371)
- *Not*I_HF® Restriction Enzyme (New England BioLabs, cat. n. R3189S)
- Purple Loading Dye 6X (New England BioLabs, cat. n. B7024S)
- rCutSmart™ buffer (New England BioLabs, cat. n. B6004S)
- Rifampicin (Duchefa Biochemie, cat. n. R0146)
- *Sfi*I Restriction Enzyme (New England BioLabs, cat. n. R0123S)
- Sodium hypochlorite 12% (VWR chemicals, cat. n. 301696S)
- Spectinomycin HCl Pentahydrate (Duchefa Biochemie, cat. n. S0188)
- T4-DNA Ligase (5 $U \cdot \mu L^{-1}$) (ThermoFisher Scientific, cat. n. EL0014)
- T4-DNA-ligase buffer 10X (ThermoFisher Scientific, cat. n. B69)
- TURBO™ DNase (2 $U \cdot \mu L^{-1}$) (Invitrogen, cat. n. AM2239)
- Tween® 20 (Sigma-Aldrich, cat. n. P1379)
- UltraPure™ Ethidium Bromide, 10 $g \cdot dm^{-3}$ (ThermoFisher Scientific, cat. n. 15585011)

Kits

- LunaScript® RT SuperMix Kit (New England BioLabs, cat. n. E3010L)
- NucleoSpin Gel and PCR Clean Up (Macherey-Nagel, cat. n. 740609)
- NucleoSpin® Plasmid (Machery-Nagel, cat. n. 740588)
- NucleoSpin® Plasmid/Plasmid (NoLid) (Machery-Nagel, cat. n. 740499)
- QIAprep® Spin Miniprep Kit (Qiagen, cat. n. 27104)
- Quick-RNA™ Plant Miniprep Kit (Zymo Research, cat. n. R2024)

Solutions

50x TAE (Tris-Acetate-EDTA): 242 g Tris base dilute in 800 ml dH_2O, add 57,1 ml acetate acid and 100 ml 0,5 $mmol \cdot dm^{-3}$ EDTA (pH 8.0), fill with dH_2O up to 1 000 ml.

Extraction buffer for DNA isolation: 200 $mmol \cdot dm^{-3}$ Tris-HCl (pH 8); 250 $mmol \cdot dm^{-3}$ NaCl; 20 $mmol \cdot dm^{-3}$ EDTA (pH 8).

Luria-Bertani medium (LB): 15,5 g LB; 9,5 g NaCl; fill with dH_2O up to 1 000 ml (pH 7.0). For solid medium add 15 g of agar.

MG/L medium (1 l): 250 mg KH_2PO_4; 100 mg NaCl; 100 mg $MgSO_4 \cdot 7\ H_2O$; 1 g L-glutamic acid; 5 g mannitol; 5 g tryptone; 2,5 g yeast extract; fill with dH_2O up to 1 000 ml (pH 7.0). Autoclave, add 0,1 g biotin. For solid medium: 12 g agar was added.

Murashige & Skoog medium (MS): 2,2 g Murashige & Skoog basal salt mixture medium; 10 g saccharose; 1 g MES monohydrate; 6 g agar powder; fill to 1 000 ml dH_2O (pH 5.8).

Plasmid isolation from *Agrobacterium tumefaciens*:

Lysis buffer: 25 $mmol \cdot dm^{-3}$ Tris/HCl (8.0); 10 $mmol \cdot dm^{-3}$ EDTA(pH 8.0); 50 $mmol \cdot dm^{-3}$ glucose; lysozyme 50 $g \cdot dm^{-3}$ in dH_2O.

Wash buffer: NaCl (1 $mol \cdot dm^{-3}$) in dH_2O.

SOC medium: 0,5% yeast extract; 2% tryptone; 10 $mmol \cdot dm^{-3}$ NaCl; 2,5 $mmol \cdot dm^{-3}$ KCl; 10 $mmol \cdot dm^{-3}$ $MgCl_2$; 10 $mmol \cdot dm^{-3}$ $MgSO_4$; 20 $mmol \cdot dm^{-3}$ glucose in dH_2O.

4.3 Vectors

- p6i-2x35S-TE9, binary vector used for barley immature embryo transformation (DNA-Cloning-Service; Leipzig, Germany)
- pSH91, vector used to express *in planta* Cas9 and the gRNA scaffold (Budhagatapalli *et al.*, 2016)

4.4 Equipment

- Analytic scales PX2244 (Ohaus)
- Axio Zoom v16 Stereo Microscope (Zeiss)
- Centrifuge Combi-spin PCV-2400 (Grant-bio Instruments^{TM})
- Centrifuge NF 400 (Nüve)
- Plant growth chamber E-41L2 (CLF Plant Climatics)
- Electrophoretic chamber for horizontal electrophoresis (Biometra)
- Electroporation system ECM399 (BTX)
- Environmental chamber MLR 351 (Sanyo)
- Gel Doc^{TM} EZ Imager (Bio Rad)

- Ice Flaker AF 80 (Scotsman)
- Incu-Shaker mini (Benchmark)
- Laminar box FlowFAST H18 (Faster S. r. l.)
- Laminar flow box Merci® TCS 2 (MERCI®)
- Magnetic stirrer IKA RCT basic (IKA)
- Microcentrifuge Model 16K (Bio Rad)
- MicroCentrifuge ScanSpeed 1730R (Labogene)
- Mix mill MM 400 (Retsch)
- NanoDrop One^{C} UV-Vis spectrophotometer (Thermo Fisher Scientific)
- Orbital incubator SI600C (Stuart)
- pH Checker® edge (Hanna instruments)
- Real time PCR QuantStudio 7 Pro (Applied Biosystems)
- Scanning system Epson Perfection V700 Photo (Epson)
- Spectrophotometer 8453 deuterium (Agilent Technologies)
- Standard Power Supply P25 (Biometra)
- Thermal cycler Biometra TAdvanced 384 G (Analytik Jena)
- Thermal cycler Veriti 9901 (Applied Biosystems)
- Thermocell Coolings&Heating block CHB-202 (Bioer)
- Ultra-Low Temperature Freezer MDF-U500VX (Panasonic)

4.5 Methods

4.5.1 Identification of putative homologs of rice genes in barley

Sequences of rice genes associated with root system architecture Os*DRO1* (Os09g0439800) (Uga *et al.*, 2013) and *qSOR1/DRL1* (Os07g0614400; DRO1-like/DRL), Os*DRL2* (Os03g0180600) and Os*DRL3* (Os03g0406300) (Kitomi *et al.*, 2020) were retrieved from the Rice Annotation Project database (RAP-DB, https://rapdb.dna.affrc.go.jp/) and used as query to search by blast homologous sequences in the genome of barley using the IPK Galaxy Blast Suite (https://galaxy-web.ipk-gatersleben.de/). The NCBI BLAST + blastn was run with default parameters against the Nucleotide BLAST two databases: of "Barley all CDS Morex v.3 (Jul 2020)" and "Barley cv. Golden Promise CDS (Jul 2018)". For further work were selected genes Horvu.Morex.r3.5HG0480470 (highest similarity with Os*DRO1*) and Horvu.Morex.r3.2HG0125600 (highest similarity with q*SOR/DRL1*).

4.5.2 Plant cultivation

4.5.2.1 *In vitro* root angle determination

Under the flow box, grains of different barley accessions (Golden Promise, Maythorpe and HOR1122) were surface sterilized with 70% EtOH for 30 sec, rinsed with dH_2O, then 5 min in 7% hypochlorite with Tween 20 with constant shaking. In the end grains were repeatedly washed with dH_2O. Embryo facing downward grains were placed into Petri dish containing 250 ml ½ MS medium (pH 5.8) along a middle line. Plate was sealed with 2 layers of parafilm, covered in aluminium foil and vernalized at 4 °C for 2 days. After 2 days, the plates with grains were transferred to phytotron with following conditions: 16 hours day, 19 °C; 8 hours night, 15 °C. Plates were standing vertically. After 5 days, the aluminium foil covering upper part of plant was removed, while root system remained covered, and plants were grown for another 10 days.

At the end of the growing period, plates were scanned with a flatted scanner Epson at a 300-dpi resolution and default parameters. Pictures were saved as .tif and analysed with ImageJ/Fiji software (Shindelin *et al.*, 2012; Schneider *et al.*, 2012). Contrasted root angles have been measured between the two outmost right and left roots, 3 cm under the junction of roots and shoots.

4.5.2.2 Crown root inducible system

4.5.2.2.1 Mini-hydroponic cultivation

Grains of different barley cv. Golden Promise and cv. Maythorpe were surface sterilized under the flow box in 70% EtOH for 30 sec, rinsed with dH_20 and then 5 min with 7% hypochlorite with Tween 20 with constant shaking. Finally, grains were thoroughly washed with dH_2O andthen put to Petri dish with filter paper wetted with 25 ml of dH_2O containing NPA (50 µmol·dm^{-3}) (inhibitor of polar auxin transport). Plates were wrapped in aluminium foil and vernalized for 48 hours at 4 °C. After 2 days, aluminium foil was removed and plates were transferred to phytotron with conditions as follow: 16 hours day, 19 °C; 8 hours night, 15 °C. After 7 days in phytotron, plants were transferred to mini-hydropony (Fig. 4) with 50 µmol·dm^{-3} NPA in dH_2O with 1 g·dm^{-3} of Kristalon solution. After 72 hours, 5 plants were harvested (as T0-days sample): roots, crown and leaves were separated with a razor blade, immediately flash frozen in liquid nitrogen, and stored in a deep freezer at -80 °C until further use. Solution was changed for 1-NAA (50 µmol·dm^{-3}) in dH_2O with 1 g·dm^{-3} of Kristalon. After 48 hours, another 5 plants were harvested as T2-days, solution was changed for Kristalon (1 g·dm^{-3}) in dH_2O. Five plants were harvested after 72 hours from T0 (sample T3-days), 96 hours (sample T4-days), and after 168 hours (sample T7-days). The plants were regularly monitored to observe first occurrence of crown roots. The time scheme of kinetics and cultivation is in Figure 5.

With the kind help of Nguyễn Diệu Thu (M.Sc) picture of emerging crown roots was taken via Axio Zoom v16 Stereo Microscope (Zeiss).

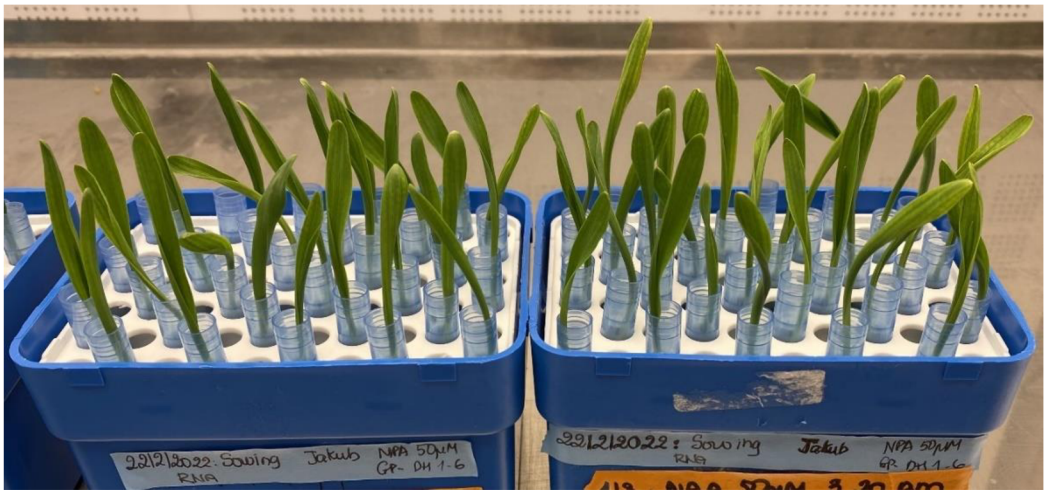

Figure 4: Home-made mini-hydropony used in this work.

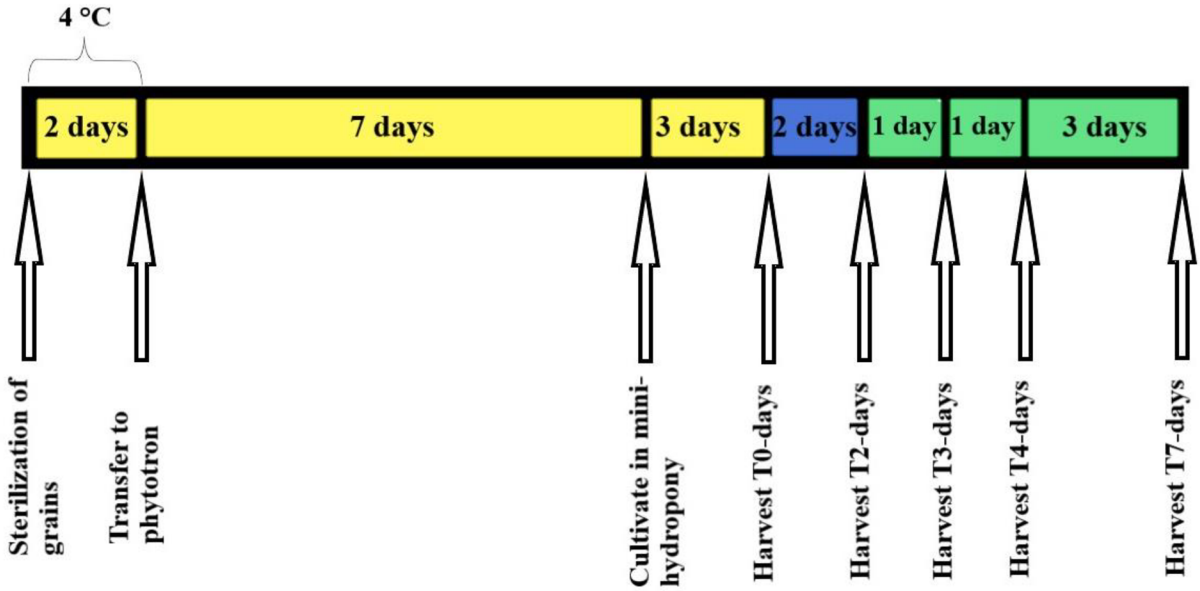

Figure 5: Time scheme of mini-hydropony cultivation. Legend: (yellow colour): 50 µmol·dm^{-3} NPA treatment; (blue colour): 50 µmol·dm^{-3} 1-NAA treatment; (green colour): no treatment.

4.5.2.2.2 RNA isolation, removal of gDNA, and cDNA synthesis

RNA was isolated by Quick-RNA™ Plant Miniprep Kit following the manufacturer's instructions, with a change of grinding frozen samples by pestle in mortar with liquid nitrogen and adding RNA Lysis Buffer to already grinded sample (not via ZR Bashing Bead™ Lysis Tube).

Genomic DNA was removed by adding DNase Reaction Buffer 10X: 0,1 volume of sample, and 1 µl TURBO™ DNase (2 U·µL^{-1}). Substances were mixed gently and incubated 30 min in 37 °C while shaking. Then was added LiCl, ½ volume of sample, and let in −20 °C for 30 min. Tube was centrifuged at 13 000 rpm for 15 min at 4 °C. Supernatant was discarded, pellet rinsed with 500 µl 70% EtOH. Sample was centrifuged 10 min at 13 000 rpm at 4 °C. Supernatant was again discarded and pellet washed with 96% EtOH (500 µl). Tube was centrifuged at 13 000 rpm at 4 °C for 10 min. Pellet was let to dry 10 min and then dissolved in 50 µl of RNA-free H_2O. Concentration was quantified by NanoDrop.

To validate the absence of gDNA contamination, PCR on RNA was performed with primers amplifying *TIP41* gene. PCR reaction mix was prepared (Tab. 1). Settings of a reaction are in Table 2. PCR products were separated by electrophoresis on

1% agarose gel prepared in 1X TAE and containing EtBr. Electrophoresis was run for 45 min at 90 V. In case of gDNA contamination, a fragment of ± 500 bp long would be expected.

Synthesis of cDNA was performed in a 20 µl-reaction containing 2 µg of total RNA and following the protocol of LunaScript® RT Super Mix kit. Samples were then purified via NucleoSpin Gel and PCR Clean Up and eluted in 100 µl dH_2O.

With all purified cDNA samples was performed PCR to validate the efficiency of cDNA synthesis. PCR reaction mix was prepared (Tab. 1), conditions of the reaction are in Table 2. PCR products were separated by electrophoresis on 1% agarose gel prepared in 1X TAE and containing EtBr. Electrophoresis was run for 45 min at 90 V.

Table 1: PCR reaction mix.

Substance	**Stock solution concentration**	**Final concentration**	**Volume [µl]** (1 reaction)
5X Green GoTaq® Reaction Buffer	5X	1X	2
qTIP41 forward*	10 µmol·dm^{-3}	0,2 µmol·dm^{-3}	0,2
qTIP41 reverse*	10 µmol·dm^{-3}	0,2 µmol·dm^{-3}	0,2
dNTP Mix	10 mmol·dm^{-3}	0,2 mmol·dm^{-3}	0,2
GoTaq® DNA Polymerase	5 U·reaction^{-1}	0,05 U·reaction^{-1}	0,1
Sample**			1
Nuclease-free water			6,3

* sequences in Table 21
** RNA, or cDNA

Table 2: Condition of PCR reaction.

Process	**Temperature [°C]**	**Time [s]**	**Number of cycles**
Initial denaturation	95	120	1
Denaturation	95	30	35
Primers annealing	58	30	
Elongation	72	30	
Final elongation	72	300	1

4.5.2.2.3 Real-Time quantitative PCR

Analysis of gene expression was performed by qPCR using the Luna® Universal qPCR Master Mix (NEB). The 10 µl reaction contained 1X reaction buffer, forward and reverse primer (final concentration 0,25 µmol·dm^{-3}), and 1 µl of cDNA diluted to 1/5 (Tab. 3). For analysis were selected specific primers for genes Hv*ACTIN*, Hv*5439,* Hv*EIF512*, and Hv*20934* and primers designed on Primer3Plus for Hv*DRO1* and Hv*DRL1* genes (Tab. 4). To each well of 96-well plate was put 9 µl of reaction mix with corresponding primers and 1 µl of cDNA sample in three technical replicates. For measurement of expression of Hv*DRO1* and Hv*DRL1* genes were used cDNAs of crown samples: T0-days, T2-days, T3-days, T4-days, and T7-days. To set efficiency of primers and select reference genes, cDNA samples T3-days of Golden promise and Maythorpe were mixed (10 µl each) and diluted to final ratio 1/5, 1/20, 1/50 and 1/200. Quantitative PCR was performed in Real time PCR QuantStudio 7 Pro cycler (Applied Biosystems) with specific conditions (Tab. 5). After amplification, a melting curve was obtained to validate the specificity of the amplified product.

Measured Ct values of diluted samples were used to calculate efficiency (E) based on equation: $E = 10^{(-1/slope)}$. As slope value was put "a" from regression equation y = ax + b. Relative expression was determined based on the efficiency-corrected ΔΔCt method described by Pfaffl (2001).

Table 3: Reaction mix for qPCR.

Substance	**Stock solution concentration**	**Final concentration**	**Volume [µl]** (1 reaction)
Luna® Universal qPCR Master Mix	2X	1X	5
Forward primer*	10 µmol·dm^{-3}	0,25 µmol·dm^{-3}	0,25
Reverse primer*	10 µmol·dm^{-3}	0,25 µmol·dm^{-3}	0,25
Nuclease-free water			3,5

* sequences are in Table 4.

Table 4: List of used primers for qPCR

Name	Sequence 5´–3´
HvACT_fwd	TTGACCTCCAAAGGAAGCTATTCT
HvACT_rev	GGTGCAAGACCTGCTGTTGA
Hv5439_fwd	GATTGAGGTGGAGAGGGTATTG
Hv5439_rev	CTCCTGGTCTGTTAGCAGTTT
HvEIF512_fwd	TTGACCCTCCAGTGGAGAGGGT
HvEIF512_rev	TGGACAACTTGCTGTTCCTCCA
Hv20934_fwd	ATTTTGCGCCCGAACATGTTC
Hv20934_rev	GATCATACGGTGTGCTAGCAGG
qDRO1_fwd	ACACCCGCAAAATTCTTCGG
qDRO1_rev	ACCCATTTTGCGCCATCATC
qDRL1_fwd	TGACACGCAGATCATACTCAGC
qDRL1_rev	AGGCGAACATGTTCTTGAGG

* if not mentioned otherwise, primers were borrowed from colleges

Table 5: Condition of qPCR reaction.

Process	Temperature [°C]	Time [s]	Number of cycles
Initial hold	25	600	1
Initial denaturation	95	600	
Denaturation	95	15	40
Primers annealing	60	60	

4.5.3 Mediated gene knock-out by CRISPR/Cas^9

4.5.3.1 Design of guide RNA (gRNA)

For both Hv*DRL1* and Hv*DRO1*, guide RNAs were designed with the on-line available CRISPOR tool (http://crispor.tefor.net/; Concordet *et al.*, 2018), using the defaults parameters and the reference genome annotated *Hordeum vulgare* subsp. *vulgare*_two-rowed barley/NCBI_GCA_904849725.1 (MorexV3_pseudomolecules_assembly) for off-target prediction.

For each genes, 2 guide RNAs (DRO1 and DRO2 for Hv*DRO1* gene, and DRL1 and DRL2 for Hv*DRL1* gene) were selected considering several criteria: i) gRNAs starting with adenine or guanin were selected, because the expression of gRNA fused to its scaffold is driven by the OsU3 Pol III promoters of small nuclear RNA (snRNA) gene that is selective for these two bases. Additionally, gRNAs with thymine at the 3rd position of PAM (TGG) sequence were omitted. Finally, the length did not exceed 20 nucleotides and the gRNA was selected upstream of functional domain of gene.

The sequence of gRNA in connection of scaffold RNA (scRNA) (Tab. 6) was designed to form specific secondary structure including 3 loops in tail section, one additional loop with 2 "antennas" and unbonded gRNA (Fig. 6). For visualisation of secondary structure was used RNAfold webserver (http://rna.tbi.univie.ac.at/cgi-bin/RNAWebSuite/RNAfold.cgi).

Forward (F) and reverse (R) oligonucleotides matching the sequence of designed gRNA were ordered, with addition of specific overhang at the 5´-end corresponding with restriction site of *Bsa*I restriction enzyme to allow cloning of gRNA into the pSH91 vector. Sequence at 5´-end of the forward oligonucleotide was `GGCG`, sequence of reverse oligonucleotide was `AAAC` (Tab. 6).

Primers were ordered from Sigma-Aldrich, diluted in water at the 100 µM. To form the double-strand gRNAs, oligonucleotides were mixed to equimolar concentration (2 µM final) in the presence of 1X T4 DNA ligase buffer and placed in a thermocycler to perform annealing as followed: 95°C in 4 minutes, 70 °C in 10 minutes, from 70 °C, ramp-down to 4 °C at 1 °C/min (66 cycles).

Table 6: Sequence of scaffold RNA and gRNA oligonucleotides.

Name	Sequence 5´–3´	Position [bp]
Scaffold RNA	GTTTTAGAGCTAGAAATAGCAAGTTAAAATAAGGCT-AGTCCGTTATCAACTTGAAAAAGTGGCACCGAGTCGGTGC	
DRL1_F	GGCGATGCTCTCCATCGGAACCCT	180
DRL1_R	AAACAGGGTTCCGATGGAGAGCAT	200
DRL2_F	GGCGAACTGCCCCTCCAGCCTCG	386
DRL2_R	AAACCGAGGCTGGAGGGGCAGTT	405
DRO1_F	GGCGAAGGCCCGGAGGAACGTGC	61
DRO1_R	AAACGCACGTTCCTCCGGGCCTT	80
DRO2_F	GGCGATGGTCATAAGTAAGGGAA	425
DRO2_R	AAACTTCCCTTACTTATGACCAT	444

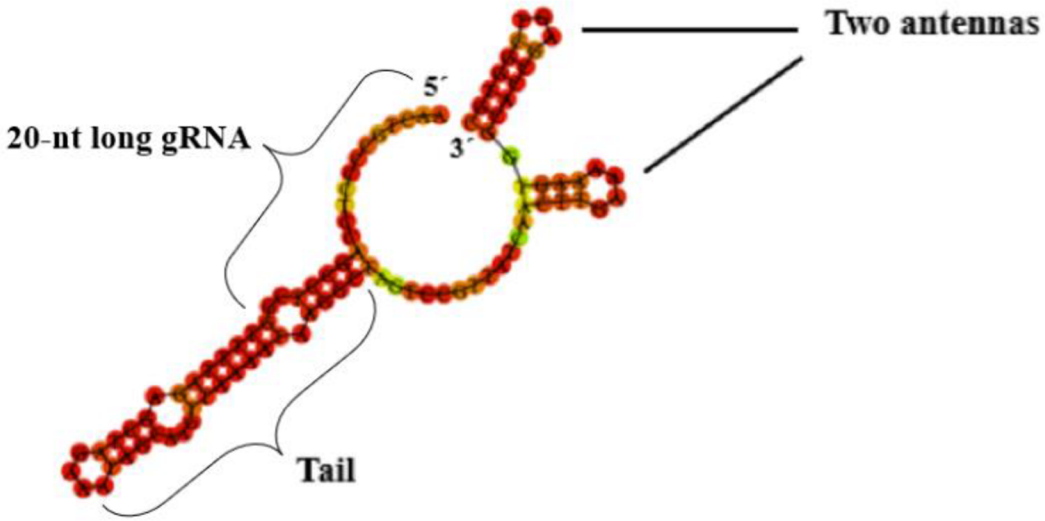

Figure 6: Secondary structure of gRNA with scaffold RNA.

4.5.3.2 Insertion of gRNA oligonucleotide duplex into pSH91 vector

The cloning vector pSH91 (Fig. 7) is 12 198 bp long plasmid, that contains all the required features for construction of CRISPR/Cas9 construct, such as ORF for Cas9, that is under strong promotor, or scaffold RNA, that fusions with cloned gRNA oligonucleotide duplex. It also contains cleavage sites for restriction enzymes to allow cloning and genes encoding resistance to antibiotics to allow selection of transformants.

The plasmid pSH91 was isolated from *Escherichia coli* TOP10 culture grown at 37°C overnight in LB medium containing Kanamycin (50 ml·dm^{-3}), using QIAprep® Spin

Miniprep Kit and following the protocol of manufacturer. The concentration and quality of the plasmid preparation were measured by NanoDrop.

Two µg of the isolated plasmid were digested by *Bsa*I HF restriction enzyme by gently mixing and spinning down (1 min) reagents (Tab. 7), and incubating for 2 hours at 37 °C.

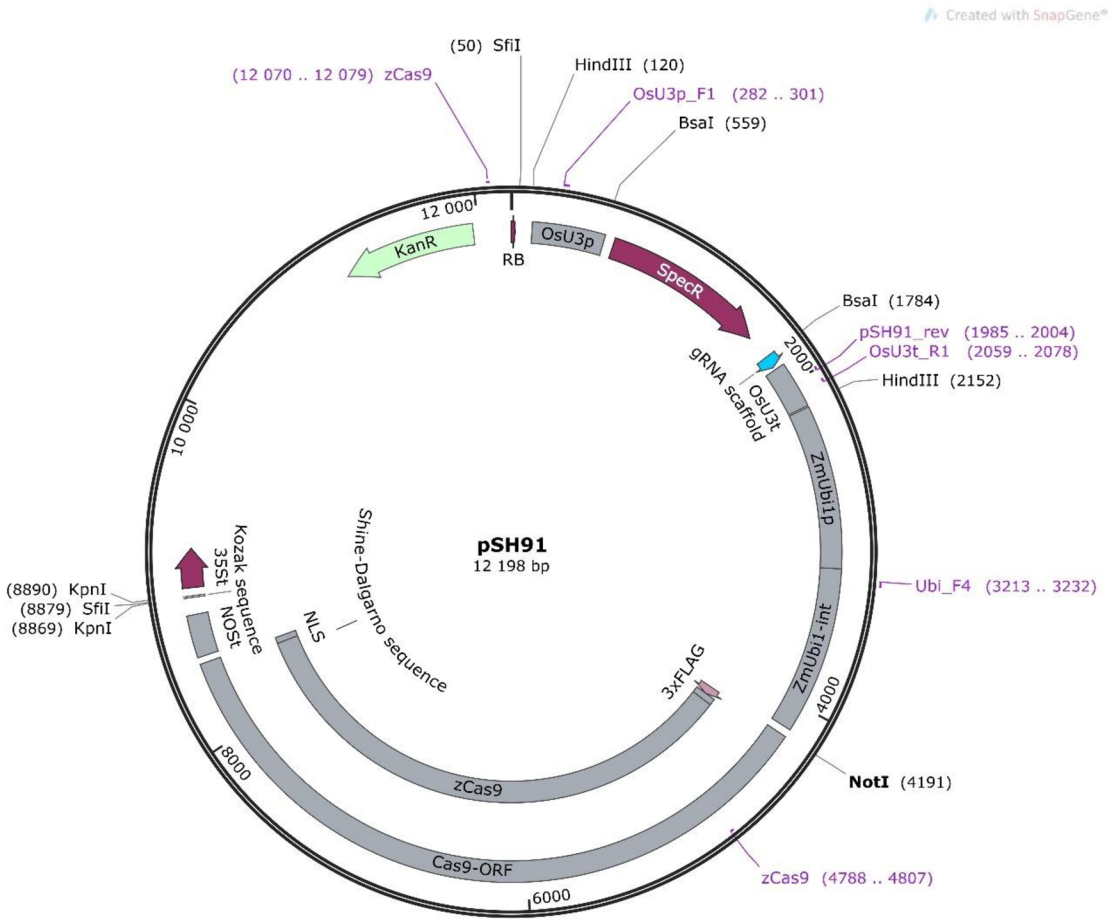

Figure 7: Map of the vector pSH91 created in SnapGene. Legend: (KanR): gene of resistance to Kanamycin; (SpecR): gene of resistance to Spectinomycin; (OsU3p/t): rice snRNA U3 promoter/terminator; (ZmUbi1p/int): maize Ubiquitin 1 promoter/first intron; (zCas9): optimized version of Cas9, (NOSt): nopaline synthase terminator; (35St): 35S terminator. Text outside of circle: in black – binding sites of restriction enzymes; in blue – binding sites of primers.

The digested plasmid was purified on column using the NucleoSpin Gel and PCR Clean Up kit, following the protocol of manufacturer. The concentration was quantified by NanoDrop, and the restriction was validated by electrophoresis on 1% agarose gel in 1X TAE containing ethidium bromide (EtBr).

The vector pSH91 contains two restriction sites for *Bsa*I HF, that borders resistance to Spectinomycin. Digestion by this enzyme created linear product 10 973 bp long (removed 1 225 bp long part with Spectinomycin resistance), that was ligated with prepared gRNA oligonucleotide duplex by gently mixing reagents (Tab. 8) and incubating overnight in 16 °C.

Table 7: Reagents for cleavage of pSH91 by *Bsa*I HF.

Substance	**Stock solution concentration**	**Final concentration**	**Volume [µl]** (1 reaction)
pSH91	410 ng·µl^{-1}	2 µg·reaction^{-1}	5
*Bsa*I HF enzyme	20 U·µL^{-1}	0,2 U·µL^{-1}	1
rCutSmart buffer	10x	1x	5
Nuclease-free water			39

Table 8: Reagents for ligation of pSH91 and gRNA oligonucleotide duplex.

Substance	**Stock solution concentration**	**Final concentration**	**Volume [µl]** (1 reaction)
Digested pSH91	43 ng·µl^{-1}	≥ 30 ng·reaction^{-1}	1
T4-DNA ligase	5 U·reaction^{-1}	0,5 U·reaction^{-1}	1
T4-DNA ligase buffer	10x	1x	1
gRNA oligonucleotide duplex			7

4.5.3.3 Heat-shock transformation of ligated product into *E. coli* TOP10 strain

The following steps took place on ice: 5 µl of ligated product was supplied into 50 µl of chemical competent *Escherichia coli* TOP10 cells, tube was mixed gently and let on ice for 20 minutes.

Mixture was let for 90 s in 42 °C and immediately put back on ice for 2 min and let 5 min at room temperature. Then 450 µl of SOC media was added and let shaking for 40 min at 180 rpm and 37 °C. Bacteria culture was then concentrated by centrifuging at 5 000 rpm for 3 min. Supernatant was removed except for 100 µl, in which the bacterial pellet was gently resuspended by pipetting. Bacterial culture was plated onto LB medium containing 50 mg·dm^{-3} of Kanamycin and 15 g·dm^{-3} agar. Plates were sealed with parafilm and incubated overnight at 37 °C.

Part of grown colony was in specific format (Fig. 8) gently transferred by toothpick to freshly prepared plate with solid LB and Kanamycin (50 mg·dm^{-3}), let overnight incubating at 37 °C and put to 4 °C for storage purposes. Toothpick was put to tube containing 3 ml of LB and 50 mg·dm^{-3} of Kanamycin and let incubating overnight at 37 °C with constant shaking at 180 rpm. 500 µl of culture was mixed with 500 µl of glycerol and stored in −80 °C.

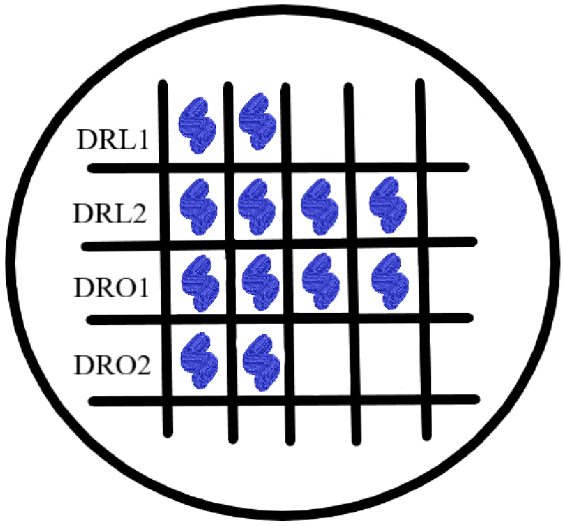

Figure 8: Visualisation of transferring pattern of *Escherichia coli* colonies containing pSH91 (blue colour) to Petri dish. Two colonies were chosen for DRL1 and DRO2 gRNA and four colonies for DRL2 and DRO1 gRNA.

4.5.3.4 Verification of gRNA insertion into pSH91 vector

Verification of gRNA cloning into pSH91 vector was done by *Hind*III HF restriction enzyme. The plasmid was isolated from 2 ml of bacterial culture (tube with toothpick) via QIAprep® Spin Miniprep Kit by following the manufacture protocol. Concentration of purified plasmid was measured on NanoDrop. The isolated plasmid was digested by *Hind*III HF restriction enzyme. For this purpose, reagents (Tab. 8) were gently mixed and incubated 90 minutes in 37 °C. Products with addition of Purple Loading Dye (6x) were separated by electrophoresis on 1% agarose gel in 1X TAE with EtBr for 45 minutes at 90 V. The restriction by *Hind*III of a plasmid containing gRNA produces 2 bands at 826−827 bp (807 bp plus length of gRNA) and 10 166 bp, whereas the restriction of an empty vector results in 2 bands of 2 032 bp and 10 166 bp.

Positive samples for *Hind*III cleavage underwent polymerase chain reaction (PCR) with OsU3P/T primers. Reagents (Tab. 9) with 0,5 µl of bacterial culture were mixed and put to thermocycler with corresponding settings (Tab. 10). Products were separated by electrophoresis on 1% agarose gel in 1X TAE with ethidium bromide for 45 minutes at 90 V. Expected result was 571−572 bp long band (552 bp plus gRNA) for vector with inserted gRNA, vector without insertion and therefore without removal of 1 225 bp part would result in 1 796 bp long band.

Table 8: Reagents for cleavage of pSH91 by *Hind*III HF.

Substance	**Stock solution concentration**	**Final concentration**	**Volume [µl]** (1 reaction)
pSH91/gRNA	*	500 ng·reaction^{-1}	*
*Hind*III HF enzyme	20 U·µL^{-1}	0,2 U·µL^{-1}	0,5
rCutSmart buffer	10x	1x	2,5
Nuclease-free water			**

* Volume of pSH91was adjusted based on measured concentration to have ±500 ng in one reaction. Concentrations are in Table 26.
** Fill volume up to 25 µl.

Table 9: PCR reaction mix.

Substance	Stock solution concentration	Final concentration	Volume [µl] (1 reaction)
5X Green GoTaq® Reaction Buffer	5X	1X	3
OsU3P_F1 primer*	10 µmol·dm^{-3}	0,167 µmol·dm^{-3}	0,25
OsU3T_R1 primer*	10 µmol·dm^{-3}	0,167 µmol·dm^{-3}	0,25
dNTP Mix	10 mmol·dm^{-3}	0,167 mmol·dm^{-3}	0,25
GoTaq® DNA Polymerase	5 U·reaction^{-1}	0,0167 U·reaction^{-1}	0,05
Nuclease-free water			11,2

* sequences are in Table 21

Table 10: PCR reaction settings.

Process	Temperature [°C]	Time [s]	Number of cycles
Initial denaturation	95	600	1
Denaturation	95	45	35
Primers annealing	61	30	
Elongation	72	105	
Final elongation	72	600	1

4.5.3.5 Insertion of pSH91/gRNA into the final binary p6i-2x35S-TE9 vector

The vector p6i-2x35S-TE9 (p6i) (Fig. 9) is 10 052 bp long plasmid that contains all the necessary elements needed for integration of DNA into the plant genome via *A. tumefaciens*. For that reason, pSH91/gRNA was cloned into p6i, creating "binary" pSH91/gRNA-p6i vector.

Vector pSH91 with inserted gRNA was digested by restriction enzyme *Sfi*I by mixing reagents (Tab. 11) and incubating 4 hours in 50 °C. Product was purified by NucleoSpin Gel and PCR Clean Up, following the protocol of developer. Concentration was quantified on NanoDrop. Products with addition of Purple Loading Dye (6x) were separated by electrophoresis in 1% agarose gel in 1X TAE with EtBr for 45 minutes at 90 V, expected results were 2 bands ± 3 300 bp and ± 8 900 bp long.

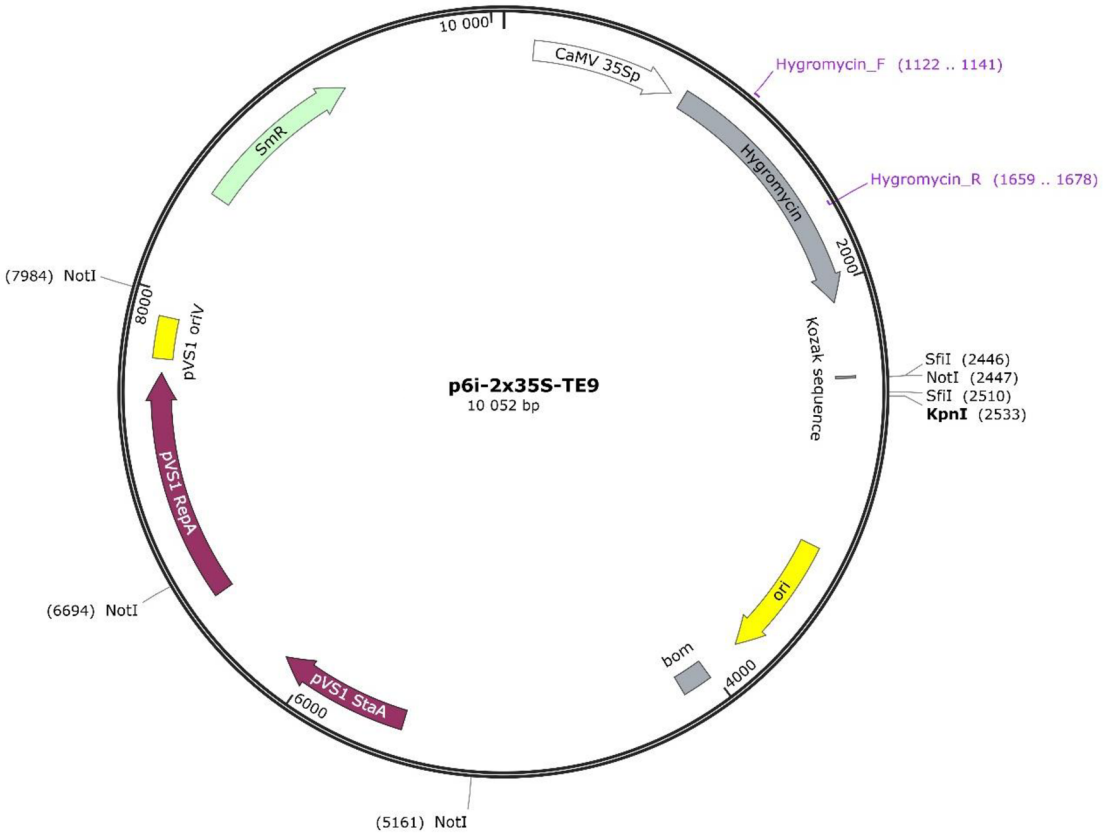

Figure 9: Map of the vector p6i-2x35S-TE9 created in SnapGene. Legend: (SmR): gene of resistance to spectinomycin; (CaMV 35Sp): cauliflower mosaic virus 35S promoter with a duplicated enhancer region; (ori): high-copy-number ColE1/pMB1/pBR322/pUC origin of replication; (bom): basis of mobility region from pBR322; (pVS1 StaA): stability protein from the *Pseudomonas* plasmid pVS1; (pVS1 RepA): replication protein from the *Pseudomonas* plasmid pVS1; (pVS1 oriV): origin of replication for the *Pseudomonas* plasmid pVS1. Text outside of circle: in black – binding sites of restriction enzymes; in blue – binding sites of primers.

Table 11: Reagents for cleavage of pSH91/gRNA by *Sfi*I.

Substance	**Stock solution concentration**	**Final concentration**	**Volume [µl]** (1 reaction)
pSH91/gRNA	Table 26	≥2 µg·reaction^{-1}	8
*Sfi*I enzyme	20 U·µL^{-1}	0,2 U·µL^{-1}	1
rCutSmart buffer	10x	1x	5
Nuclease-free water			36

The vector p6i-2x35S-TE9 was cut by restriction enzyme *Sfi*I. Reagents (Tab. 12) were mixed and incubated 4 hours at 50 °C. Product was isolated by NucleoSpin Gel and PCR Clean Up, following the protocol of manufacturer. Concentration was measured on NanoDrop. Product with addition of Purple Loading Dye (6x) was separated by electrophoresis on 1% agarose gel in 1X TAE with EtBr for 45 minutes at 90 V. The vector p6i has *Sfi*I restriction sites only 64 bp apart. For that reason, expected result was one ±10 000 bp large band.

Digested pSH91/gRNA and p6i underwent ligation by gently mixing substances (Tab. 13) and incubating overnight at 16 °C.

Table 12: Reagents for cleavage of p6i by *Sfi*I.

Substance	**Stock solution concentration**	**Final concentration**	**Volume [µl]** (1 reaction)
p6i	415 ng·µl^{-1}	≥2 µg·reaction^{-1}	5
*Sfi*I enzyme	20 U·µL^{-1}	0,2 U·µL^{-1}	1
rCutSmart buffer	10x	1x	5
Nuclease-free water			39

Table 13: Reagents for ligation of p6i and pSH91/gRNA.

Substance	**Stock solution concentration**	**Final concentration**	**Volume [µl]** (1 reaction)
Digested p6i	30 ng·µl^{-1}	≥ 30 ng·reaction^{-1}	1
T4-DNA ligase	5 U·reaction^{-1}	0,5 U·reaction^{-1}	1
T4-DNA ligase buffer	10x	1x	1
Digested pSH91/gRNA			7

Ligated product (5 µl) was transferred into 50 µl of chemical competent *Escherichia coli* TOP10 cells, gently mixed tube was let on ice for 20 minutes, then put to 42 °C for 90 s and immediately after let back on ice for 2 min and 5 min at room temperature. Then was added 450 µl of SOC media and the reagents were 40 min shaking at 180 rpm and 37 °C. By centrifuging at 5 000 rpm for 3 min the bacteria culture was concentrated, supernatant was removed except for 100 µl, that was used for resuspending bacterial pellet. Culture was transferred to Petri dish with solid LB containing 50 mg· dm^{-3} of Spectinomycin antibiotic to select p6i clones and let incubating overnight in 37 °C.

Two colonies per plate were gently touched by toothpick, that was put to tube containing 3 ml of LB and 50 mg· dm^{-3} of Spectinomycin. Tubes were let to incubate overnight in 37 °C with constant shaking at 180 rpm. 500 µl of bacteria culture was mixed with 500 µl of glycerol and stored in −80 °C.

Binary plasmid pSH91/gRNA-p6i was purified from 2 ml of bacterial culture by QIAprep® Spin Miniprep Kit by following the manufacture protocol, concentration was quantified on NanoDrop. Isolated binary plasmid was digested by *Not*I HF restriction enzyme to verify insertion and ligation of pSH91/gRNA and p6i vectors. Cleavage was performed by gently mixing reagents (Tab. 14) and incubating 90 minutes at 37 °C. Purple Loading Dye (6x) was added to digested products. Electrophoresis was run in 1% agarose gel in 1X TAE with EtBr for 45 minutes at 90 V to separate products, expected bands were 1 298 bp, 1 541 bp, 5 605 bp and 9 172 bp long.

Binary plasmid was also sent for sequencing. Sample mixture (Tab. 15) was prepared based on recommendation of StandardSeq Sanger sequencing of SEQme company (www.seqme.eu), that performed the sequencing.

Table 14: Reagents for cleavage of pSH91/gRNA-p6i by *Not*I.

Substance	**Stock solution concentration**	**Final concentration**	**Volume [µl]** (1 reaction)
pSH91/gRNA-p6i	Table 27	≥1 µg·$reaction^{-1}$	3
*Not*I_HF enzyme	20 U·$µL^{-1}$	0,2 U·$µL^{-1}$	0,5
rCutSmart buffer	10x	1x	2,5
Nuclease-free water			19

Table 15: Mixture for sequencing of pSH91/gRNA-p6i.

Substance	Stock solution concentration	Final concentration	Volume [µl] (1 reaction)
pSH91/gRNA-p6i	Table 27	500 ng·reaction^{-1}	1,5
pSH91_rev primer*	10 µmol·dm^{-3}	5 µmol·dm^{-3}	5
Nuclease-free water			3,5

* sequence in Table 21

4.5.3.6 Transformation of *Agrobacterium tumefaciens* AGL1 strain with the pSH91/gRNA-p6i vector.

Following steps took place on ice: 1 µl of pSH91/gRNA-p6i vector was added to *Agrobacterium tumefaciens* strain AGL1. 50 µl of mixture was transferred into pre-cooled electroporation cuvette, placed to electroporator and 1 800 V pulse was emitted. Immediately after voltage stopped, 450 µl of SOC media was added and content of cuvette was returned to microtube.

Tube was incubated 90 min at 28 °C with constant shaking at 180 rpm. Culture was centrifuged at 5 000 rpm for 3 min, 100 µl of supernatant was kept for resuspending the pellet. Bacterial culture was sowed to Petri dish with solid MG/L media, containing Carbenicillin (100 mg·dm^{-3}), Rifampicin (50 mg·dm^{-3}) and Spectinomycin (50 mg·dm^{-3}) to select positives AGL1 clones. Plates were kept 3 days in dark in 28 °C.

Colony was transferred by toothpick to 3 ml of liquid MG/L containing Carbenicillin (100 mg·dm^{-3}), Rifampicin (50 mg·dm^{-3}) and Spectinomycin (50 mg·dm^{-3}) and incubated overnight at 28 °C with constant shaking at 180 rpm. Stocks were prepared by mixing 500 µl of bacteria culture with 500 µl of glycerol and stored in −80 °C.

To verify the successful transformation of the binary plasmid into AGL1 bacterial cells, plasmid was isolated from 2 ml of bacteria culture (tube with toothpick) via NucleoSpin® Plasmid kit and NucleoSpin® Plasmid/Plasmid (NoLid) following manufacture protocol (from step 2) with addition of Lysis buffer and Wash buffer. Concentration of purified plasmid was quantified via NanoDrop.

Before transformation of barley by binary vector, the quality of vector and absence of any mutation that might have occurred during *A. tumefaciens* transformation was double checked by transferring isolated plasmid into 50 µl of chemical competent TOP10 cells of *Escherichia coli*. Steps were the same as in the chapter 4.5.3.5.

Purified plasmids from *E. coli* (via QIAprep® Spin Miniprep Kit) were digested by restriction enzymes *Not*I_HF® and *Kpn*I_HF®. Reagents (Tab. 16) were gently mixed and incubated 90 min in 37 °C. To separate products electrophoresis was run with purple loading dye (6x) in 1% agarose gel in 1X TAE with EtBr for 45 minutes at 90 V, expected bands for *Not*I_HF were 1 298 bp, 1 541 bp, 5 605 bp and 9 172 bp long, for *Kpn*I_HF two large bands over 7 000 bp long.

Reaction mixture (Tab. 17) was sent for StandardSeq Sanger sequencing to SEQme company.

Table 16: Reagents for cleavage of AGL1 pSH91/gRNA-p6i by *Not*I_HF and *Kpn*I_HF.

Substance	**Stock solution concentration**	**Final concentration**	**Volume [µl]** (1 reaction)
AGL1 pSH91/gRNA-p6i	Table 29	≥1 µg·reaction^{-1}	4
Restriction enzyme	20 U·µL^{-1}	0,2 U·µL^{-1}	0,5
rCutSmart buffer	10x	1x	2,5
Nuclease-free water			18

Table 17: Mixture for sequencing of AGL1 pSH91/gRNA-p6i plasmid.

Substance	**Stock solution concentration**	**Final concentration**	**Volume [µl]** (1 reaction)
AGL1 pSH91/gRNA-p6i	Table 29	100 ng·reaction^{-1}	1
pSH91_rev primer*	10 µmol·dm^{-3}	5 µmol·dm^{-3}	5
Nuclease-free water			4

* sequence in Table 21

4.5.3.7 *Agrobacterium*-mediated stable transformation of immature barley embryo

Small amount of upper layer of still frozen glycerol stock with binary vector in AGL1 was transferred into 5 ml of MG/L with Carbenicillin (100 mg·dm^{-3}), Rifampicin (50 mg·dm^{-3}) and Spectinomycin (50 mg·dm^{-3}). Sample was incubated 36 hours in 28 °C with constant shaking at 180 rpm, and OD_{600} was measured on spectrophotometer, needed value was 2−3. Another glycerol stocks, that were later used for transformation of immature embryos, were prepared by mixing 200 µl of culture with 200 µl glycerol.
Isolation of barley immature embryos and transformation by AGL1 inoculum was performed following the method of Marthe *et al.* (2015) and with the help of Bc. Vendula Svobodová.
Plants grew first few weeks inside culture box, then approximately two months inside small pot in Plant growth chamber in 16 °C and 60 % humidity. They were after replanted to big pot and put to greenhouse.

4.5.3.8 Genotyping of transformed T0 generation plants

Genomic DNA was isolated from a piece of leaf, not bigger than 0,5 cm^2, that was placed inside a 1.5ml Eppendorf tube alongside with a homogenization ball, 300 µl of extraction buffer and 100 µl Chloroform:IAA (24:1). Sample was homogenised twice in grind mill (25 rpm per min) and centrifuged 3 min at 13 000 rpm at room temperature (RT). Clear supernatant was transferred to a fresh 1.5ml Eppendorf tube and 700 µl 96% EtOH was added; mixture was gently mixed by inverting the tube to precipitate gDNA. Sample was incubated 5 min at room temperature and centrifuged 15 min at 13 000 rpm at RT. Supernatant was discarded by pipetting; pellet was washed by 70 µl 70% EtOH and centrifugated 2 min at 13 000 rpm at RT. Supernatant was discarded and pellet let to dry 10 min. To tube was added 50 µl of TE buffer, sample was vortexed and let overnight in 4 °C.
PCR reaction mix with isolated genomic DNA was prepared (Tab. 18). PCR was ran with OsU3P/U3T primers, Hygromycin primers, and Ubi_F4/zCas9_R1 primers (Tab. 19). Electrophoresis was run with PCR products and purple loading dye (6x) on 1% agarose gel in 1X TAE with EtBr for 45 minutes at 90 V.

Table 18: PCR reaction mix for genotyping.

Substance	Stock solution concentration	Final concentration	Volume [µl] (1 reaction)
5X Green GoTaq® Reaction Buffer	5X	1X	2
Forward primer*	10 µmol·dm^{-3}	0,2 µmol·dm^{-3}	0,2
Reverse primer*	10 µmol·dm^{-3}	0,2 µmol·dm^{-3}	0,2
dNTP Mix	10 mmol·dm^{-3}	0,2 mmol·dm^{-3}	0,2
GoTaq® DNA Polymerase	5 U·reaction^{-1}	0,05 U·reaction^{-1}	0,1
gDNA Sample			1
Nuclease-free water			6,3

* sequences in Table 21

Table 19: Condition of PCR reaction for genotyping.

Process	Temperature [°C]	Time [s]	Number of cycles
Initial denaturation	95	120	1
Denaturation	95	30	35
Primers annealing	*	30	
Elongation	72	45	
Final elongation	72	600	1

* annealing temperature specific for each primers in Table 21

PCR was ran with the samples that showed specific product (based on the type of used set of primers) with the use of DRO1_seq, DRO2_seq and DRL1_seq primers, that were designed on Primer3Plus website to border gRNA in binary vector (Tab. 21). PCR reaction mix was prepared the same as in Table 18 only with double volumes for each substance (final concentration remained the same). Condition of PCR was set based on Table 19.

PCR products were purified via NucleoSpin Gel and PCR Clean Up following the manufacture protocol. Concentration was quantified on NanoDrop. Sequencing mixture (Tab. 20) was prepared and sent to SEQme for StandardSeq sequencing.

With the help of DECODR v3.0 software (Bloh *et al.*, 2021) mutations were predicted in obtained sequences.

Table 20: Sequencing mixture of gDNA.

Substance	Stock solution concentration	Final concentration	Volume [µl] (1 reaction)
Isolated gDNA	40–50	≥100 ng·reaction^{-1}	2
Forward or reverse primer*	10 µmol·dm^{-3}	5 µmol·dm^{-3}	5
Nuclease-free water			3

* DRO1_seq, DRO2_seq or DRL1_seq primers based on a type of sample.

Table 21: List of used primers**.**

Name	Sequence 5´–3´	Size of PCR product [bp]	Annealing temperature [°C]
qTIP41_fwd	TGGTTGGTTTCTGCTCTTGC	± 500	58
qTIP41_rev	CGGCTTTGCTTCCTCCTTAC		
OsU3P_F1	CAGGGACCATAGCACAAGAC	1 796 / 571–572	61
OsU3T_R1	TCAGCGGGTCACCAGTGTTG		
pSH91_rev	AATGTGGCGCCGTAAATAAG	-	-
UBI_F4	TGGTTAGGGCCCGGTAGTTC	1594	62
zCas9_R1	TTAATCATGTGGGCCAGAGC		
Hygromycin_F	GAATTCAGCGAGAGCCTGAC	556	60
Hygromycin_R	ACATTGTTGGAGCCGAAATC		
DRO1_seq_F	TTCAGCTGGATGGCGAACAA	573	55
DRO1_seq_R	GGCAAATTGCTTTGACGCTG		
DRO2_seq_F	CACAAGTGCAGGACGCTT	590	55
DRO2_seq_R	TGCATCCTCGAGGCATTCG		
DRL1_seq_F	CATGAAAATGTGGCGCCGTA	606	60
DRL1_seq_R	GCATTTCGTAGTGGGCCATG		

* if not mentioned otherwise, primers were borrowed from colleges

5 RESULTS

The goal of the thesis was to study root angle determination in barley (*Hordeum vulgare* L.). Sequences of genes associated with root system architecture in rice (Uga *et al.*, 2013; Kitomi *et al.*, 2020) were used as query to find putative homologs in barley. Cultivars of barley Golden Promise, Maythorpe and the landrace HOR1122 (internal number: 181) were *in vitro* screened for potential contrasted root angle. Expression of candidate genes was measured throughout 7 days of Golden Promise and Maythorpe cultivation in mini-hydropony. Additionally, using CRISPR-Cas^9 methodology, T_0 generation of transformed plants was prepared and via software DECODR v3.0 (Bloh *et al.*, 2021) screened for potential mutations.

5.1 Finding putative rice homologs in barley

Genes associated with root system architecture in rice Os*DRO1* (Os09g0439800) (Uga *et al.*, 2013), q*SOR1/DRL1* (Os07g0614400), Os*DRL2* (Os03g0180600) and Os*DRL3* (Os03g0406300) (Kitomi *et al.*, 2020) were used as templates to search for putative homologs in barley database for cultivar Morex and Golden Promise. Highest similarity with Os*DRO1* 81,6 % showed Horvu.Morex.r3.5HG0480470 and Horvu.GOLDEN.5H01G311500 with 81,5% identity. Horvu.Morex.r3.2HG0125600 showed highest identity with Os*DRL1* (94,7 %) and Os*DRL3* (87,7 %), same as Horvu.GOLDEN.2H01G175600 (94,7 % with Os*DRL1* and 84,4 % with Os*DRL3*) (Tab. 22). Horvu.Morex.r3.5HG0480470 and Horvu.Morex.r3.2HG0125600 were selected for further work as they showed 99,9% identity with Golden Promise cultivar.

Table 22: Barley putative homologs of rice genes.

Rice gene	Database hit	Identical matches [%]
DRO1	HORVU.MOREX.r3.5HG0480470	81,6
	HORVU_GOLDEN_5H01G311500	81,5
DRL1	HORVU.MOREX.r3.2HG0125600	94,7
	HORVU_GOLDEN_2H01G175600	94,7
DRL2	HORVU.MOREX.r3.6HG0616790	96,7
	HORVU_GOLDEN_6H01G422900	96,7
DRL3	HORVU.MOREX.r3.2HG0125600	87,7
	HORVU_GOLDEN_2H01G175600	84,4

5.2 Root angle determination

The landrace HOR1122 (Fig. 10), as well as the barley cultivars Golden Promise (Fig. 11) and Maythorpe were cultivated *in vitro* for 17 days, scanned and their root angles measured via Fiji/ImageJ. Average angles were computed. Widest angle showed the landrace HOR1122 : 53,8°, Golden Promise resulted with slightly narrower angle 45,5°, while Maythorpe's 37,9° had the narrowest observed angle (Tab. 23, Fig. 12).

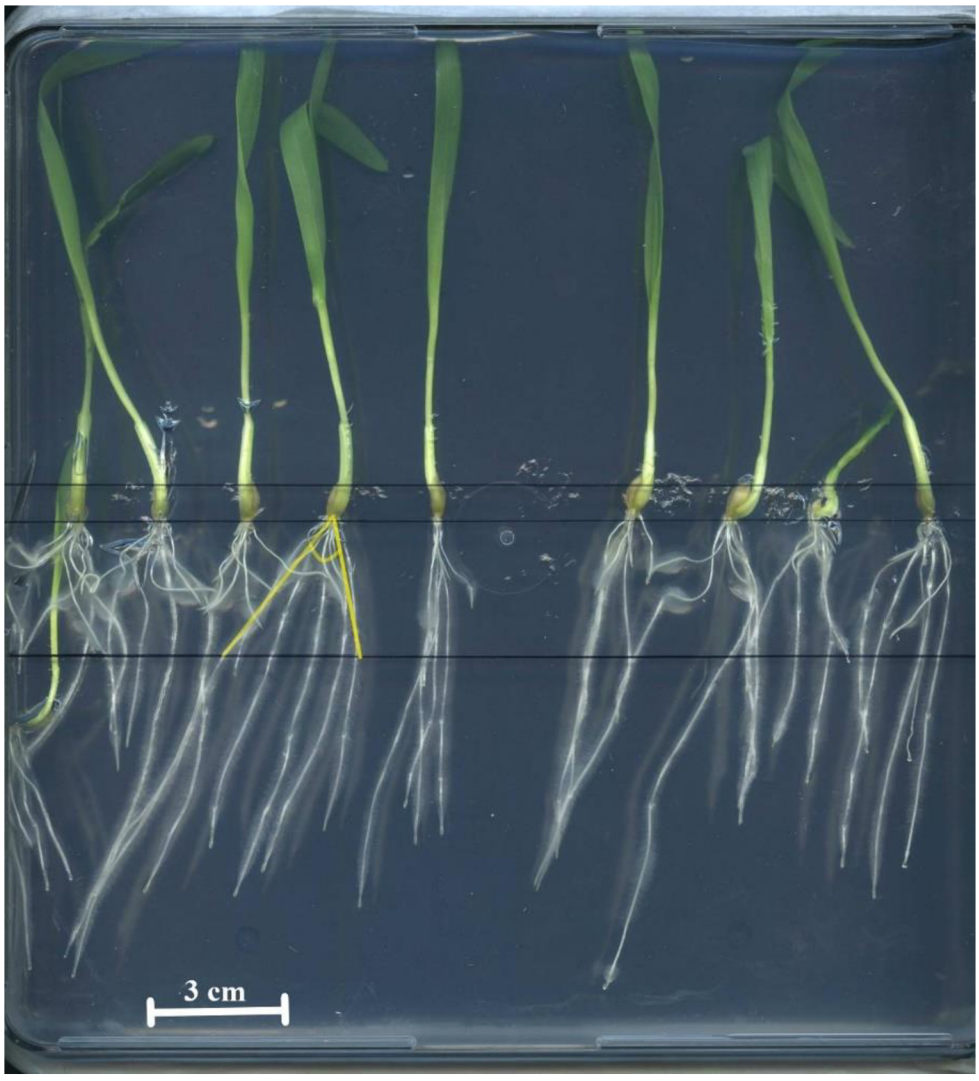

Figure 10: The landrace HOR1122 plants grown 17 days *in vitro* on 250 ml ½ MS medium. Yellow lines show example of root angle measurement.

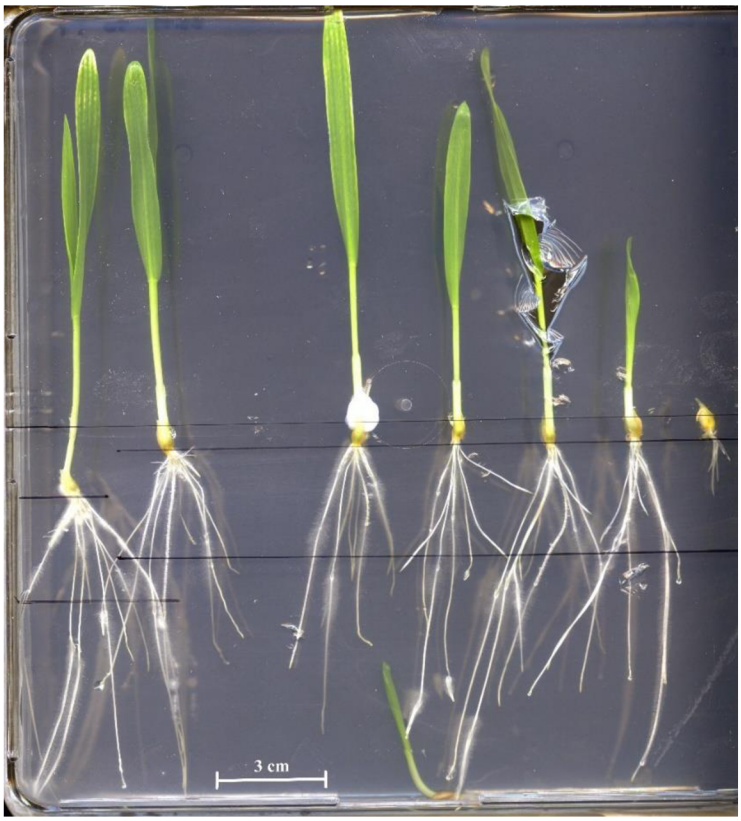

Figure 11: Golden Promise plants grown 17 days *in vitro* on 250 ml ½ MS medium.

Table 23: Measured root angles of *in vitro* cultivated plants.

	HOR1122		Golden Promise		Maythorpe
Measured root angles [°]	58,3	27,9	81,7	22,9	52,0
	38,9	49,5	39,4	44,3	40,0
	31,4	44,0	42,4	45,7	47,2
	80,7	43,5	46,0	45,0	23,3
	58,5	40,3	22,4	67,1	29,3
	44,0	46,0	57,8	52,5	41,2
	38,0	47,8	80,0	39,1	34,0
	63,0	45,5	39,4	50,6	30,9
	68,2	15,6	84,2	45,0	43,3
	52,9	53,6	70,2	40,9	
	34,2	56,3	29,1	20,3	
	69,0	58,2	69,4	36,0	
	57,6	30,0	24,1	25,3	
	78,5	76,3	24,3	67,9	
	92,6	35,6	50,5	43,0	
	65,7	44,0	27,9	21,6	
	66,0	48,6			
	50,7	45,2			
SEM	2,55		3,24		2,90

Legend: (SEM): Standard error of a mean.

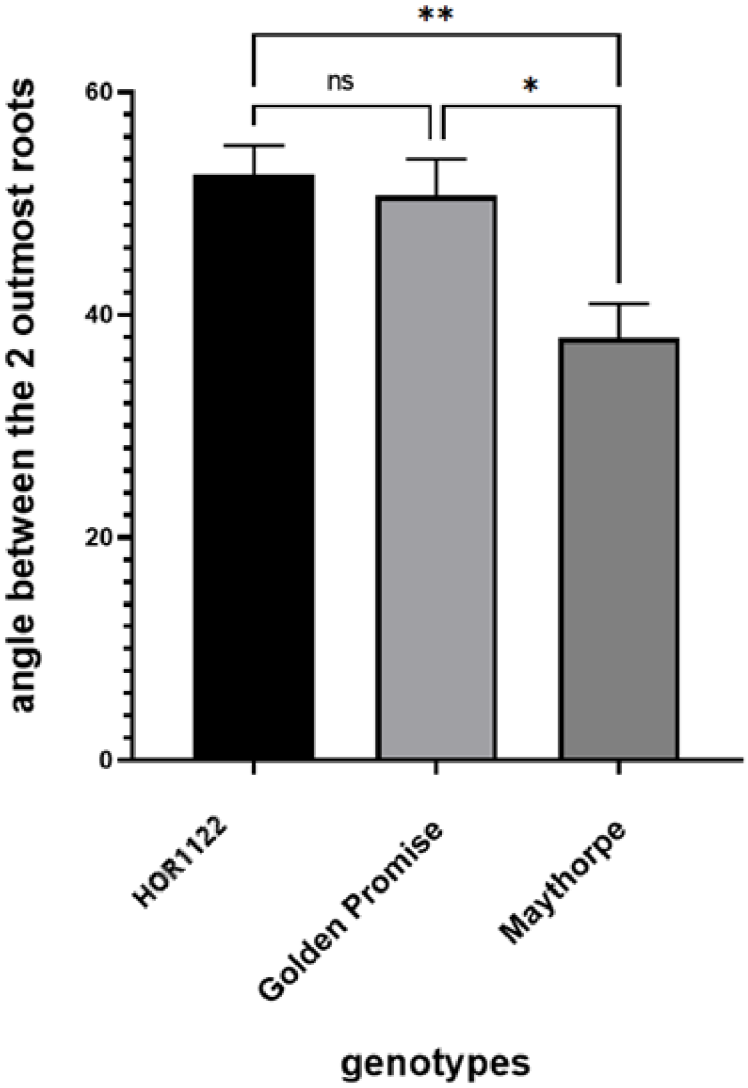

Figure 12: Comparison of average angles of three barley genotypes.

5.3 Crown root inducible system

5.3.1 Cultivation

Two days after treatment with 1-NAA, one could observe the enlargement of the stem base and the presence of a small “bud”. (Fig. 13). A set of several new emerged crown root was clearly observed at the stem base of seedlings 4 days after ignition of the treatment. (Fig. 14).

Extracted RNA from plants showed no contamination by genomic DNA, observed bands correspond with degraded RNA and mixture of PCR reagents (Fig. 15). Later synthetized cDNA occurred properly in all samples, showing homogenous signal (Fig. 16)

Figure 13: Sample T2-days of a Golden Promise genotype with visible enlargement of the stem base (labelled with an arrow). Grown 48 hours under 1-NAA (50 µM).

Figure 14: Crown roots emergence of barley Golden Promise genotype sample T4-days. Grown 4 days without the NPA (50 µM), 2 days without 1-NAA (50 µM). Crown roots are encircled.

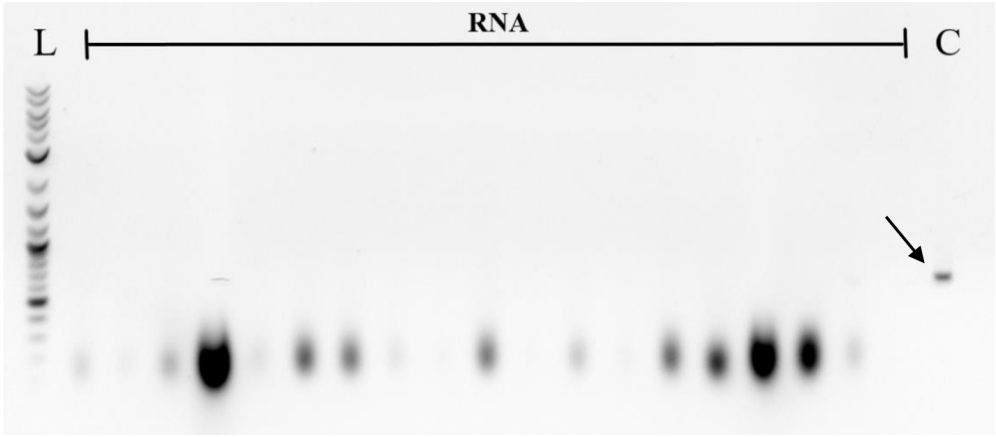

Figure 15: Validation of genomic DNA contamination in extracted RNA.

Legend: (L): standard GeneRuler 1kb Plus DNA ladder; (RNA): samples of RNA; (C): control – genomic DNA of wild type Golden Promise, band ± 500 bp labelled with an arrow.

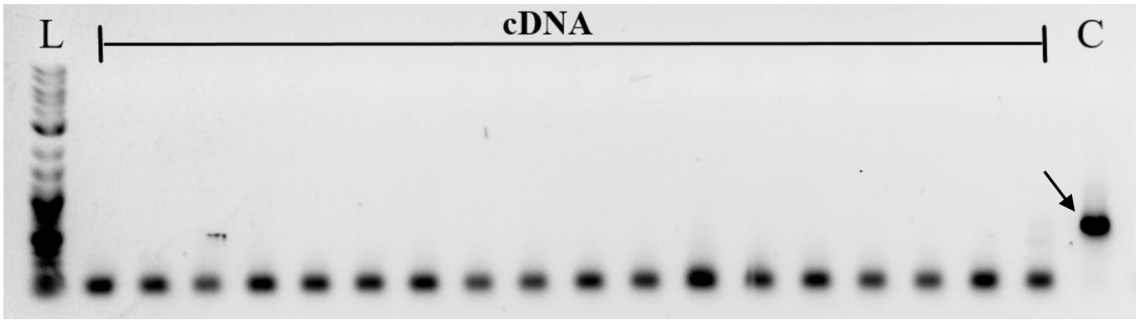

Figure 16: Validation of cDNA synthesis.

Legend: (L): standard GeneRuler 1kb Plus DNA ladder; (cDNA): samples of cDNA; (C): control – genomic DNA of wild type Golden Promise, band ± 500 bp labelled with an arrow.

5.3.2 Expression of candidate genes

The highest efficiency 99 % showed primers for gene Hv*5439*. Primers for Hv*ACTIN* and Hv*20934* showed 94 % efficiency. Efficiency of gene Hv*DRO1* was 95 %, while efficiency of Hv*DRL1* and Hv*EIF512* resulted in value above 100 % (Tab. 24).

In figures 15, 16, 17, 18, 19 and 20 is showed graph of Ct values dependent on $\log_{10}$ dilution for each gene, with displayed regression equation, that served for calculating the efficiency. Hv*5439* and *HvACTIN* were selected as reference genes.

Table 24: Computed efficiency of selected genes.

	Efficiency		Slope
Hv*ACTIN*	1,88	94 %	-3,63
Hv*20934*	1,88	94 %	-3,63
Hv*5439*	1,98	99 %	-3,37
Hv*EIF512*	2,07	103,5 %	-3,17
Hv*DRO1*	1,90	95 %	-3,60
Hv*DRL1*	2,29	114,5 %	-2,77

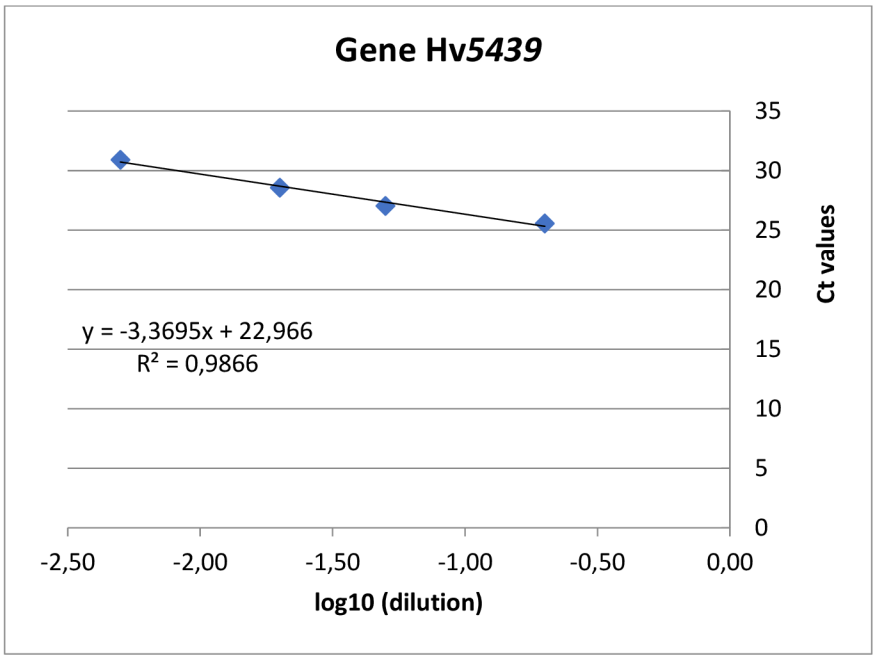

Figure 17: Graph of Ct values dependent on $\log_{10}$ of dilution for gene Hv*5439*.

Legend: (R^2): reliability squared; regression equation is displayed above R^2.

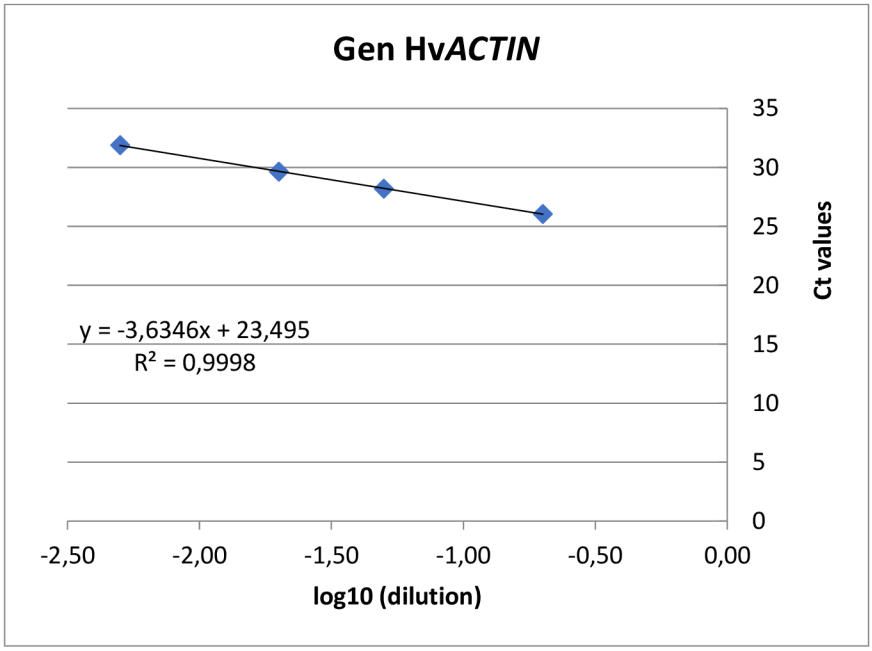

Figure 18: Graph of Ct values dependent on $\log_{10}$ of dilution for gene Hv*ACTIN*.

Legend: (R^2): reliability squared; regression equation is displayed above R^2.

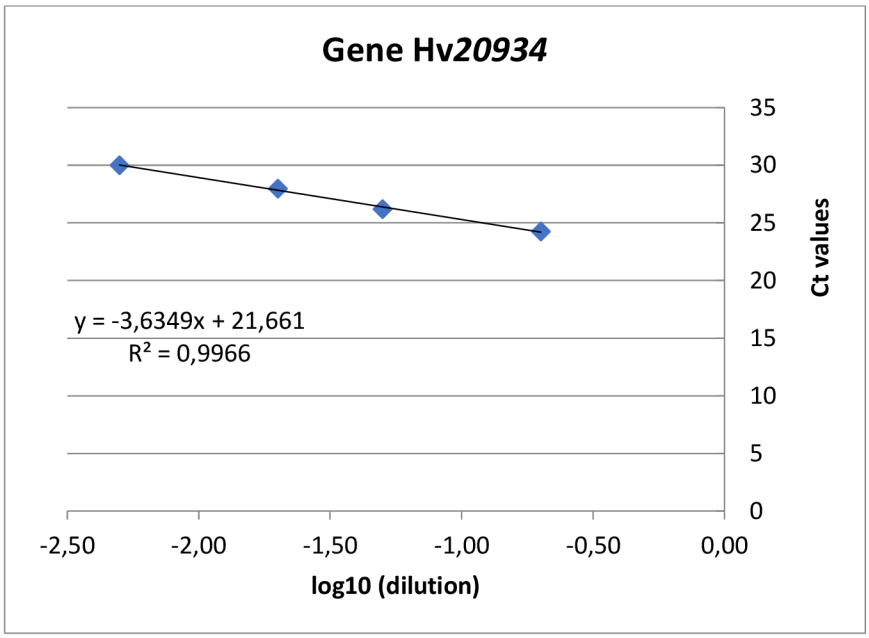

Figure 19: Graph of Ct values dependent on $\log_{10}$ of dilution for gene Hv*20934*.

Legend: (R^2): reliability squared; regression equation is displayed above R^2.

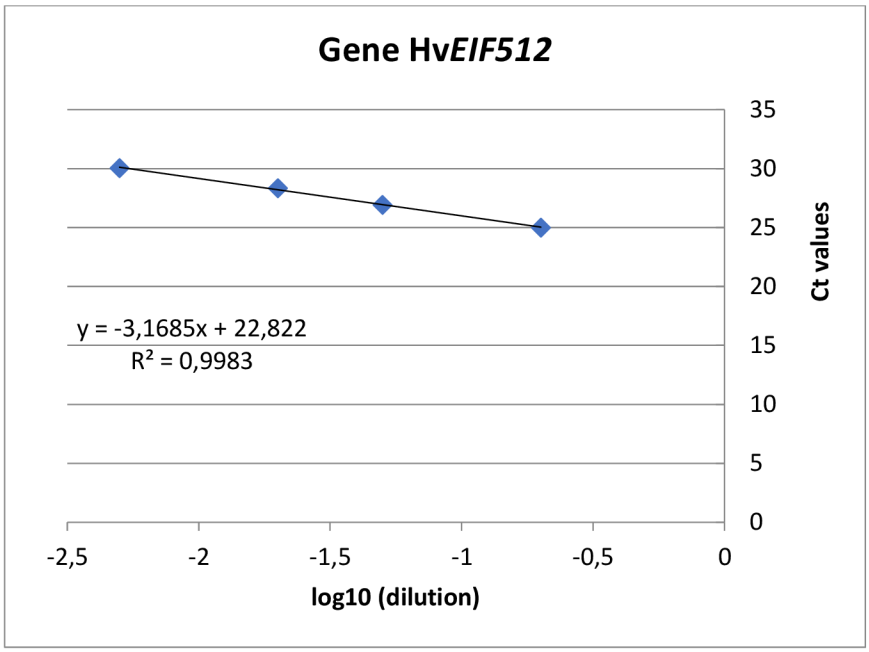

Figure 20: Graph of Ct values dependent on $\log_{10}$ of dilution for gene Hv*EIF512*.

Legend: (R^2): reliability squared; regression equation is displayed above R^2.

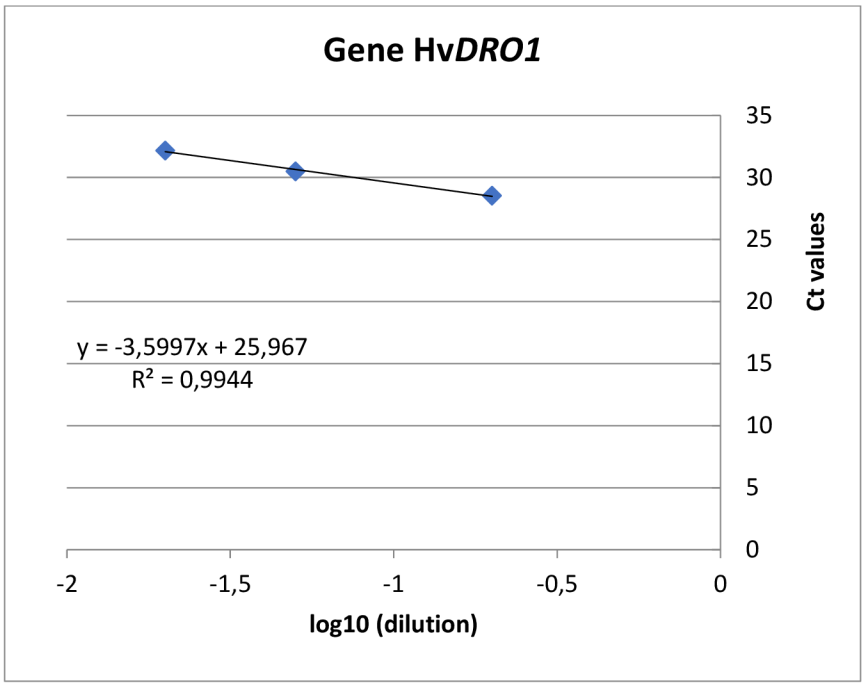

Figure 21: Graph of Ct values dependent on $\log_{10}$ of dilution for gene Hv*DRO1*.

Legend: (R^2): reliability squared; regression equation is displayed above R^2.

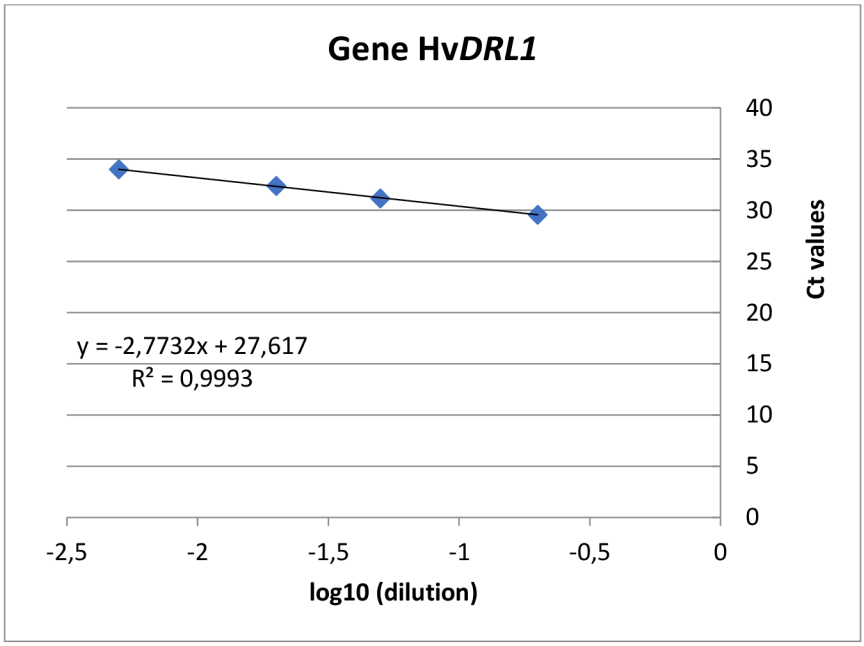

Figure 22: Graph of Ct values dependent on $\log_{10}$ of dilution for gene Hv*DRL1*.

Legend: (R^2): reliability squared; regression equation is displayed above R^2.

Melting curves of Hv*ACTIN* are displayed in Figure 23, melting curves of Hv*5439* are showed in Figure 24. Hv*DRO1* and Hv*DRL1* have their melting curves displayed in Figures 25 and 26, and computed expressions in Figure 27 and Figure 28. Expression of Hv*DRL1* was not conclusively observed in T0-days and T2-days.

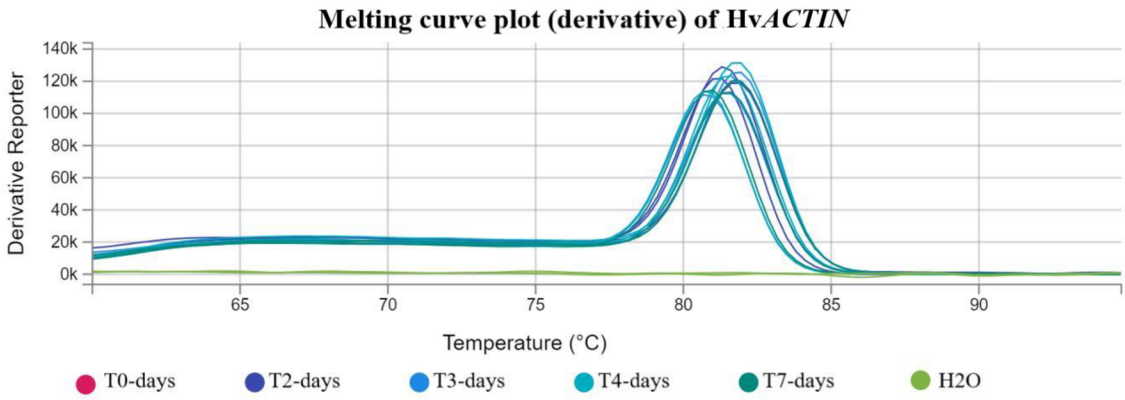

Figure 23: Melting curve of *HvACTIN* in Golden Promise.

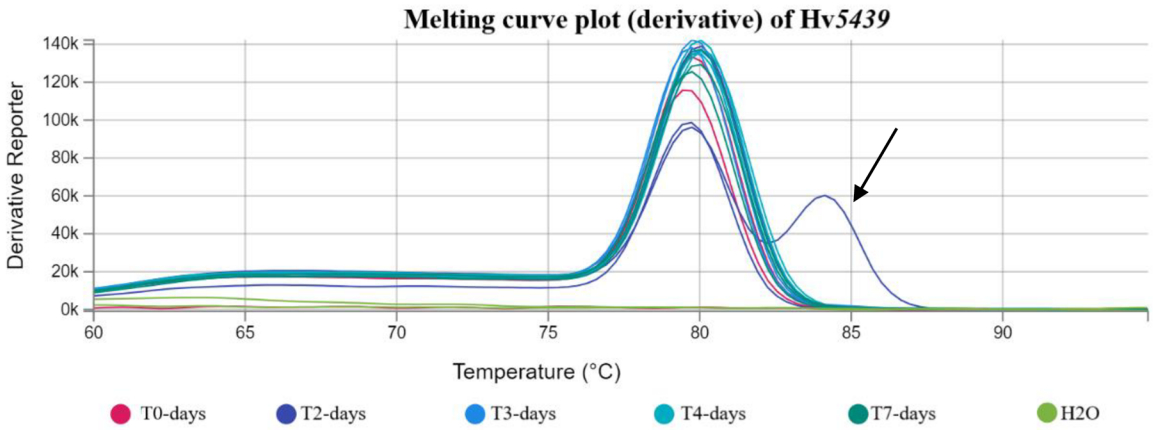

Figure 24: Melting curve of Hv*5439* in Maythorpe. Unspecific product labelled with an arrow.

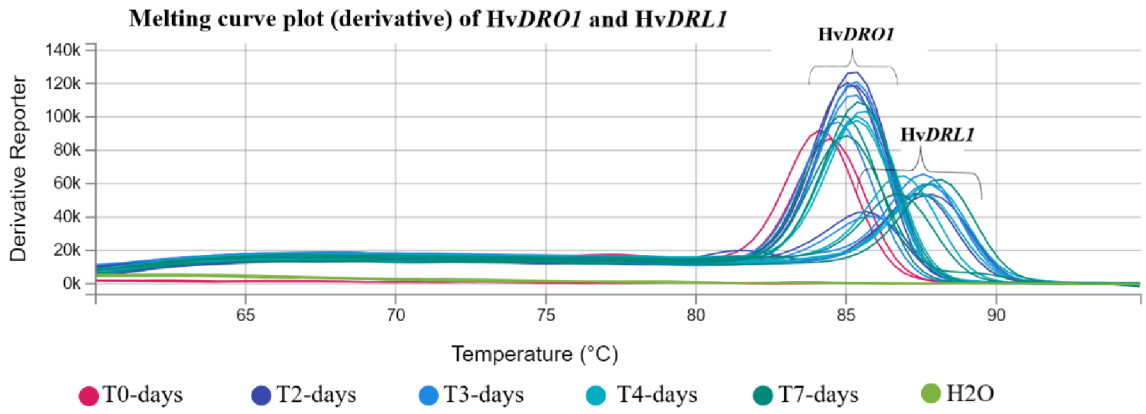

Figure 25: Melting curve of Hv*DRO1* and Hv*DRL1* in Golden Promise cultivar.

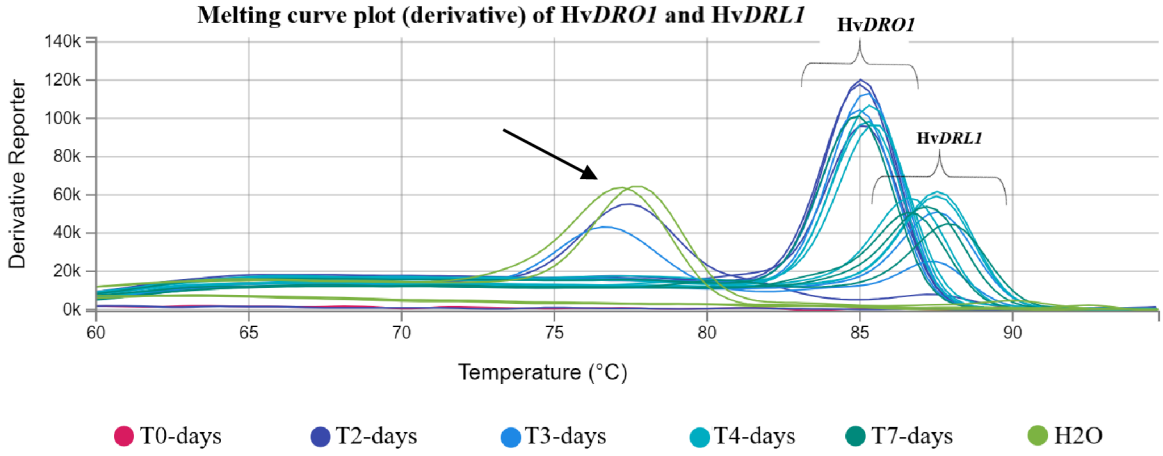

Figure 26: Melting curve of Hv*DRO1* and Hv*DRL1* in Maythorpe cultivar. Unspecific product labelled with an arrow.

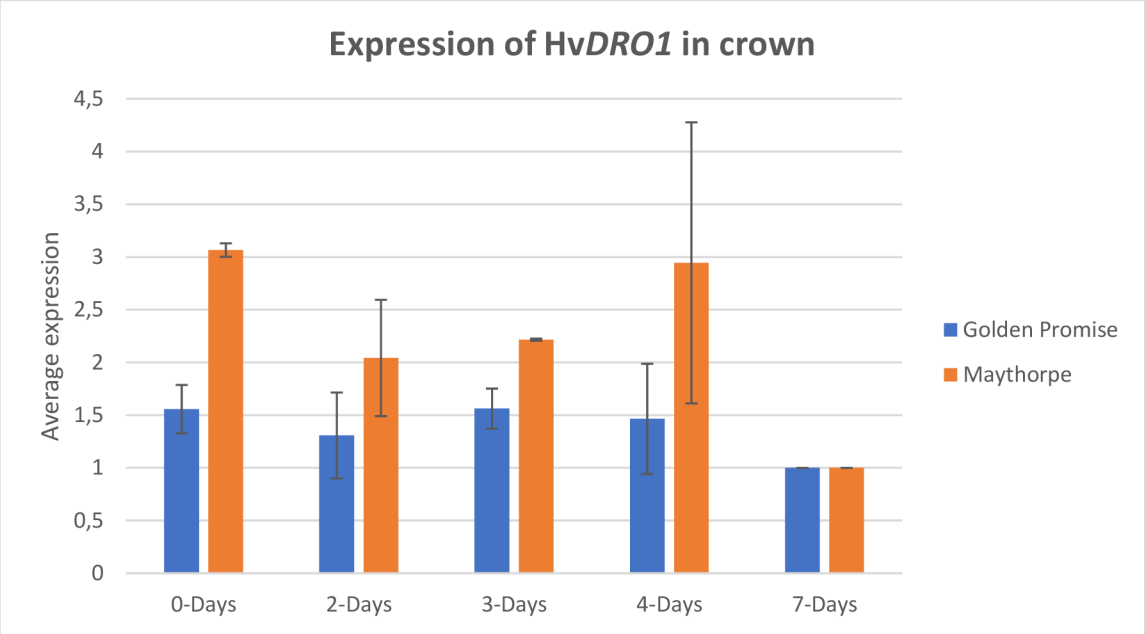

Figure 27: Expression of Hv*DRO1* gene in the crown of barley. The bars indicate average ± standard error of the mean. n= 2. Samples at 7 days after initiation of the treatment were taken as reference sample.

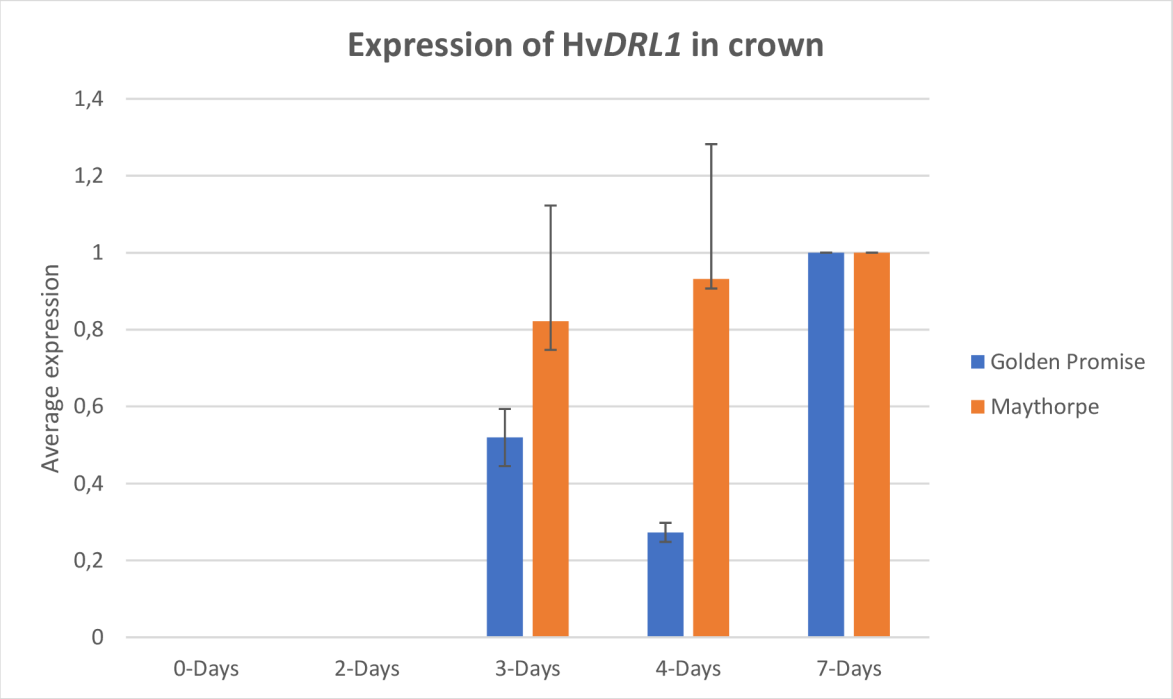

Figure 28: Expression of Hv*DRL1* gene in the crown of barley. The bars indicate average ± standard error of the mean. n= 2. Samples at 7 days after initiation of the treatment were taken as reference sample.

5.4 CRISPR-Cas^{9} mediated knock-out

5.4.1 Design of gRNA

For each Os*DRO1* and Os*DRL1* homolog were designed 2 gRNAs via CRISPOR website (Tab. 25). Corresponding secondary structures of gRNAs associated with scaffold RNA are showed in Figures 29, 30, 31 and 32.

Table 25: Guide RNA properties.

Name		**Sequence**		**Position**
Target gene	gRNA	gRNA	PAM	[bp]
DRO1	DRO1	AAGGCCCGGAGGAACGTGC	CGG	61
	DRO2	ATGGTCATAAGTAAGGGAA	AGG	425
DRL1	DRL1	ATGCTCTCCATCGGAACCCT	CGG	180
	DRL2	AACTGCCCCTCCAGCCTCG	AGG	386

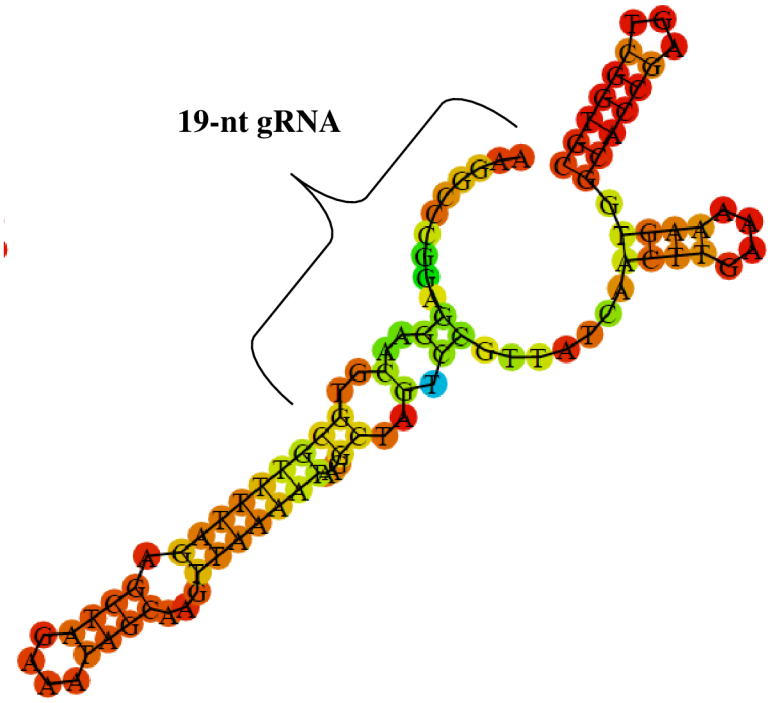

Figure 29: Secondary structure of DRO1 gRNA-scRNA. Created on CRISPOR website.

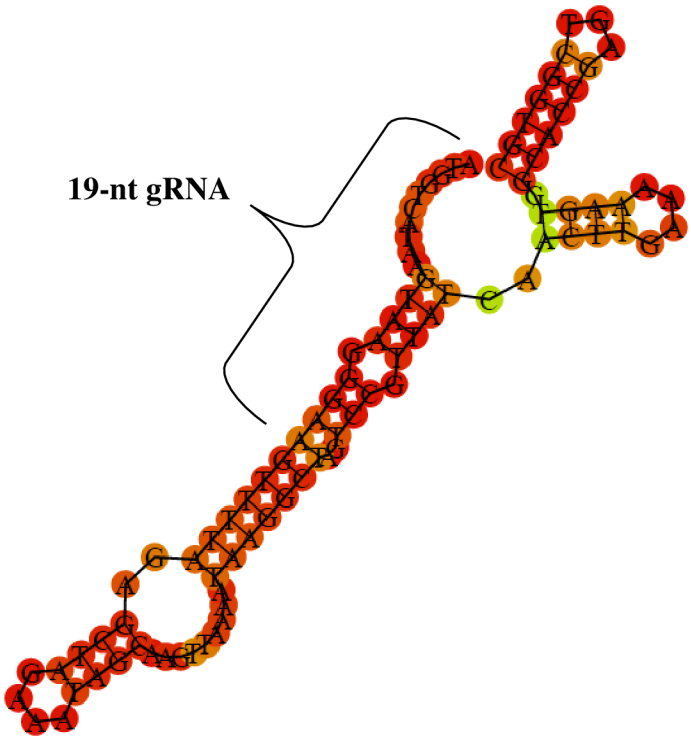

Figure 30: Secondary structure of DRO2 gRNA-scRNA. Created on CRISPOR website.

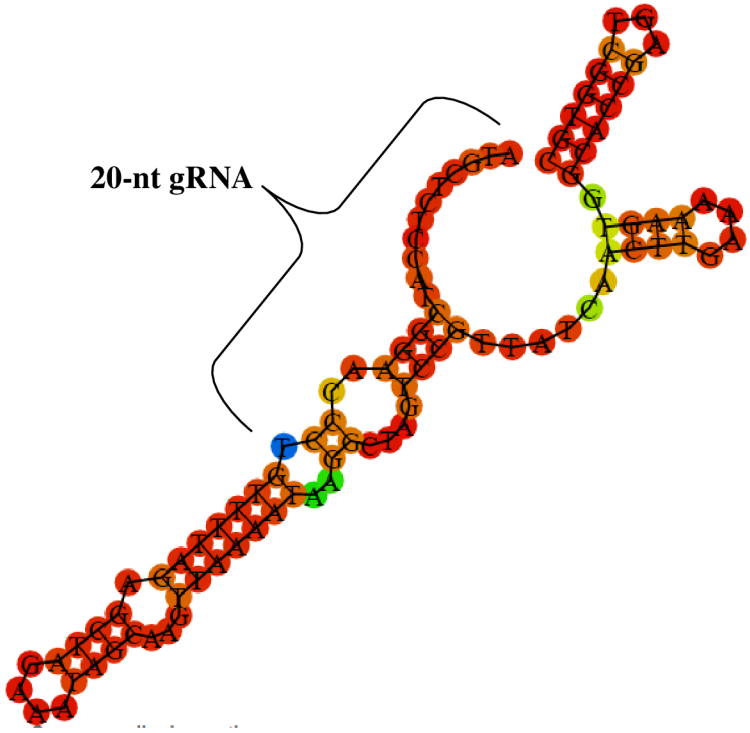

Figure 31: Secondary structure of DRL1 gRNA-scRNA. Created on CRISPOR website.

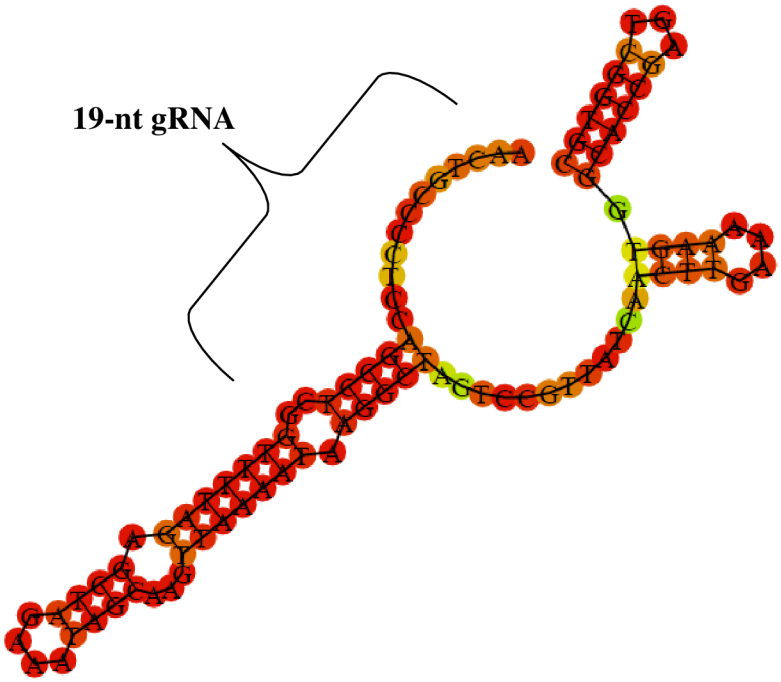

Figure 32: Secondary structure of DRL2 gRNA-scRNA. Created on CRISPOR website.

5.4.2 Insertion of oligonucleotide duplex gRNA into pSH91

First, concentrations of isolated plasmids pSH91/gRNA from *E. coli* quantified on NanoDrop (Tab. 26) were used to compute volumes for reaction mix of *Hind*III_HF cleavage (500 ng·reaction^{-1}), that was performed to verify insertion of prepared oligonucleotide duplex gRNA into pSH91. Seven out of 12 samples (DRL1A, DRL1B, DRL2C, DRO1A, DRO1D, DRO2A, DRO2B) showed after subsequent electrophoresis two bands of expected length 826−827 bp and 10 166 bp. Remaining samples showed unspecific product that did not match expected length (Fig. 33).

Table 26: Concentration and A260/A280 ratio of pSH91/gRNA.

	DRL1		DRL2				DRO1				DRO2	
Sample	A	B	A	B	C	D	A	B	C	D	A	B
Concentration [ng·µl^{-1}]	258	372	415	389	398	334	334	404	373	309	341	328
A260/A280	1,84	1,85	1,85	1,85	1,85	1,85	1,85	1,84	1,85	1,84	1,85	1,86

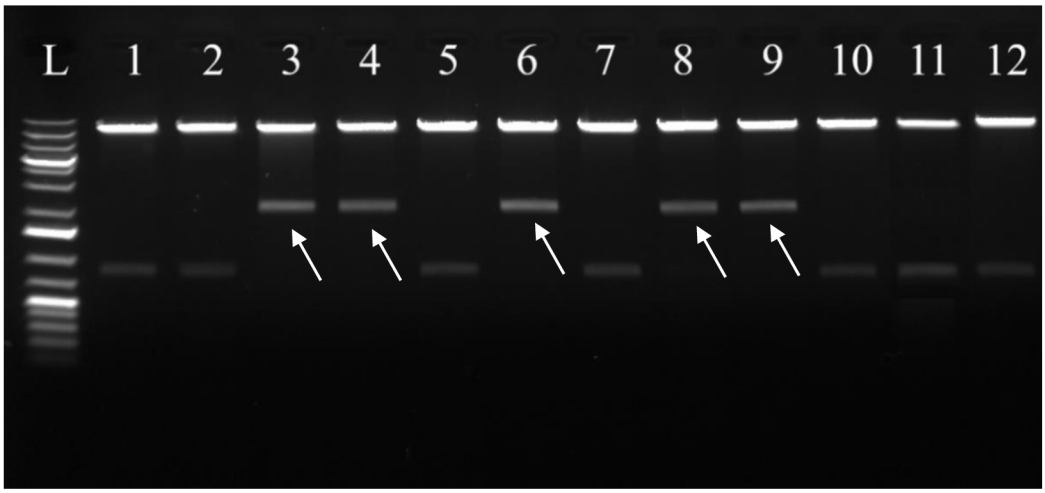

Figure 33: Cleavage of pSH91/gRNA by *Hind*III_HF.

Legend: (L): standard GeneRuler 1kb Plus DNA ladder, (1): DRL1A, (2): DRL1B, (3): DRL2A, (4): DRL2B, (5): DRL2C, (6): DRL2D, (7): DRO1A, (8): DRO1B, (9): DRO1C, (10): DRO1D, (11): DRO2A, (12): DRO2B, nonspecific product is labelled with an arrow.

With the samples that showed specific products was ran PCR with OsU3P_F1 and OsU3T_R1 primers to amplify specific region of pSH91 that covers cloning site for gRNA. Specific product with the length 571−572 bp corresponding with successful cloning was obtained for each of 7 samples (Fig. 34).

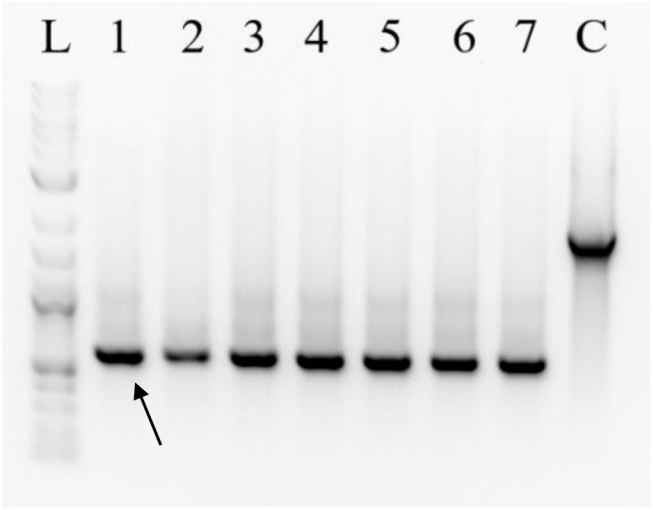

Figure 34: Amplification of cloning site of pSH91 vector.

Legend: (L): standard GeneRuler 1kb Plus DNA ladder, (1): DRL1A, (2): DRL1B, (3): DRL2C, (4): DRO1A, (5): DRO1D, (6): DRO2A, (7): DRO2B, (C): negative control – plain pSH91 without insert 1 796 bp long; specific product of 571−572 bp labelled with an arrow.

5.4.3 Creation of binary vector pSH91/gRNA-p6i

DRL1B, DRL2C, DRO1A, DRO2A samples (pSH91/gRNA) and p6i vector were selected for restriction by *Sfi*I. Each of the DRO and DRL samples showed 2 bands with expected length ± 3 300 bp and ± 8 900 bp, same as the p6i showed expected one large band, proving successful cleavage (Fig. 35).

From transformed *Escherichia coli* (by ligated pSH91/gRNA-p6i) were isolated pSH91/DRO1-p6i plasmids from 3 bacterial colonies, pSH91/DRO2-p6i from 3 colonies as well, pSH91/DRL1-p6i from 4 colonies (Tab. 27). For pSH91/DRL2-p6i did not grow a single colony of *E. coli* and this sample was excluded from further work.

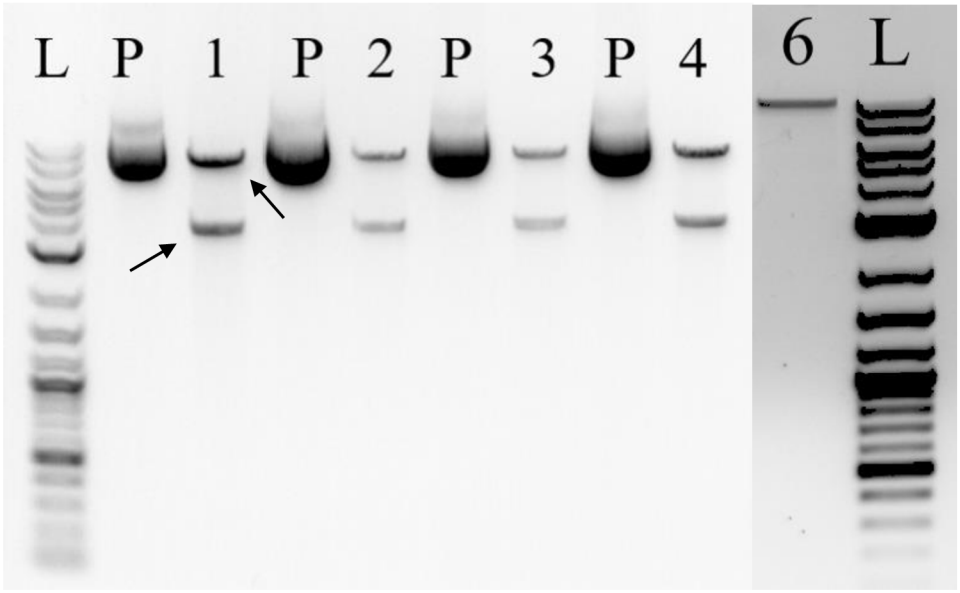

Figure 35: Cleavage of pSH91/gRNA and p6i by *Sfi*I restriction enzyme.

Legend: (L): standard GeneRuler 1kb Plus DNA ladder, (P) undigested pSH91 plasmid, (1): digested DRO1A, (2): digested DRO2A, (3): digested DRL1B, (4): digested DRL2C, (6): digested p6i vector; specific products of ± 3 300 bp (lower) and ± 8 900 bp (higher) labelled with an arrow.

Table 27: Concentration and A260/A280 ratio of binary vector pSH91/gRNA-p6i.

	DRO1			**DRO2**			**DRL1**			
Sample	A	B	C	A	B	C	A	B	C	D
Concentration [ng·µl^{-1}]	274	308	276	16	468	265	275	366	351	44
A260/A280	1,84	1,85	1,84	1,79	1,84	1,84	1,86	1,84	1,85	1,86

The samples were cut by *Not*I_HF restriction enzyme. Samples DRO1A, DRO1B, DRO1C, DRO2C, DRL1A, DRL1B and DRL1C showed expected 4 bands 1 298 bp, 1 541 bp, 5 605 bp, 9 172 bp long. Sample DRO2B showed unspecific products that did not match expected length. DRL1D lacked 1 298 bp and 1 541 bp long bands and DRO2A, as its concentration hinted, showed no result (Fig. 36).

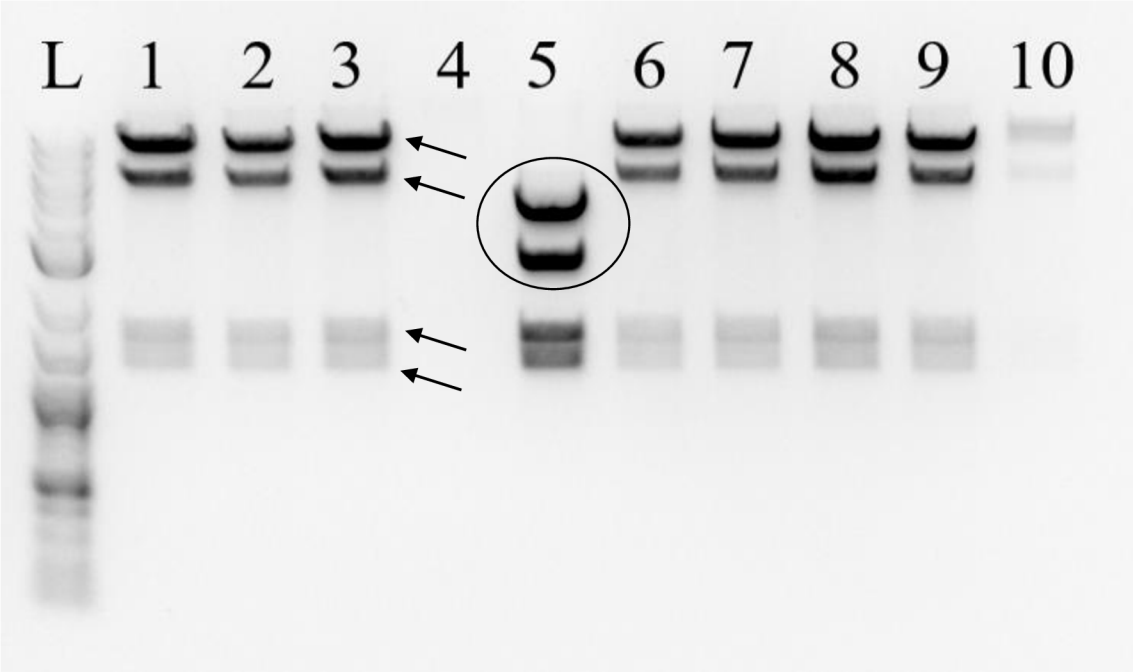

Figure 36: Cleavage of the binary vector by *Not*I_HF restriction enzyme.
Legend: (L): standard GeneRuler 1kb Plus DNA ladder, (1): DRO1A, (2): DRO1B, (3): DRO1C, (4): DRO2A, (5): DRO2B, (6): DRO2C, (7): DRL1A, (8): DRL1B, (9): DRL1C, (10): DRL1D; specific products are labelled with an arrow, from the bottom: 1 298 bp, 1 541 bp, 5 605 bp, 9 172 bp; nonspecific products are encircled.

5.4.4 Transformation of *Agrobacterium tumefaciens* by binary vector

DRO1A, DRO1B, DRO1C, DRO2C, DRL1A, DRL1B and DRL1C samples were after positive sequencing selected for transformation of *Agrobacterium tumefaciens* AGL1.

For plasmid isolation, 3 grown colonies were selected for samples DRO1A and DRL1A, plasmid of remaining samples was isolated from 2 colonies. Concentrations of purified plasmids are in Table 28.

Isolation of first and second colony of DRO1A sample same as second colony of DRL1B sample was not successful as measured concentration was very low and therefore these samples were not included in further transformation of *Escherichia coli*.

Plasmids isolated from transformed *E. coli* (concentration in Tab. 29) and cleaved by *Not*I_HF and *Kpn*I_HF restriction enzymes all showed bands of expected length (Fig. 37). Samples DRO1A3, DRO1B2, DRO1C1, DRO2C2, DRL1A2, DRL1B1 and DRL1C1 were sent for sequencing and based on results glycerol stocks of DRO1A3, DRO2C2 and DRL1A2 were used for transformation of immature embryos.

Table 28: Concentration of pSH91/gRNA-p6i vector isolated from *A. tumefaciens.*

	DRO1 A			**DRO1 B**		**DRO1 C**		**DRO2 C**		**DRL1 A**			**DRL1 B**		**DRL1 C**	
Sample	1	2	3	1	2	1	2	1	2	1	2	3	1	2	1	2
Concentration [ng·µl^{-1}]	0	0	46	127	101	98	46	124	183	69	22	32	225	9	35	28

Table 29: Concentration of pSH91/gRNA-p6i transferred to *A. tumefaciens*, isolated from *E. coli*.

	DRO1 A	**DRO1 B**		**DRO1 C**		**DRO2 C**		**DRL1 A**			**DRL1 B**	**DRL1 C**	
Sample	3	1	2	1	2	1	2	1	2	3	1	1	2
Concentration [ng·µl^{-1}]	233	286	293	266	245	299	311	320	376	275	205	269	320

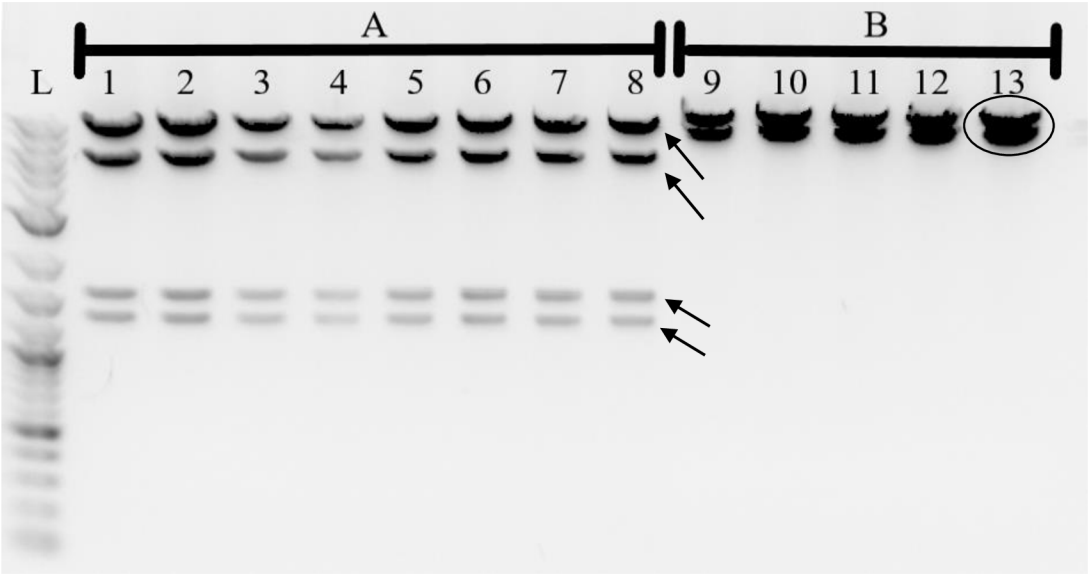

Figure 37: Binary vector isolated from *A. tumefaciens* and *E. coli* restricted by *Not*I_HF and *Kpn*I_HF enzymes.

Legend: (L): standard GeneRuler 1kb Plus DNA ladder, (A): samples cleaved by *Not*I_HF, (B): samples cleaved by *Kpn*I_HF, (1): DRL1A1, (2): DRL1A2, (3) DRL1A3, (4) DRL1B1, (5): DRL1C1, (6): DRL1C2, (7): DRO1A3, (8): DRO1B1, (9): DRO1B2, (10): DRO1C1, (11): DRO1C2, (12): DRO2C1, (13): DRO2C2; specific products for *Not*I_HF are labelled with an arrow, from the bottom: 1 298 bp, 1 541 bp, 5 605 bp, 9 172 bp; specific products for *Kpn*I_HF are encircled, 2 bands over 7 000 bp.

5.4.5 Genotyping of transformed barley

Total number of 105 plants, 39 plants for DRL1, 33 for DRO1 and 33 for DRO2, was tested for transformation by binary vector via PCR with specific primers. For OsU3p/U3t primers, 6 plants transformed by DRL1 were positive, 17 DRO1 plants were positive and 28 DRO2 plants were positive, 51 in total. For hygromycin 17 plants were positive: 1 for DRL1, 8 for DRO1 and 8 for DRO2. Only 5 plants out of 105 were positive for Cas9 sequence, 1 transformed by DRL1 and 4 by DRO2, which makes 4,76% transformation successfulness. No plant transformed by DRO1 gRNA was positive in Cas9 sequence. All the samples positive for Hygromycin were positive for OsU3p/t and all five samples positive for Cas9 were also positive in Hygromycin sequence. Samples with specific product for each set of primers are showed in figures 38, 39 and 40. Each sample positive in at least 2 out of 3 tested primers

(17 samples) was sent for sequencing. DECODR v3.0 software predicted that 3 base deletion occurred in 1 sample of DRO2-transformed plants, sample DRO2/S_4 3 (Fig. 41).

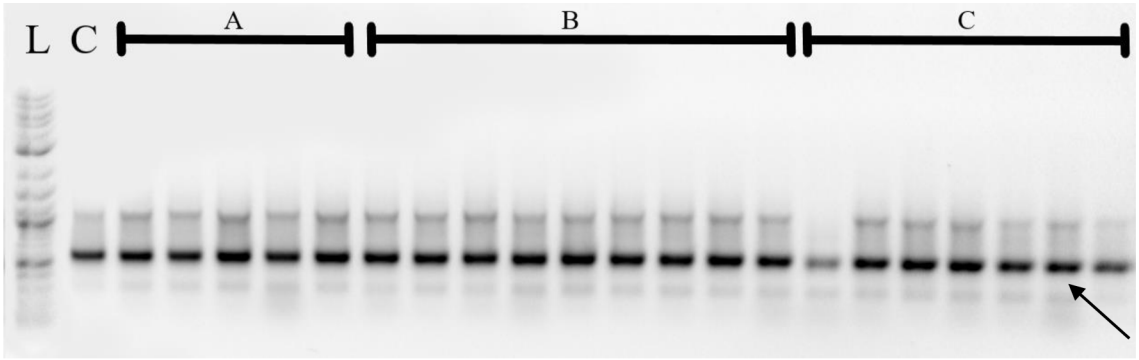

Figure 38: Amplification with OsU3p/U3t primers.

Legend: (L): standard GeneRuler 1kb Plus DNA ladder, (C) positive control - DRO2 construct ligated in pSH91, (A): DRL1 samples, (B): DRO1 samples, (C): DRO2 samples; specific band of the mutated sample DRO2/S_4 3 is labelled with an arrow, 571−572 bp long.

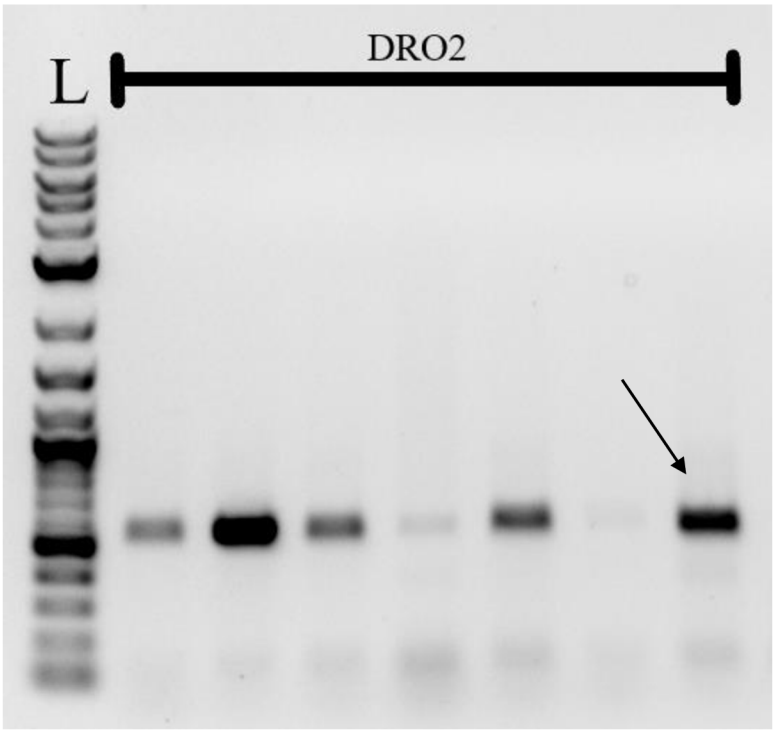

Figure 39: Amplification of DRO2 samples with the use of Hygromycin primers.

Legend: (L): standard GeneRuler 1kb Plus DNA ladder; specific band of the mutated sample DRO2/S_4 3 is labelled with an arrow, 556 bp long.

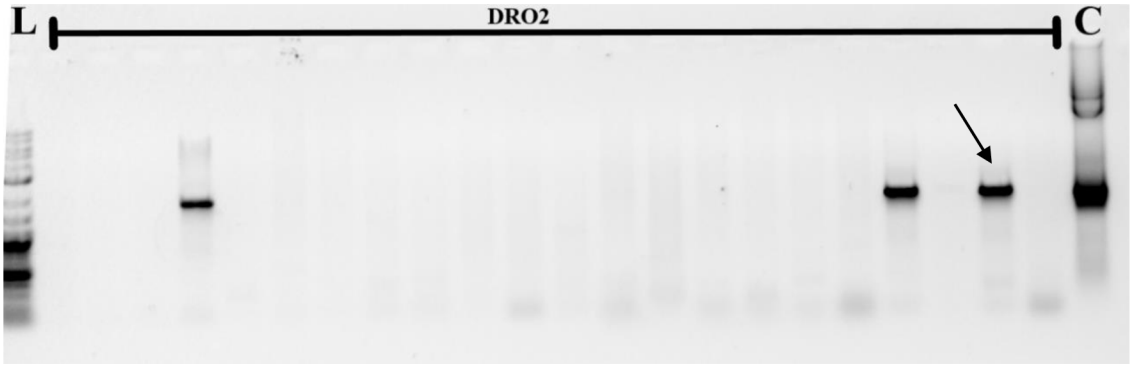

Figure 40: Amplification of DRO2 samples with the use of Ubi_F4/zCas9 primers.
Legend: (L): standard GeneRuler 1kb Plus DNA ladder, (C) positive control - DRO2 construct ligated in pSH91; specific band of the mutated sample DRO2/S_4 3 is labelled with an arrow, 1 594 bp long.

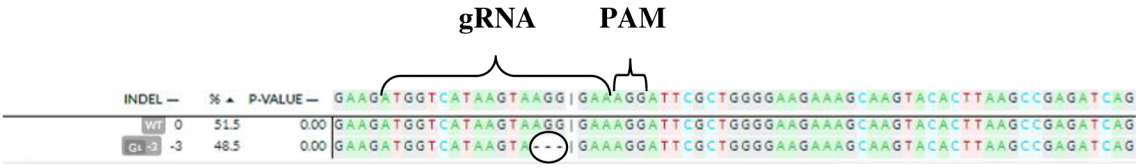

Figure 41: Predicted 3 base deletion of DRO2 S_4 3 sample (sequence in a last row) by Decodr v3 software. Deletion is encircled. Legend: (WT): wild-type sequence.

No visible difference in the phenotype of plant above-ground part was observed between plant carrying mutation and plant without mutation (Fig. 42).
Plant with mutation DRO2/S_4 3 was 61,5 cm high and 4,5 cm wide. Plant DRO2/S_4 2 that was positive in OsU3p/U3t and Hygromycin set of primers but negative in Cas9 primers was 68 cm high and 5 cm wide. Number and density of stems was similar.

Figure 42: Transformed barley 91 days old. On the left: plant DRO2/S_4 2 without mutation; on the right: plant DRO2/S_4 3 carrying 3-base deletion.

6 DISCUSSION

For the past few decades, due to changing climate plants are more often exposed to harsh and stressful conditions such as floods, temperature fluctuation, or long periods of droughts, which in agriculture negatively affects crop yield. Focus of many scientists across the world is on producing more sustainable crops with higher yield in challenging environment, as increasing growth of population demands more sophisticated supply of food. In the last 40 years of 20th century, worldwide production of grain doubled thanks to progress in agronomic practice and molecular biology. Study of genotype, rather than phenotype, helped for better understanding of a plant development and its cellular pathways, response to stressful stimulus and variety of pathogens on a molecular level, and especially to identify molecular markers and QTL related to specific traits of interest and to study their function in organism. The newest method CRISPR/Cas9 allows researchers to precisely edit DNA of studied organism. For importance of this tool speaks a fact, that pioneers of this technology won a Nobel prize in chemistry in 2020, less than 10 years from its discovery (NP, 2023). Just recently, among other features studied for potential association with yield increase, plant´s root architecture received more attention of researchers. Roots are not only mechanical support of above-ground part of a plant, but also play a vital role in exploring and acquiring resources from the soil. Spatial distribution of root system and its growth angle is closely related to that, as some nutrients and water tend to be in a deeper levels of soil, and hence plant with deeper root system could exploit these resources and be less prone to drought (Barber, 1995; Lynch, 1995; Khush, 2001; Manschadi *et al.*, 2008; Godfray *et al.*, 2010; Uga *et al.*, 2013; Arora, 2019; Nawaz & Chung, 2020).

In this work, we used IPK Galaxy Blast Suite to identify putative homologs of rice genes Os*DRO1* (Os09g0439800) and *qSOR1/DRL1* (Os07g0614400) in two barley cultivars Golden Promise and Morex v3. Gene Os*DRO1* plays a role in drought tolerance by affecting root growth angle (Uga *et al.*, 2013), while *qSOR/DRL1* is associated with root system architecture (Kitomi, *et al.*, 2020). Barley (*Hordeum vulgare* L.) was selected as a close ortholog to rice (*Oryza sativa* L.), additionally rice homologs of drought-tolerance genes have already been identified in barley (Fedorowicz-Stronska *et al.*, 2017).

Putative homologs Hv*DRO1* and Hv*DRL1* for Morex cultivar (Os*DRO1*: 81,6% identity, Os*DRL1*: 94,7% identity) and for Golden Promise cv. (Os*DRO1*: 81,5% identity, Os*DRL1*: 94,7% identity) (Tab. 22) differed only in 0,01 % of sequence, suggesting that the sequence of both targets is potentially stable across the genotypes.

In the next experimental part of this thesis, we focused on three different genotypes of barley: cv. Golden Promise, cv. Maythorpe and the landrace HOR1122. The cv. Golden Promise was chosen as it is the model for immature embryo transformation via *Agrobacterium tumefaciens*. Golden Promise is a gamma-ray induced mutant of cultivar Maythorpe and was selected for its desirable agronomic traits such as short stature and earliness, and became a popular malting variety. Moreover, screening experiment conducted at the Scottish Crop Research Institute uncovered that Golden Promise was more tolerant to salt (Forster, 2001; Walia *et al.*, 2007). The landrace HOR1122 was chosen based on GWAS conducted in the laboratory aiming to unravel new QTL related to root growth development under osmotic stress. In this experiment, HOR1122 showed to have large root angle and to be sensitive to drought as shown by shorter root length (data not shown; Khodaeiaminjan *et al.*, 2023). They were grown *in vitro* on ½ MS medium, in order to measure their contrasted root angles. Grown plants were easily and fast scanned and their root growth angle measured. Experiment was restarted several times due to occurrence of contamination, despite thorough sterilization. Measured angles showed relatively high standard deviation (18,4 for GP; 16,1 for #181 and 8,7 for Maythorpe). This could have been a result of the small size of Petri dish where the plants were cultivated, as already proposed by Bengough *et al*. (2004) and Hargreaves *et al.* (2009) as one of the cons of this technique, because the roots of different samples often overlapped and could potentially interfered with the root growth. Moreover, aluminium foil used to cover bottom half of Petri dish could not fully prevent root exposure to light, and therefore roots did not grow in same conditions as they would in natural environment (Xu *et al.*, 2013). However, for the purpose of this thesis the condition of experiment was satisfactory. Golden Promise and Maythorpe cultivars were selected for further gene expression study because they showed narrow angle (GP 45,5 °; Maythorpe 37,9 °), that is supposedly associated with the genes of our interest *DRO1* and *DRL1* (Uga *et al.*, 2013; Kitomi *et al.*, 2020).

The expression of Hv*DRO1* and Hv*DRL1* genes was measured in the crown of barley cultivars Golden Promise and Maythorpe by extracting RNA and running qPCR with synthetized cDNA (Fig. 33, 34). Plants were cultivated in mini-hydropony following specific kinetics (chapter 4.5.2.2.1). In one hand, determined expression of Hv*DRO1* gene showed no significant changes and divergence across the samples in both cultivars. On the other hand, transcript of Hv*DRL1* gene was not detected in the crown of seedlings before treatment with 50 µM of 1-NAA (sample T0-days), nor after the 48 hours treatment (sample T2-days). The potential explanation is, that the gene is not expressed in selected plant organ after our chosen kinetics. Nevertheless, Kitomi *et al.* (2020) proved, that Os*DRL1* is regulated by auxin, and is mostly expressed in root tips and the shoot base with crown root primordia. The accumulation of Hv*DRL1* transcript in sample T3-days corresponds with observed CR primordium. That suggests plausible explanation, that in samples T0-days and T2-days primordium was not yet formed and the gene expressed. However, to confirm this hypothesis and to determine the different phases of root meristem development, histology study should be made, and potentially followed by fluorescent *in situ* hybridisation targeting Hv*DRL1* and Hv*DRO1*. The fact, that expression of Hv*DRO1* was detected in samples T0-days and T2-days unlike Hv*DRL1* is with agreement of Kitomi *et al.* (2020), as they proposed that these two genes might be expressed in rice in different tissues. The dissimilarity in barley may be even bigger.

Overall, the expression was higher in Maythorpe cultivar in both genes. No association with screened root growth angles and gene expression was observed, as detected expression was too weak and difference between the two cultivars too little to make any conclusions.

In the final part of experimental section of this thesis was performed CRISPR/Cas^9 mediated knock-out in order to prepare mutated T_0 plants for further study of function of Hv*DRO1* and Hv*DRL1* genes. This approach of gene editing and targeted mutation is becoming more popular and promise a long-term solution to agriculture problems (Nawaz and Chung, 2020).

Designed gRNAs for each gene were successfully inserted into pSH91 cloning vector (Fig. 39, 40). Isolated vector from *E. coli* pSH91/gRNA and p6i vector were successfully cleaved by *Sfi*I_HF restriction enzyme (Fig. 41) and attempted to ligate. After transformation of *E. coli* with ligated product, on plate concerning gRNA sample

named DRL2 did not grow a single colony of bacteria. The error might have occurred in ligation step, or in step of transformation by heat-shock, but as a result *Escherichia coli* did not bear plasmid containing gene for Spectinomycin resistance and therefore could not grow on selective media with 50 $mg \cdot dm^{-3}$ of Spectinomycin antibiotic. Remaining gRNAs in pSH91 were successfully ligated with p6i, creating binary vector, by which was transformed *Agrobacterium tumefaciens* strain AGL1. Successful transformation was verified by restriction enzyme *Not*I and by Sanger sequencing. The AGL1 strain of Agrobacterium tumefaciens served for transformation of immature Golden Promise cv. barley embryos, that were later genotyped using specific primers, to determine successfulness of transformation and possible occurrence of mutation caused by CRISPR/Cas^9 construct.

Only 5 plants out of 105 (4,76 %) were successfully transformed by AGL1 carrying CRISPR/Cas^9 construct. This low rate of transformation could have been caused by poor quality of embryos, that were over a year old by the time of transformation. In DRO2 S_4 3 sample was predicted 3-base deletion in the Hv*DRO1* gene, that was 3 bp upstream of PAM sequence, which corresponds with findings of Fischer *et al.* (2012). Mutation occurred in 1 out of 5 plants, that were tested positive for Cas^9 sequence, which makes a high 20% success rate. This only proves the efficiency and usefulness of a CRISPR/Cas^9 tool (Doudna & Charpentier, 2014).

By comparing phenotype of DRO2 S_4 3 with a sample DRO2 S_4 2, that tested positive in Cas^9 sequence, but did not bear a mutation, was not found any differences. Mutation had no effect on morphology of above-part of a plant. Underground part was not phenotyped, because invasive nature of a screening method could cause stress and potential harm to the plant, that is going to be a subject of further studies.

Whether the mutation led to knock-out of the Hv*DRO1* gene, and potentially increased tolerance of barley to drought, like it was observed in rice (Uga *et al.*, 2013), is the potential subject of future studies.

7 CONCLUSION

Putative homologs of rice genes Os*DRO1* and *qSOR1/DRL1* were identified in barley, showing 81,6% and 94,7% identity. Three barley cultivars were cultivated *in vitro,* and their root growth angle was measured (the landrace HOR1122: 53,8 °; cv. GP: 45,5 °; cv. Maythorpe: 37,9 °). After treatment of auxin-based inducible system, in mini-hydropony grown plants of cv. GP and cv. Maythorpe was detected a basal level of expression of the Hv*DRO1* gene in all studied crown samples. The expression of the Hv*DRL1* gene was not observed in the beginning of the crown-root initiation and development. First accumulation of its transcript was detected 3 days after auxin treatment and at this moment, visible "buds" at the crown surface were observed. The expression of *HvDRL1* gene then remained constant for the duration of the experiment. The two cultivars did not show any significant difference in expression of Hv*DRO1* and Hv*DRL1*.

Five plants were successfully transformed by AGL1 strain containing CRISPR/Cas9 construct. One T_0 plant was predicted to bear a 3-base deletion in the Hv*DRO1* gene, located 3 bp upstream of PAM sequence. No morphology difference was observed between mutated and nonmutated above-ground part of plants. The effect of the deletion in the Hv*DRO1* gene on the root system architecture and overall, the plant fitness will be studied in the next plant generation.

Identifying more genes and learning their function is desired in order to produce plants adapted to nowadays needs and challenges.

8 REFERENCES

Abas L., Benjamins R., Malenica N., Paciorek T., Wiśniewska J., Moulinier-Anzola J. C., Sieberer T., Friml J., Luschnig C. (2006): Intracellular trafficking and proteolysis of the *Arabidopsis* auxin-efflux facilitator PIN2 are involved in root gravitropism. Nature cell biology, 8: 249–256.

Arite T., Kameoka H., Kyozuka J. (2012): Strigolactone positively controls crown root elongation in rice. Journal of Plant Growth Regulation, 31 :165–172.

Arora N.K. (2019): Impact of Climate Change on Agriculture Production and Its Sustainable Solutions. Environment, Development and Sustainability, 2: 95–96.

Aziz A. A., Lim K. B., Rahman E. K. A., Nurmawati M. H., Zuruzi A. S. (2020) Agar with embedded channels to study root growth. Scientific Reports, 10: 14231.

Bailey D. W. (1971): Recombinant-inbred strains. An aid to finding identity, linkage, and function of histocompatibility and other genes. Transplantation, 11: 325–327.

Barber, S. A. (1995): Soil Nutrient Bioavailability: A Mechanistic Approach. 2nd Edition, John Wiley, New York.

Bates G. H. (1937): A device for the observation of root growth in the soil. Nature 139: 966-967.

Bellini C., Pacurar D. I., Perrone I. (2014): Adventitious Roots and Lateral Roots: Similarities and Differences. Annual Review of Plant Biology 65: 639−666.

Bengough A. G., Gordon D. C., Al-Menaie H., Ellis R. P., Allan D., Keith R., *et al.* (2004): Gel observation chamber for rapid screening of root traits in cereal seedlings. Plant and Soil, 262: 63−70.

Bian H. W., Xie Y. K., Guo F., Han N., Ma S., Zeng Z., Wang J., Yang Y., Zhu M. (2012): Distinctive expression patterns and roles of the miRNA393/TIR1 homolog module in regulating flag leaf inclination and primary and crown root growth in rice. (*Oryza sativa* L.). New Phytologist, 196: 149–161.

Bloh K., Kanchana R., Bialk P., Banas K., Zhang Z., Yoo B. C., Kmiec E. B. (2021): Deconvolution of Complex DNA Repair (DECODR): Establishing a Novel Deconvolution Algorithm for Comprehensive Analysis of CRISPR-Edited Sanger Sequencing Data. The CRISPR journal, 4: 120–131.

Boonsirichai K., Sedbrook J. C., Chen R., Gilroy S., Masson P. H. (2003): Altered response to gravity is a peripheral membrane protein that modulates gravity-induced cytoplasmic alkalinization and lateral auxin transport in plant statocytes. Plant Cell, 15: 2612–2625.

Bortesi L., & Fischer R. (2015): The CRISPR/Cas9 system for plant genome editing and beyond. Biotechnology Advances, 33: 41–52.

Budhagatapalli N., Schedel S., Gurushidze M., Pencs S., Hiekel S., Rutten T., *et al.* (2016): A simple test for the cleavage activity of customized endonucleases in plants. Plant Methods, 12: 6.

Chen X., Shi J., Hao X., Liu H., Shi J., Wu Y., Wu Z., Chen M., Wu P., Mao C. (2013): OsORC3 is required for lateral root development in rice. Plant Journal, 74: 339–350.

Cho S. H., Yoo S. C., Zhang H., Pandeya D., Koh H. J., Hwang J. Y., Kim G. T., Paek N. C. (2013): The rice narrow leaf2 and narrow leaf3 loci encode WUSCHEL–related homeobox 3A (OsWOX3A) and function in leaf, spikelet, tiller and lateral root development. New Phytologist, 198: 1071–1084.

Cho S. H., Yoo S. C., Zhang H., Lim J. H., Paek N. C. (2014): Rice narrow leaf1 regulates leaf and adventitious root development. Plant Molecular Biology Reporter, 32: 270–281.

Concordet J. & Haeussler M. (2018): CRISPOR: intuitive guide selection for CRISPR/Cas9 genome editing experiments and screens, Nucleic Acids Research, 46: 242–245.

Coudert Y., Perin C., Courtois B., Khong N. G., Gantet P. (2010): Genetic control of root development in rice, the model cereal. Trends in Plant Science 15: 219–226.

Cui P., Liu H., Ruan S., Ali B., Gill R. A., Ma H., Zheng Z., Zhou W. (2017): A zinc finger protein, interacted with cyclophilin, affects root development via IAA pathway in rice. Journal of Integrative Plant Biology, 59: 496–505.

Doudna J. A., Charpentier E. (2014): Genome editing. The new frontier of genome engineering with CRISPR-Cas9. Science, 346.

Dun E. A., Brewer P. B., Beveridge C. A. (2009): Strigolactones: discovery of the elusive shoot branching hormone. Trends in Plant Science, 14: 364–72.

Drew M. C., Saker L. R., Ashley T. W. (1973): Nutrient supply and the growth of the seminal root system in barley I. Journal of Experimental Botany 24: 1189−1202.

Ennos A. R., Fitter A. H. (1992): Comparative functional morphology of the anchorage systems of annual dicots. Functional Ecology 6: 71−78.

Fedorowicz-Strońska O., Koczyk G., Kaczmarek M., Krajewski P., Sadowski J. (2017): Genome-wide identification, characterisation, and expression profiles of calcium-dependent protein kinase genes in barley (*Hordeum vulgare* L.). Journal of Applied Genetics, 58: 11−22.

Feng S., Shen Y., Sullivan J. A., Rubio V., Xiong Y., Sun T. P., Deng X. W. (2004): Arabidopsis CAND1, an unmodified CUL1-interacting protein, is involved in multiple developmental pathways controlled by ubiquitin/proteasome-mediated protein degradation. Plant and Cell, 16: 1870−1882.

Fire A., Xu S., Montgomery M. K., Kostas S. A., Driver S. E., Mello C. C. (1998): Potent and specific genetic interference by double-stranded RNA in *Caenorhabditis elegans*. Nature, 391: 806–811.

Fischer S., Maier L. K., Stoll B., Brendel J., Fischer E., Pfeiffer F., Dyall-Smith M., & Marchfelder A. (2012): An archaeal immune system can detect multiple protospacer adjacent motifs (PAMs) to target invader DNA. Journal of Biological Chemistry, 287: 33351–33365.

Fogel R. (1985): Roots as primary producers in below ground ecosystems. In A. H. Fitter, D. Atkinson, D. J. Read, M. B. Usher, eds. Ecological interaction in soil plants, microbes and animals. British Ecological Society, Blackwell Scientific Publications, 23−26.

Forster B. P. (2001): Mutation genetics of salt tolerance in barley: An assessment of Golden Promise and other semi-dwarf mutants. Euphytica, 120: 317–328.

Gahoonia T. S., Nielsen N. E. (2004): Barley genotypes with long root hairs sustain high grain yields in low-P field. Plant and Soil, 262: 55–62.

Gao S., Fang J., Xu F., Wang W., Sun X., Chu J., Cai B., Feng Y., Chu C. (2014): Cytokinin oxidase/dehydrogenase 4 integrates cytokinin and auxin signalling to control rice crown root formation. Plant Physiology, 165: 1035–1046.

Godfray H. C. J., Beddington J. R., Crute I. R., Haddad L., Lawrence D., Muir J. F., Pretty J., Robinson S., Thomas S. M., & Toulmin C. (2010): Food security: The challenge of feeding 9 billion people. Science, 327: 812–818.

Goffinet B., Gerber S. (2000): Quantitative trait loci: a meta-analysis. Genetics, 155: 463–473.

Gowda V. R. P., Henry A., Yamauchi A., Shashidha H. E., Serraj R. (2011): Root biology and genetic improvement for drought avoidance in rice. Field Crops Research, 122: 1−13.

Gregory P. J., Hutchison D. J., Read D. B., Jenneson P. M., Gilboy W. B., Morton E. J. (2003): Non-invasive imaging of roots with high resolution X-ray microtomography. Plant and Soil, 255: 351−9.

Han H. (2018): RNA Interference to Knock Down Gene Expression. Methods of Molecular Biology, 1706: 293−302.

Hasan N., Choudhary S., Naaz N. *et al.* (2021): Recent advancements in molecular marker-assisted selection and applications in plant breeding programmes. Journal of Genetic Engineering and Biotechnology, 19: 128−154.

Havlin, J. L., Beaton, J. D., Tisdale, S. L., Nelson, W. L. (2013): Soil Fertility and Fertilizers: An Introduction to Nutrient Management. 8th Edition, Pearson Educational, Inc., New Jersey.

Hargreaves C., Gregory P., Bengough A. G. (2009): Measuring root traits in barley (*Hordeum vulgare* ssp. *vulgare* and ssp. *spontaneum*) seedlings using gel chambers, soil sacs and X-ray microtomography. Plant and Soil, 316: 285−297.

Hodge A. (2004): The plastic plant: root responses to heterogeneous supplies of nutrients. New Phytologist 162, 9–24.

Hsu Y. Y., Chao Y. Y., Kao C. H. (2012): Methyl jasmonate-induced lateral root formation in rice: the role of heme oxygenase and calcium. Journal of Plant Physiology, 170: 63–69.

Huang C. T., Klos K. E., Huang Y. F. (2020): Genome-Wide Association Study Reveals the Genetic Architecture of Seed Vigor in Oats. G3 (Bethesda), 10: 4489−4503.

Inukai Y., Sakamoto T., Ueguchi-Tanaka M., Shibata Y., Gomi K., Umemura I., Hasegawa Y., Ashikari M., Kitano H., Matsuoka M. (2005): CROWN ROOTLESS1, which is essential for crown root formation in rice, is a target of an AUXIN RESPONSE FACTOR in auxin signalling. Plant Cell, 17: 1387–1396.

Jia L., Zhang B., Mao C., Li J., Wu Y., Wu P., Wu Z. (2008): OsCYT-INV1 for alkaline/neutral invertase is involved in root cell development and reproductivity in rice (*Oryza sativa* L.). Planta, 228: 51–59.

Jiang H., Wang S., Dang L., Wang S., Chen H., Wu Y., Jiang X., Wu P. (2005): A novel short-root gene encodes a glucosamine-6-phosphate acetyltransferase required for maintaining normal root cell shape in rice. Plant Physiology, 138: 232–242.

Johnson M. G., Meyer P. F. (1998): Mechanical advancing handle that simplifies minirhizotron camera registration and image collection. Journal of Environmental Quality 27: 710−714.

Johnson M. G., Tingey D. T., Phillips D. L., Storm M. J. (2001): Advancing fine root research with minirhizotrons. Environmental and Experimental Botany 45: 263−289.

Joslin J. D., Gaudinski J. B., Torn M. S., Riley W. J., Hanson P. J. (2006): Fine-root turnover patterns and their relationship to root diameter and soil depth in a 14C-labeled hardwood forest. New Phytology 172: 523–535.

Kang B., Zhang Z., Wang L., Zheng L., Mao W., Li M., Wu Y., Wu P., Mo X. (2013): OsCYP2, a chaperone involved in degradation of auxin–responsive proteins, plays crucial roles in rice lateral root initiation. Plant Journal 74:86–97.

Khan S., Purohit A., & Vadsaria N. (2021): Hydroponics: current and future state of the art in farming, Journal of Plant Nutrition, 44: 1515−1538.

Khodaeiaminjan M., Knoch D., Ndella Thiaw M. R., Marchetti C. F., Kořínková N., Techer A., Nguyen T. D., Chu J., Bertholomey V., Doridant I., Gantet P., Graner A., Neumann K., & Bergougnoux V. (2023): Genome-wide association study in two-row spring barley landraces identifies QTL associated with plantlets root system architecture traits in well-watered and osmotic stress conditions. Frontiers in Plant Science, 14: 1125672.

Khush G. (2001): Green revolution: the way forward. Nature Reviews Genetics, 2: 815–822.

Kitomi Y., Ogawa A., Kitano H., Inukai Y. (2008): CRL4 regulates crown root formation through auxin transport in rice. Plant Root, 2: 19−28.

Kitomi Y., Ito H., Hobo T., Aya K., Kitano H., Inukai Y. (2011): The auxin responsive AP2/ERF transcription factor CROWNROOTLESS5 is involved in crown root initiation in rice through the induction of OsRR1, a type-a response regulator of cytokinin signalling. Plant Journal, 67: 472–484.

Koiwai H., Tagiri A., Katoh S., Katoh E., Ichikawa H., Minami E., Nishizawa Y. (2007): RING-H2 type ubiquitin ligase EL5 is involved in root development through the maintenance of cell viability in rice. Plant Journal, 51: 92–104.

Kumar R., Kaur A., Pandey A., Mamrutha H. M., Singh G. P. (2019): CRISPR-based genome editing in wheat: a comprehensive review and future prospects, 46: 3557-3569.

Laplaze L., Benkova E., Casimiro I., Maes L., Vanneste S., Swarup R., Weijers D., Calvo V., Parizot B., Herrera-Rodriguez M. B., Offringa R., Graham N., Doumas P., Friml J., Bogusz D., Beeckman T., Bennett M. (2007): Cytokinins act directly on lateral root founder cells to inhibit root initiation. The Plant Cell, 19: 3889−3900.

Lavenus J., Goh T., Roberts I., Guyomarc'h S., Lucas M., De Smet I., Fukaki H., Beeckman T., Bennett M., Laplaze L. (2013): Lateral root development in Arabidopsis: fifty shades of auxin. Trends in plant science, 18: 450–458.

Li J., Zhu S., Song X., Shen Y., Chen H., Yu J., Yi K., Liu Y., Karplus V. J., Wu P., Deng X. W. (2006): A rice glutamate receptor-like gene is critical for the division and survival of individual cells in the root apical meristem. Plant Cell, 18: 340–349.

Li J., Han Y., Liu L., Chen Y., Du Y., Zhang J., Sun H., Zhao Q. (2015): qRT9, a quantitative trait locus controlling root thickness and root length in upland rice. Journal of Experimental Botany, 66: 2723–2732.

Liu H., Wang S., Yu X., Yu J., He X., Zhang S., Shou H., Wu P. (2005): ARL1, a LOB-domain protein required for adventitious root formation in rice. Plant Journal, 43: 47–56,

Liu S., Wang J., Wang L., Wang X., Xue Y., Wu P., Shou H. (2009): Adventitious root formation in rice requires OsGNOM1 and is mediated by the OsPINs family. Cell Research, 19: 1110−1119.

Lontoc-Roy M., Dutilleul P., Prasher S., Liwen H., Brouillet T., Smith D. (2006): Advances in the acquisition and analysis of ct scan data to isolate a crop root system from the soil medium and quantify root system complexity in 3-d space. Geoderma Journal, 137: 231−41.

Lucas M., Godin C., Jay-Allemand C., Laplaze L. (2008): Auxin fluxes in the root apex co-regulate gravitropism and lateral root initiation. Journal of Experimental Botany, 59: 55−66.

Lynch J., van Beem J. (1993): Growth and architecture of seedling roots of common bean genotypes. Crop Science 33: 1253−1257.

Lynch J. P. (1995): Root Architecture and Plant Productivity. Plant Physiology, 109: 7−13.

Lynch J. P. (2013): Steep, cheap and deep: an ideotype to optimize water and N acquisition by maize root systems. Annals of Botany, 112, 347–357.

Lynch J. P. (2019): Root phenotypes for improved nutrient capture: an underexploited opportunity for global agriculture. New Phytologist, 223: 548–564.

Mairhofer S., Zappala S., Tracy S., Sturrock C., Bennett M. J., Mooney S. J., Pridmore T. P. (2013): Recovering complete plant root system architectures from soil via X-ray mu-computed tomography. Plant Methods, 9: 8.

Majdi H. (1996): Root sampling methods – Applications and limitations of the minirhizotron technique. Plant and Soil, 185: 255-258.

Malamy J. E. (2005): Intrinsic and environmental response pathways that regulate root system architecture. Plant Cell and Environment, 28: 67−77.

Manolio T. A. (2010): Genomewide association studies and assessment of the risk of disease. The New England Journal of Medicine, 363: 166–76.

Manschadi A. M., Christopher J., deVoil P., Hammer G. L. (2006): The role of root architectural traits in adaptation of wheat to water-limited environments. Functional Plant Biology, 33: 823−837.

Manschadi A. M., Hammer G. L., Christopher J. T., deVoil P. (2008): Genotypic variation in seedling root architectural traits and implications for drought adaptation in wheat (*Triticum aestivum* L.). Plant and Soil, 303: 115–129.

Mao C., Wang S., Jia Q., Wu P. (2006): OsEIL1, a rice homolog of the Arabidopsis EIN3 regulates the ethylene response as a positive component. Plant Molecular Biology, 61: 141–152.

Marthe C., Kumlehn J., Hensel G. (2015): Barley (*Hordeum vulgare* L.) transformation using immature embryos. Methods in molecular biology, 1223: 71–83.

McMichael B. L., Taylor H. M. (1987): Applications and limitations of rhizotrons and minirhizotrons. In: Taylor H. M. (ed): Minirhizotron observation tubes: methods and applications for measuring rhizosphere dynamics. American Society of Agronomy, Madison, 1−13.

Mori M., Nomura T., Ooka H., Ishizaka M., Yokota T., Sugimoto K., Okabe K., Kajiwara H., Satoh K., Yamamoto K., Hirochika H., Kikuchi S. (2002): Isolation and characterization of a rice dwarf mutant with a defect in brassinosteroids biosynthesis. Plant Physiology, 130: 1152–1161.

Mooney S. J., Pridmore T. P., Helliwell J., Bennett M. J. (2012): Developing X-ray computed tomography to non-invasively image 3-D root systems architecture in soil. Plant and Soil, 352: 1−22.

Morita M. T., Tasaka M. (2004): Gravity sensing and signaling. Current opinion in plant biology, 7: 712–718.

Morita M. T. (2010): Directional gravity sensing in gravitropism. Annual Review of Plant Biology, 61: 705–720.

Murashige T., Skoog F. (1962): A revised medium for rapid growth and bioassays with tobacco tissue cultures. Physiology of Plant, 15: 473–497.

Nagel K. A., Putz A., Gilmer F., Heinz K., Fischbach A., Pfeifer J., *et al*. (2012): GROWSCREEN-Rhizo is a novel phenotyping robot enabling simultaneous measurements of root and shoot growth for plants grown in soil-filled rhizotrons. Functional Plant Biology, 39: 891−904.

Nawaz M. A., & Chung G. (2020): Genetic Improvement of Cereals and Grain Legumes. Genes, 11: 1255−1263.

Neumann G., George T. S., Plassard C. (2009): Strategies and methods for studying the rhizosphere − the plant science toolbox. Plant and Soil, 321: 431–456.

Ni J., Wang G., Zhu Z., Zhang H., Wu Y., Wu P. (2011): OsIAA23-mediated auxin signaling defines postembryonic maintenance of QC in rice. Plant Journal, 68: 433–442.

Nishimasu H., Ran F. A., Hsu P. D., Konermann S., Shehata S. I., Dohmae N., Ishitani R., Zhang F., Nureki O. (2014): Crystal structure of Cas9 in complex with guide RNA and target DNA. Cell, 156: 935–949.

Oliviera M. R. G., van Noorwijk M., Gaze S. R., Brouwer G., Bona S., Mosca G., Hairiah K. (2000): Auger sampling, ingrowth cores and pinboard methods. In: Smit A. L., Sobotik M., eds. Root methods. Springer, Berlin Heidelberg, 175–210.

Ongaro V., Leyser O. (2008): Hormonal control of shoot branching. Journal of Experimental Botany, 59: 67–74.

Orman-Ligeza B., Parizot B., Gantet P. P., Beeckman T., Bennett M. J., Draye X. (2013): Post-embryonic root organogenesis in cereals: branching out from model plants. Trends in Plant Science, 18: 459−67.

Oyanagi A. (1994): Gravitropic response growth angle and vertical distribution of roots of wheat (*Triticum aestivum* L.). Plant and Soil 165: 323−326.

Pearson T. A., Manolio T. A. (2008): How to interpret a genome-wide association study. JAMA, 299: 1335–44.

Perret J. S., Al-Belushi M. E., Deadman N. (2007): Non-Destructive visualization and quantification of roots using computed tomography. Soil Biology and Biochemistry, 39: 391–399.

Pfaffl M. W. (2001): A new mathematical model for relative quantification in real-time RT-PCR. Nucleic acids research, 29: 45.

Pierret A., Moran C., Doussan C. (2005): Conventional detection methodology is limiting our ability to understand the roles and functions of fine roots. New Phytologist, 166: 967–980.

Pollard D. A. (2012): Design and construction of recombinant inbred lines. Methods in molecular biology, 871: 31–39.

Pritchard S. G., Rogers H. H. (2000): Spatial and temporal deployment of crop roots in CO2-enriched environments. New Phytologist, 147: 55−71.

Pritchard S. G., Strand A. E., McCormack M. L., Davis M. A., Oren R. (2008): Mycorrhizal and rhizomorph dynamics in a loblolly pine forest during 5 years of free-air-CO2-enrichment. Global Change Biology, 14: 1−13.

Qi Y., Wang S., Shen C., Zhang S., Chen Y., Xu Y., Liu Y., Wu Y., Jiang D. (2012): OsARF12, a transcription activator on auxin response gene, regulates root elongation and affects iron accumulation in rice (*Oryza sativa* L.). New Phytologist, 193: 109–120.

Qin C., Li Y., Gan J., Wang W., Zhang H., Liu Y., Wu P. (2013): OsDGL1, a homolog of an oligosaccharyltransferase complex subunit, is involved in N-glycosylation and root development in rice. Plant and Cell Physiology, 54: 129–137.

Ramirez-Carvajal G. A., Morse A. M., Dervinis C., Davis J. M. (2009): The cytokinin type-B response regulator PtRR13 is a negative regulator of adventitious root development in *Populus*. Plant Physiology, 150: 759−71.

Richard C. A., Hickey L. T., Fletcher S., Jennings R., Chenu K., Christopher J. T. (2015): High-throughput phenotyping of seminal root traits in wheat. Plant Methods, 11: 13.

Rosa C., Kuo Y. W., Yan Z., Falk B. W. (2018): RNA Interference mechanisms and applications in plant pathology. Annual review of Phytopathology, 56: 581–610.

Rundel P. W., Nobel P. S. (1991): Structure and function in desert root systems. In D. Atkinson, eds. Plant Root Growth: An Ecological Perspective. British Ecological Society, Blackwell Scientific Publications, 349−378.

Saad A. I. M., Elshahed A. M. (2012) Plant Tissue Culture Media. In: Leva A., Rinaldi L. M. R., Recent Advances in Plant in vitro Culture. InTech Open, 2: 29−40.

Schneider C. A., Rasband W. S., Eliceiri, K. W. (2012): NIH Image to ImageJ: 25 years of image analysis. Nature Methods, 9: 671–675.

Schindelin J., Arganda-Carreras I., Frise E., Kaynig V., Longair M., Pietzsch T., Tomancak P., Schmid B., Saalfeld S., Cardona, A., *et al.* (2012): Fiji: an open-source platform for biological-image analysis. Nature Methods, 9: 676–682.

Shafiq S., Chen C., Yang J., Cheng L., Ma F., Widemann E., Sun Q. (2017): DNA Topoisomerase 1 prevents R-loop accumulation to modulate auxin-regulated root development in rice. Molecular Plant, 10: 821–833.

Shelley I. J., Nishiuchi S., Shibata K., Inukai Y. (2013): SLL1, which encodes a member of the stearoyl-acyl carrier protein fatty acid desaturase family, is involved in cell elongation in lateral roots via regulation of fatty acid content in rice. Plant Science, 207: 12–17.

Sherman J. H., Munyikwa T., Chan S. Y., Petrick J. S., Witwer K. W. (2015): RNAi technologies in agricultural biotechnology: The Toxicology Forum 40th Annual Summer Meeting. Regulatory Toxicology and Pharmacology, 73: 671−680.

Shimizu-Sato S., Tanaka M., Mori H. (2009): Auxin-cytokinin interactions in the control of shoot branching. Plant molecular biology, 69: 429–435.

Smit A. L., Vamerali T. (1998): The influence of potato cyst nematodes (*Globodera pallida*) and drought on rooting dynamics of potato (*Solanum tuberosum L.*). Europeaan Journal of Agronomy, 9: 137−146.

Sun H., Tao J., Hou M., Huang S., Chen S., Liang Z., Xie T., Wei Y., Xie X., Yoneyama K., Xu G., Zhang Y. (2015): A strigolactone signal is required for adventitious root formation in rice. Annals of Botany, 115: 1155–1162.

Taina I. A., Heck R. J., Elliot T. R. (2008): Application of X-ray Computed Tomography to soil science: A literature review. Canadian Journal of Soil Science, 88: 1–19.

Thimann K. V., Skoog F. (1933): Studies on the Growth Hormone of Plants: III. The Inhibiting Action of the Growth Substance on Bud Development. Proceedings of the National Academy of Sciences of the United States of America, 19: 714–716.

Thorneycroft D., Sherson S. M., Smith S. M. (2001): Using gene knockouts to investigate plant metabolism. Journal of Experimental Botany, 361: 1593–1601.

Trachsel S., Kaeppler S., Brown K., Lynch J. (2011): Shovelomics: high throughput phenotyping of maize (*Zea mays* L.) root architecture in the field. Plant and Soil, 341: 75−87.

Uffelmann E., Huang Q. Q., Munung N. S., Vries de J., Okada Y., Martin A. R., Martin H. C., Lappalainen T., Posthuma D. (2021): Genome-wide association studies. Nature Reviews Methods Primers, 1: 59.

Uga Y., Okuno K., Yano M. (2011): Dro1, a major QTL involved in deep rooting of rice under upland field conditions. Journal of experimental botany, 62: 2485–2494.

Uga Y., Sugimoto K., Ogawa S., Rane J., Ishitani M., Hara N., Kitomi Y., Inukai Y., Ono K., Kanno N., Inoue H., Takehisa H., Motoyama R., Nagamura Y., Wu J., Matsumoto T., Takai T., Okuno K., Yano M. (2013): Control of root system architecture by DEEPER ROOTING 1 increases rice yield under drought conditions. Nature Genetics 45, 1097–1102.

Urnov F. D., Ronald P. C., Carroll D. (2018): A call for science-based review of the European court's decision on gene-edited crops. Nature Biotechnology, 36: 800–802.

Vamerali T., Ganis A., Bona S., Mosca G. (2003): Fibrous root turnover and growth in sugar beet (*Beta vulgaris* var *saccharifera*) as affected by nitrogen shortage. Plant and Soil, 255: 169−177.

Vamerali T., Bandiera M., Mosca G. (2011): Minirhizotrons in Modern Root Studies. In S. Mancuso, Measuring Roots. Springer Berlin, Heidelberg, 341−361.

Van Der Meer, P., Angenon, G., Bergmans, H., Buhk, H., Callebaut, S., Chamon, M., Zimny, T. (2023): The Status under EU Law of Organisms Developed through Novel Genomic Techniques. European Journal of Risk Regulation, 14: 93−112.

Vives-Vallés J. A., & Collonnier C. (2020): The Judgment of the CJEU of 25 July 2018 on Mutagenesis: Interpretation and Interim Legislative Proposal. Frontiers in Plant Science, 10.

Wahbi A., Gregory, P. J. (1995): Growth and development of young roots of barley (*Hordeum Vulgare* L.) genotypes. Annals of Botany, 75: 533–539.

Walia H., Wilson C., Condamine P. *et al.* (2007): Array-based genotyping and expression analysis of barley cv. Maythorpe and Golden Promise. BMC Genomics, 8: 87.

Wang X. F., He F. F., Ma X. X., Mao C. Z., Hodgman C., Lu C. G., Wu P. (2011): OsCAND1 is required for crown root emergence in rice. Molecular Plant, 4: 289–299.

Wang S., Xu Y., Li Z., Zhang S., Lim J. M., Lee K. O., Li C., Qian Q., Jiang A., Qi Y. (2014a): OsMOGS is required for N-glycan formation and auxin-mediated root development in rice (*Oryza sativa* L.). Plant Journal, 78: 632–645.

Wang Y., Ma N., Qiu S., Zou H., Zang G., Kang Z., Wang G., Huang J. (2014b): Regulation of the α-expansin gene OsEXPA8 expression affects root system architecture in transgenic rice plants. Molecular Breeding, 34: 47–57.

Wang Y., Wang D., Gan T., Liu L., Long W., Wang Y., Niu M., Li X., Zheng M., Jiang L., Wan J. (2016): CRL6, a member of the CHD protein family, is required for crown root development in rice. Plant Physiology and Biochemistry, 105: 185–194.

Wilson R. C., & Doudna, J. A. (2013): Molecular mechanisms of RNA interference. Annual review of biophysics, 42: 217–239.

Withers P. J., Bouman C., Carmignato S., Cnudde V., Grimaldi D., Hagen C. K., Maire E., Manley M., Du Plessis A., Stock S. R. (2021): X-ray computed tomography. Nature Reviews Methods Primers, 1: 18.

Xia J., Yamaji N., Che J., Shen R. F., Ma J. F. (2014): Normal root elongation requires arginine produced by argininosuccinate lyase in rice. Plant Journal, 78: 215–226.

Xu W., Ding G., Yokawa K., Baluška F., Li Q., Liu Y., Shi W., Liang J., Zhang J. (2013): An improved agar-plate method for studying root growth and response of *Arabidopsis thaliana*. Scientific Reports, 3: 1273.

Xu L., Zhao H., Ruan W., Deng M., Wang F., Peng J., Luo J., Chen Z., Yi K. (2017): ABNORMAL INFLORESCENCE MERISTEM1 functions in salicylic acid biosynthesis to maintain proper reactive oxygen species levels for root MERISTEM activity in rice. Plant Cell, 29: 560–574.

Yamamoto Y., Kamiya N., Morinaka Y., Matsuoka M., Sazuka T. (2007): Auxin biosynthesis by the YUCCA genes in rice. Plant Physiology, 143: 1362–1371.

Yang T. H., Kon M., DeLisi C. (2013): Genome-wide association studies. Methods in molecular biology, 939: 233–251.

Yokawa K., Kagenishi T., Kawano T., Mancuso S., Baluška F. (2011): Illumination of Arabidopsis roots induces immediate burst of ROS production. Plant Signalling Behaviour, 6: 1460–1464.

Zhang C., Lim S., Kim J., Song J., Yook M., Nah G., Valverde B., Kim D. (2015): Quantifying herbicide dose-response and resistance in *Echinochloa* spp. by measuring root length in growth pouches. Canadian Journal of Plant Science, 95: 1181−1192.

Zhang J., Xu L., Wu Y., Chen X., Liu Y., Zhu S., Ding W., Wu P., Yi K. (2012): OsGLU3, a putative membrane-bound endo-1,4-beta-glucanase, is required for root cell elongation and division in rice (*Oryza sativa* L.). Molecular Plant, 5:176–186.

Zhao C., Xu J., Chen Y., Mao C., Zhang S., Bai Y., Jiang D., Wu P. (2012): Molecular cloning and characterization of OsCHR4, a rice chromatin-remodeling factor required for early chloroplast development in adaxial mesophyll. Planta, 236: 1165–1176.

Zhao Y., Hu Y., Dai M., Huang L., Zhou D. X. (2009): The WUSCHEL-related homeobox gene WOX11 is required to activate shoot-borne crown root development in rice. Plant Cell, 21: 736–748.

Zhao Y., Cheng S., Song Y., Huang Y., Zhou S., Liu X., Zhou D. X. (2015): The interaction between rice ERF3 and WOX11 promotes crown root development

by regulating gene expression involved in cytokinin signaling. Plant Cell, 27: 2469–2483.

Zhou S., Jiang W., Long F., Cheng S., Yang W., Zhao Y., Zhou D. X. (2017): Rice homeodomain protein WOX11 recruits a histone acetyltransferase complex to establish programs of cell proliferation of crown root meristem. Plant Cell, 29: 1088–1104.

Online:

BTC, Bartz Technology Corporation [online].

Visited: 1. 2. 2023

Website: https://www.bartztechnology.com/

Heiney A. (2004): Farming for the Future. NASA.gov, 8. 27. 04. [online].

Visited: 15. 4. 2023

Website: https://www.nasa.gov/missions/science/biofarming.html

IPK, IPK Galaxy Blast Suite [online].

Visited 1. 9. 2021

Website: https://galaxy-web.ipk-gatersleben.de/

NP, Nobel prize press release [online].

Visited 10. 3. 2023

Website: https://www.nobelprize.org/prizes/chemistry/2020/summary/

Pierce M. (2021): NASA Research Launches a New Generation of Indoor Farming. Nasa.gov, 12. 13. 21. [online].

Visited: 15. 4. 2023

Website: https://www.nasa.gov/directorates/spacetech/spinoff/NASA_Research_Launches_a_New_Generation_of_Indoor_Farming

RAP, The Rice Annotation Project [online].

Visited 1. 9. 2021

Website: https://rapdb.dna.affrc.go.jp/

VSI, Vienna Scientific Instruments [online].

Visited: 1. 2. 2023

Website: https://www.vienna-scientific.com/